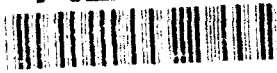


AD-A262 739



DOCUMENTATION PAGE

Form Approved
OMB No 0704-0188

1b. RESTRICTIVE MARKINGS	
3. DISTRIBUTION/AVAILABILITY OF REPORT Approved for public release; distribution is unlimited.	
2b. DECLASSIFICATION/DOWNGRADING SCHEDULE APPROX 1993	
4. PERFORMING ORGANIZATION REPORT NUMBER(S)	
5. MONITORING ORGANIZATION REPORT NUMBER(S) AFOSR	
6a. NAME OF PERFORMING ORGANIZATION The Board of Trustees of the University of Illinois	6b. OFFICE SYMBOL (If applicable)
7a. NAME OF MONITORING ORGANIZATION AFOSR/PKD	
6c. ADDRESS (City, State, and ZIP Code) 506 S. Wright St. Urbana, IL 61801	
7b. ADDRESS (City, State, and ZIP Code) Bldg. #410 Bolling AFB, DC 20332-6448	
8a. NAME OF FUNDING/SPONSORING ORGANIZATION AFOSR	8b. OFFICE SYMBOL (If applicable) ME
9. PROCUREMENT INSTRUMENT IDENTIFICATION NUMBER 91-0380	
8c. ADDRESS (City, State, and ZIP Code) Bldg. #410 Bolling AFB, DC 20332-6448	
10. SOURCE OF FUNDING NUMBERS	
PROGRAM ELEMENT NO.	PROJECT NO.
TASK NO.	WORK UNIT ACCESSION NO.
11. TITLE (Include Security Classification) International Conference on Martensitic Transformations (ICOMAT 92)	
12. PERSONAL AUTHOR(S) C. M. Wayman	
13a. TYPE OF REPORT Final	13b. TIME COVERED FROM 9/30/91 TO 12/31/92
14. DATE OF REPORT (Year, Month, Day) 93/03/05	15. PAGE COUNT 2
16. SUPPLEMENTARY NOTATION	
17. COSATI CODES	
FIELD	GROUP
SUB-GROUP	
18. SUBJECT TERMS (Continue on reverse if necessary and identify by block number)	
19. ABSTRACT (Continue on reverse if necessary and identify by block number) Abstracts of presentations made at the International Conference on Martensitic Transformations (ICOMAT 92), July 20-24, 1992.	
20. DISTRIBUTION/AVAILABILITY OF ABSTRACT <input type="checkbox"/> UNCLASSIFIED/UNLIMITED <input type="checkbox"/> SAME AS RPT <input type="checkbox"/> DTIC USERS	
21. ABSTRACT SECURITY CLASSIFICATION	
22a. NAME OF RESPONSIBLE INDIVIDUAL	22b. TELEPHONE (Include Area Code)
	22c. OFFICE SYMBOL

93-07443

ICOMAT-92

Sponsors

The Organizing Committee of ICOMAT-92 is extremely grateful for the generous financial sponsorship of the conference by the following companies and organizations. The contributions received from these sources will enable us to significantly enhance the quality of the conference, which will benefit all who attend. In view of the difficult economic conditions at present, these sponsors are to be especially applauded by all of us for their support.

Furakawa Electric	Japan
Tokin Corporation	Japan
Raychem Corporation	USA
Sumitomo Metal Mining Co.	Japan
U.S. Nitinol	USA
Daido Steel	Japan
Inland Steel	USA
G. Rau GmbH	Germany
Martin Marietta	USA
NKK Corporation	Japan
Flexmedics Corporation	USA
Kobe Steel	Japan
University of Illinois	USA
Shape Memory Applications, Inc.	USA
Nippon Steel	Japan
n.v. A.M.T.	Belgium
Memry Corporation	USA
Naval Postgraduate School	USA
National Science Foundation	USA
Office of Naval Research	USA
Army Research Office-Durham	USA
Air Force Office of Scientific Research	USA
Electric Power Research Institute	USA

ICOMAT-92

International Advisory Committee

M. Ahlers	Argentina	T. Ko	China
J. Beyer	Netherlands	Y.N. Koval	USSR
H. Bhadeshia	England	T. Maki	Japan
L. Delaey	Belgium	G.B. Olson	USA
D.V. Edmonds	England	J. Orin	Spain
F. Fujita	Japan	K. Otsuka	Japan
R. Gotthardt	Switzerland	J. Perkins	USA
G. Guenin	France	K. Shimizu	Japan
E. Hornbogen	Germany	V. Stchastlivtsev	USSR
T.Y. Hsu	China	J. Van Humbeeck	Belgium
P. Kelly	Australia	C.M. Wayman	USA
N. Kennon	Australia		

Honorary Members

J.W. Christian	England
M. Cohen	USA
L.G. Khandros	USSR
G. Kurdyumov	USSR
Z. Nishiyama	Japan
W.S. Owen	USA
V. Sadovsky	USSR
I. Tamura	Japan

Organizing Committee

C.M. Wayman (Chairman)
Jeff Perkins (Secretary/Program)
Darel Hodgson (Posters/Exhibitions)
Shellee Perkins (Social Director)
Marge Meyer (Registration)
Janine Hodgson (Liaison)

ICOMAT-92 Secretariat
Jeff Perkins
Naval Postgraduate School
Code ME/PS
Monterey, CA 93943, USA
(408) 646-2216
FAX (408) 484-9999

Accession For	
NTIS CRA&I	<input checked="" type="checkbox"/>
DTIC TAB	<input type="checkbox"/>
Unannounced	<input type="checkbox"/>
Justification	
By	
Distribution	
Availability Codes	
Avail and/or	
Spec	

A-1

ABSTRACTS

ABSTRACTS LISTED BY NUMBER IN THE PROGRAM

1. Studies of Martensitic Transformations in the Last Forty Years

Ken'ichi Shimizu

The author has studied the martensitic transformations and related phenomena, such as shape memory and superelasticity effects, in various ferrous and non-ferrous alloys for 41 years after graduation from a university in 1951. Main research results obtained by his group in the recent 41 years are introduced referring to those by other researchers, and unsolved problems are discussed. Then, future research subjects and their solvable techniques are surveyed with a little dogmatic view.

2. Views from Physics on Martensitic Transformations

James A. Krumhansl and Gerhard R. Barsch

A number of new experimental and theoretical advances in both materials science and physics have been applied to the study of displacive phase transformations. Among the experimental techniques there have been great advances in electron imaging and diffraction, in precision x-ray and neutron diffraction, in inelastic neutron scattering, and in materials preparation and control. In condensed matter physics attention has turned away from energy band and lattice details to more general global methods: renormalization group and mappings, methods for random and amorphous systems, the use of phenomenological (Landau-Ginzburg) free energies, intrinsically nonlinear theoretical methods, and widespread developments in computer simulation. Together these experimental and theoretical advances have given us much more information about martensitic materials than was available at the time of the formulation of much of the traditional methodology of the description of martensitic transformations, in many cases supplementing but in others calling for revisions or additions. In this review talk we discuss: 1) Lattice correspondences in systems where both x-ray and neutron diffraction data are available. There are three subclasses of materials: strongly martensitic dominated by elastic instabilities, intermediate martensities where both lattice strains and shuffles are inseparably operable, and martensitic transformations where shuffles dominate. 2) We address the physics of 'mesoscopic' behavior at the 10-1000 nanometer scale: characteristic of twinning patterns and habit plane structures. The new approach used is to employ nonlinear, nonlocal (strain gradient) continuum mechanics; we show how topological solitary excitations may be used as a basis for constructing phenomenological free energies. We compare this approach with elastic continuum methods in dislocation theory. 3) We discuss a number of special applications in the context of these approaches, including twinned precursors, the effect of composition variations, and defect induced nucleation. Supported by the U.S. Department of Energy, Grants DE-FG02-88ER45364 and DE-FG02-85ER45214.

3. Polydomain Phases in Martensitic Transformations

Alexander L. Roytburd

The discovery of polydomain phases has been one of the fundamental results of the experimental and theoretical studies of martensitic transformation. These phases consist of the alternation of domains: twins of a product phase or layers of different product phases. Elastic interactions between domains lead to the formation of an equilibrium polydomain structure corresponding to the free energy minimum. Thus, these domains have been named "elastic domains". The elastic domains form the polydomain phase whose average properties (e.g. a self-strain) are dependent on its domain structure. Hence, parameters of the domain structure are the additional degrees of freedom of a polydomain phase. This fact considerably determines the properties of the polydomain phase, as well as the thermodynamics and kinetics of a phase transformation with its participant. The thermodynamic aspects of polydomain phases are considered using a tetragonal-orthorhombic phase transformation as an example.

4. Atomistic Modeling of Ni-Ti

Hermann J.P. van Midden

The shape memory properties of NiTi alloys are well known to be influenced by lattice defects such as point defects, dislocations interfaces etc. In order to study the transformation mechanism and the way it is influenced by these defects an atomistic model is being developed. In this model an semi-empirical many body interatomic potential (Finnis-Sinclair, EAM theory) defines the material at an atomic level. The potentials are determined so as to fit several experimental quantities. A large variety of properties can be calculated from these potentials and compared with measured quantities, thus guaranteeing an adequate description of the material. Numerical simulations, such as Minimum energy calculations and Molecular dynamics simulations can give detailed information about defect structures, structural transformations and the dynamical development of the atomic system.

The paper will discuss the application of atomistic modelling to the NiTi, the procedure of determining the potentials and the first results of the simulations.

5. Topological Soliton Models for Interfaces in Proper Ferroelastic Martensites

Gerhard R. Barsch, W. Cao, A. Saxena and James A. Krumhansl

Coherent interfaces and modulated structures in martensites without shuffle displacements may be described in terms of quasi-1D soliton solutions obtained from a Landau-Ginzburg free energy functional for a fully 3D nonlinear, nonlocal anisotropic elastic continuum. This approach is illustrated for (110) twin boundaries, twin bands and pretransformation structural modulations in proper ferroelastic martensites undergoing a cubic - tetragonal (O_h - D_{4h}) transformation. With model parameters obtained from experimental elastic constant, x-ray lattice parameter and phonon dispersion data the theory has been applied numerically to $\text{In}_{1-x}\text{Tl}_x$ and $\text{Fe}_{1-x}\text{Pd}_x$ alloys. Starting from a very small (large) value at the transition temperature, the twin boundary energy (width) increases (decreases) strongly with decreasing temperature in the tetragonal phase of these two materials, respectively. The relevance of this approach and of these results for the martensite nucleation mechanism are discussed.

6. Theory for the Microstructure of Martensite and Applications

John M. Ball and Richard D. James

We present recent results on a new theory for the microstructure of martensite developed by the authors. The theory is capable of predicting the detailed patterns of microstructure that result from a martensitic transformation as well as the behavior of a martensitic crystal subject to applied loads and displacements. The crystallographic theory of martensite follows from the theory as a special case. A consequence of the theory is the extreme sensitivity of the patterns of microstructure to the precise lattice parameters, which has been explored by Bhattacharya for wedge-like microstructures appearing in shape-memory materials. We present recent predictions that relate to the deformations possible by rearranging variants and compare with experiment. Our approach is related to a theory of Khachaturyan, Roitburd and Shatalov. We explain the similarities and differences between the two approaches.

7. Surface Energy and Microstructure

Robert V. Kohn and Stefan Muller

Martensitic phase transitions lead to microstructures with rather special fine scale structures. Bulk energy considerations can predict gross features such as the directions of the twin planes. However, they are unable to predict finer details such as the length scale on which twinning occurs. Such details are generally explained by the inclusion of surface energy. A standard approach is to minimize the sum of bulk and surface energy within a restricted class of "twinned" configurations. This leads to the conclusion that the twin width w and the twin length l should satisfy $w \approx \epsilon^{1/2} l^{1/2}$, where ϵ is a constant with the dimensions of length. While this seems to be the rule, a different structure is sometimes observed, for example in Indium Thallium. It involves a coarsening of the twins away from the austenite-twinned martensite interface.

We have developed a new theoretical approach to this problem, based on a strain gradient model for the inclusion of surface energy. Our analysis differs from prior ones in that it permits configurations which are not "one dimensional" to compete in the minimization. We find that the global minimum of energy can be either "one-dimensional" or "branched," depending on the relative values of the elastic moduli in the austenite and martensite phases. The situation is quite analogous to the structure of magnetic domains near the boundary of a ferromagnetic material, a problem that was studied some time ago by Lifshitz.

8. **Computational Results for Martensitic Twinning**

Mitchell Luskin and C. Collins

We present computational results for martensitic fine-scale twinning and the austenitic-martensitic interface. We approximate a continuum model for InTi developed by Ericksen and James by the finite element method, and we utilize a variant of the conjugate gradient algorithm to compute minimum energy configurations. Our simulations have obtained twinning on the scale of the computational mesh for arbitrary orientations of the computational mesh with respect to the twin planes and the austenitic-martensitic interface. Our computations show the path of our algorithm to a local minimum of the bulk energy. The microstructure organizes itself so that the energy density is small in disjoint regions. As these regions coalesce or approach the boundary, a microstructure that is compatible with the applied loads is chosen throughout the entire crystal.

9. **Total Energy Calculations for Structural Phase Transformations**

K.M. Ho, Y.Y. Ye, Che-Ting Chan and Bruce N. Harmon

Advances in modern supercomputers and calculational techniques have made it possible to obtain accurate values for the energies of crystalline structures by performing first principles electronic structure calculations. These calculations have been used to obtain detailed information in the energy and the microscopic forces that arise as atoms are collectively displaced from one crystalline structure to another. Such results are useful in determining the path and energy barriers for martensitic phase transformations and in estimating the energy of the parent-martensite interface.

10. **Electronic Structure Calculations of Martensitic Transformations in Ti-Alloys**

Patrick Slavenburg and J.E. Inglesfield

Bandstructure calculations, which have been performed within our group for many years on complex systems, have recently been applied to a number of binary Ti-based alloys, important as memory alloys. The systems which have been looked at are: Ti-Fe, Co, Ni, Pd, Rh, Pt, Au. Calculations have been done, using different programs as ASW (Augmented Spherical Wave Method) and the LAPW (Linearised Augmented Plane Wave Method). Each method has different strengths and weaknesses, though the full potential version of the LAPW is considered to give the most precise basis-set, to date.

We have calculated the bandstructures, density of states and charge densities of the cubic as well as the orthorhombic structure, (martensite or close to martensite).

The martensitic transformation in these alloys must be driven by a lower energy of the low temperature martensitic phase. We are currently investigating how far this is due to a difference in bonding energy (i.e. the sum of the one-electron energies). With this work, we hope to make contact to the work of Pettifor. The instability of the high temperature phase may be connected with a high peak at the density of states as suggested by others before. There may also be Charge Density Wave effects due to flattened pieces at the Fermi surface. Furthermore, we try to make a link to the beta-phase Hume-Rothery alloys, which, in many cases exhibit almost the same macroscopic features as the Ti alloys.

11. **The Origin of Pre-Transitional Effects in Alloys With ω -Transformation**

David A. Vul

The theory of the β -to- ω displacive transformation and the elastic diffuse scattering anomalies above the transition temperature is presented. The phase diagram for this type of transformation is constructed. It is shown that the diffraction anomalies are the result of scattering on an oscillating component of static displacements around interstitial impurities (O, N, C). The oscillations arise due to a dip in the longitudinal phonon mode $L[111]$ at the position $2/3(111)$ and have the same wave vector. The β -to- ω transition is found to be a point of local instability of the bcc lattice around these impurities.

12. On the Constitutive Relations for δ to α Martensitic Transformation Plasticity in Plutonium Alloys

Paul H. Adler and Gregory B. Olson

A constitutive model for transformation plasticity based on isothermal martensitic kinetics is applied to the $\delta \rightarrow \alpha$ transformation in Pu alloys. The model is in good agreement with available data for $\delta \rightarrow \alpha$ transformation plasticity behavior of PuGa alloys in uniaxial compression as a function of composition, temperature and strain rate.

13. Microstructural Changes Occurring During Ageing of the Thermoelastic Martensite of γ -Quenched U-6 wt.% Nb Alloy Below 450 C

G. Beverini and David V. Edmonds

The chemical and morphological changes occurring during ageing U-6.0wt.% Nb have been studied using Atom Probe field Ion Microscopy (APFIM), Position Sensitive Atom Probe (PoSAP) analysis and Transmission Electron Microscopy (TEM). Statistical analysis of APFIM data has shown that phase separation occurs during ageing this alloy below 450 °C in a manner consistent with spinodal decomposition. Various PoSAP data representation techniques support this result since the solute atoms form a percolated (sponge-like) structure. However, TEM observations of the aged material revealed a complex microstructure which could not result solely from spinodal decomposition. It is believed that an isothermal martensitic transformation occurs at some point during the spinodal process as a result of solute depletion of the matrix. The martensitic transformation believed to occur isothermally is the same transformation responsible for the formation of the thermoelastic martensite encountered in water quenched U-6Nb, however, during ageing this transformation is restricted in the spinodally decomposed parent phase and therefore the resultant microstructure of the aged alloy is drastically different to that of the water quenched alloy. A mechanism is proposed to explain the concurrent occurrence of spinodal decomposition and martensitic transformation which could account for the large strength increments observed when material is aged below 450 °C.

14. On the Martensitic Transformation in a Dual Phase α/β Cu-Zn Alloy

Y.F. Hsu, W.H. Wang and C. Marvin Wayman

Martensitic transformation in a Cu-38.5wt% Zn alloy containing 15% volume fraction of α particles has been studied. The crystal structure and characteristic of the martensitic transformation of dual phase α/β CuZn alloy are similar to those for single phase alloy. The martensite formed upon subcooling possesses M9R LPSO structure with internal stacking faults on the (001) basal plane. Most of the soft α particles are deformed by slip, in order to accommodate the shape strain accompanied during the martensitic transformation. Besides, deformation twin, an unusual deformation mode in fcc structure, has been found in some α particles.

15. 9R Martensite in the TiPd-Fe Alloys

Kazuyuki Enami and Y. Nakagawa

In the TiPd alloys around equiatomic composition range, it was reported in the previous papers that the 9R martensite(M) phase appears besides the ordinary 2H (D019)M phase when palladium is substituted by 3d elements other than nickel. In the present experiment the crystal structure, internal structure and morphology of 9RM phase of the TiPd-Fe alloys were investigated by using electron microscopy and X-ray analysis. It was found that the 9RM phase begins to appear when the iron content is higher than 6.3at% in the alloys 50Ti-(50-x)Pd-xFe. In the alloys x=6.3 to 8.0, the 9RM phase has a monoclinic structure and the monoclinicity increases with increasing iron content. The internal structure of the 9RM phase is found to be {114} twin which corresponds to {128} twin in the 18RM phase in the Cu-Al base alloys. Besides this the basal plane (001) twin was found to exist due to the monoclinicity of the crystal symmetry. Quite unique features of the manner of coexistence of 9R and 2H M phases have been found. In the present alloys, it was frequently observed that the both the phases were involved in a variant crystal, that is, they make "two-in-one" morphology of the two M phases. There are two types of such morphology. First 9RM crystal is sandwiched by 2HM crystals or vice versa in a variant. The second, the 9R and 2H M crystals join together on the common "twinning" plane ($\bar{1}11$)2H/($\bar{1}14$)9R, that is 9R and 2H M phases become twin-related with each other in a variant. These results are well explained when considering the similarity of the atomic arrangements of the facet or twinning planes of both phases.

16. **Transmission Electron Microscope Investigations of 9R Martensite Formation in Copper Precipitates in Thermally Aged Iron-Copper Alloys**
Peter J. Othen, M.L. Jenkins and G.D.W. Smith

Conventional transmission electron microscopy (CTEM) and high resolution electron microscopy (HREM) experiments have been carried out on thermally aged Fe 1.30 wt.% Cu and Fe 1.28 wt.% Cu 1.43 wt.% Ni alloys to study the structure of small overaged copper precipitates ($d=10-15$ nm) in the α -Fe matrix. Evidence for the existence of a previously unexpected 9R phase in almost pure (> 95 at.%) copper particles has been found in diffraction pattern, optical diffractogram and interference fringe information. The 9R phase is believed to form by martensitic transformation from metastable bcc copper-rich particles coherent with the bcc ferrite matrix, and is thought to be a metastable intermediate phase formed prior to the precipitates assuming the thermodynamically stable fcc structure at larger sizes. A precipitate 9R structure is consistent with results from molecular dynamics calculations modelling the precipitate transformation from bcc. The bcc-9R martensitic transformation is well known in beta-brass, but this is believed to be the first time it has been seen in almost pure copper.

17. **Electron Microscopic Study of Twin Sequences and Branching in Ni₆₆Al₃₄ 3R Martensite**

Dominique Schryvers and Joseph T. Van Landuyt

Microtwin sequences in Ni₆₆Al₃₄ martensite plates of different size were investigated by electron microscopy. Although mostly irregular sequences were observed an average twin width w can be determined which increases with twin length L following the expected relation $w \propto \sqrt{L}$. High resolution electron microscopy was used to study the twin branching close to the plate boundaries and an atomic model for the branching of a microtwin and the changes in twin thickness is suggested.

18. **Differential Scanning Calorimetry Study of Aging in a Ti-Pd-Ni-B Shape Memory Alloy**

Ming-Hsiung Wu, Scott M. Russell and C.C. Law

An aging effect in a B2 Ti₅₀Pd₄₀Ni₁₀ alloy has been studied by differential scanning calorimetry. The aging changes the subsequent martensitic transformation kinetics to become "burst-like" where the transformation occurs in a narrow temperature range. Further aging shifts the transformation to lower temperatures. The activation energy for the change of the transformation kinetics is 627.5 KJ/mole while the activation energy for the depression of the transformation temperature is determined to be 420.6 KJ/mole. The aging effect occurs only in the first cooling cycle. Thermal cycling or thermal exposure of the alloy in the martensitic state restores the original transformation kinetics.

19. **Effect of Constrained-Heating Temperature on Microstructure in Ni-Ti Alloy**

L.H. Liu, J.H. Jiang and Liancheng Zhao

The effect of constrained-heating temperature on the microstructure of martensite and R-phase in a near-equiatomic NiTi alloy has been studied by means of metalloscope, X-ray diffraction analysis, SEM and TEM. It is shown that the microstructure of the alloy can be remarkably influenced by the constrained-heating temperature. The microstructure is the same as that of the sample with no constrained-heating at lower temperature. It is composed of parent phase and martensite at room temperature; the martensite variant is plate, and it is possessed of obvious direction when constrained-heating at lower temperature. The microstructure of the sample with constrained-heating at about 450°C will consist of R-phase and martensite with the dislocation forms. With increasing the constrained-heating temperature to 550°C, the microstructure is the same as that of the sample with no constrained-heating. In present paper, the cause of the microstructure difference has been discussed in detail, and considered that it is related to the different initial stress fields introduced by the constrained-heating in the parent phase.

20. Effects of Thermal Treatments on the Respective Behavior of "R" and Martensitic Phases in Ni-Ti-Co Shape Memory Alloys

L. Jordan, M. Masse, A. Villafana and G. Bouquet

NiTiCo shape memory alloys are materials commonly devoted to orthodontical applications. Nevertheless such uses imply reproducible mechanical properties depending on the structural evolutions occurring as a function of temperature. The aim of this work is to determine the structural modifications induced by various thermal treatments.

The chemical content of the NiTiCo alloys we elaborated, provides materials exhibiting a martensitic transformation in the 0°C to 30°C temperature range, corresponding to the hysteresis width.

The structural evolution of these alloys, as a function of temperature, was followed by internal friction spectrometry measurements and D.S.C. (Differential Scanning Calorimetry) experiments. These experimental methods detect clearly the "R" phase occurrence, on cooling, thanks to its net separation from the martensitic phenomenon, however, on heating, stepped thermal treatments are needed in order to separate the respective contribution of the "R" phase and the inverse martensitic transformation.

Thermal cycling appears as a very efficient way of shifting the martensite occurrence towards lower temperatures whereas the "R" phase is detected at a fixed temperature. This behaviour is explained in terms of structural phenomena taking place at the interfaces between martensitic variants.

Thermal treatments, such as annealings at high temperatures (500-700°C), induce transition temperatures displacements due to structural modifications concerning precipitated phases.

Finally, the determination of the elastic modulus evolution of our alloys, coupled to the internal friction measurements, proves the mechanical efficiency of the "R" phase compared to the one of the martensite. This result raises the question of the real structural nature of the "R" phase.

21. Recent Works on Crystal Structure Determination of Martensites

Kazuhiro Otsuka and Takuya Ohba

To know the structures of martensites is the first step to understand the mechanism of martensitic transformations. Despite the fact, the structures of some martensites remain unsolved until recently, since martensite single crystals are not easily available because of multiplicity of variants of martensites. Recently, however, a remarkable progress has been made in the structure analysis from two respects. First is the introduction of 4-circle diffractometer, which makes the accurate determination of structures possible for single crystal martensites produced by stress-induced transformation technique, followed by absorption correction and the least squares analysis of atomic parameters. Second is the site occupancy determination in ternary alloys by ALCHEMI (Atom Location by Channeling Enhanced Microanalysis) method and Synchrotron Radiation, which makes various x-ray wave lengths available. These are extensively reviewed for the monoclinic Ti-Ni martensite, trigonal ζ_2 Au-Cd martensite and other β -phase martensites. Based on these, a classification scheme of structural change in martensitic transformations will be presented. Ageing effects in martensites, which are responsible for the increase of Af temperature and rubber-like behavior in some alloys, will also be discussed from the structural point of view.

22. Nucleation of Martensite

Armen G. Khachaturyan

The homogeneous and heterogeneous nucleation of the martensitic phase is discussed. Different accommodation modes making possible to overcome the strain-induced nucleation barrier are considered. The cases of classical and nonclassical nucleation are analyzed. A concept of an adaptive martensitic phase is proposed and a role of the adaptive phase in the martensitic transformation and especially in the homogeneous nucleation process is discussed.

23. Computer Simulations of Heterogeneous Coherent Nucleation of Martensite in B2 NiAl

Philip C. Clapp, Y. Shao, Y. Zhao and Jonathan A. Rifkin

We have fitted the parameters of the Ginzburg-Landau strain free energy functional to the strain energy characteristics of B2 NiAl as determined from empirical data and Embedded Atom Method Ni-Al potentials. During Monte Carlo simulations, pseudoelastic behavior with hysteresis has been observed, caused by stress induced martensite during tensile stress cycling.

In separate atomistic studies of B2 NiAl using Molecular Dynamics simulations, both thermally induced and stress induced coherent martensitic nucleation and growth processes have been observed, including the formation of self-accommodating martensite variants. Nucleation is found to occur only at special heterogeneous sites that can be well characterized. Prior to nucleation, clear evidence of the buildup of large amplitude localized soft modes can be seen. A discussion of the kinetics of these processes will be presented, and evidence in the form of computer movies will be shown.

24. Computer Simulation of the Nucleation Process of the Martensite in a Small Particle

Tetsuro Suzuki and Ken'ichiro Takahashi

The famous classical experiment by Cech and Turnbull has shown that the nucleation process of the martensite becomes difficult as the size of the specimen decreases. This experimental result has been interpreted in terms of the decrease of the probability in finding lattice defects responsible for the nucleation process of the martensite with the decrease of the volume of the specimen. In order to find out whether the nucleation of the martensite is possible without the presence of the lattice defects, small particle models with two kinds of interaction potential between constituent atoms have been constructed and the molecular dynamical study of the martensite nucleation process has been carried out. In the small particle model with the Lennard-Jones potential, the nucleation of the martensite has been found possible without the presence of lattice defects. However, the nucleation has not been found possible without the presence of the lattice defects in the small crystal model with a longer interaction range potential than the Lennard-Jones potential.

25. Cellular Automaton Model of a Martensitic Transformation in a Hexagonal Array

Daniel Maeder and M. Droz

In previous work the possibilities of a mesoscopic model with 4 cell states was explored, which could change between one high temperature state ("0") and three martensitic states called "A", "B", "Z" as a function of two variables, temperature T and stress S [1]. The transformation rules were based on minimizing the sum of all interaction energies between nearest neighbours in a square array, plus the bulk energies which were assumed proportional to temperature for each A and B state, and one half of it for each Z. To explain the familiar formation of martensitic needles at the beginning of the transformation, special rules had to be introduced for second-nearest neighbours, and would have to be more complex for a complete model incorporating the additional variants commonly denoted "C" and "D". We have found that a cellular automaton on a hexagonal lattice allows a much simpler transformation rule producing all four martensitic variants. A mixed cell state "Y" must accompany C and D, in a way analogous to Z which allows a reversible change between A/B. The hexagonal plane is particularly attractive for such models, as the differences between various martensitic needle propagations can be traced to minute differences of interaction energies between close-packed pairs. Apart from the hexagonal lattice plane transition rules, each cell has information on the third dimension neighbourhood stored with it. Such "germs" remain unseen inside the crystal at high temperature but can start nucleation which may also be aided by weaker coupling with germ bits from nearest neighbours. The bulk energies depend not only on temperature, but on three stress components so that any combination of two variants can be favoured in the simulation. The Program will be displayed live on a IBM-compatible PC.

[1] D.G.Maeder and M.Droz: Proc.ICOMAT-89, Sydney(Australia), 1990, p.119.

26. Martensite Nucleation Through Spinodal Decomposition

Alexander L. Roytburd

A new model of martensitic nucleation is considered. It is shown that at large driving force the nucleation of the twinned martensite phase proceeds through the creation of an intermediate unstable state in a local volume. This state then decomposes into an alternation of the twin domains. The tendency to minimize the energy of the interaction of the transforming volume with the surrounding matrix takes the role of a condition of conservation of average strain. Thermodynamics and kinetics of such a mode of nucleation are considered and compared with other models of martensitic nucleation. The nucleation barrier has been found to be of 10^3 times less than other estimations that had rejected any possibility of the homogeneous nucleation of martensite.

27. *In Situ* High-Resolution Transmission Electron Microscope Study of Martensite Nucleation and Growth in a Co-32 wt. % Ni Alloy

James M. Howe

In situ hot-stage high-resolution transmission electron microscopy (HRTEM) was used to study the interfacial and internal structures, thickness and growth kinetics of the h.c.p. \rightarrow f.c.c. martensitic transformation in a Co-32wt.%Ni alloy. The results from these studies show that the interface is perfectly coherent and propagates by the motion of transformation dislocations on alternate close-packed planes. Initial lamellae are often four or six close-packed planes thick and defect free. These data support models of martensite nucleation that are based on the simultaneous formation of several overlapping stacking faults on alternate close-packed planes. The advancing martensite interfaces propagated across the field of view in less than 1/30th sec, placing a lower limit on the interface velocity of 440 nm/sec.

28. Homogeneous Martensitic Nucleation in Iron-Cobalt Precipitates Formed in a Copper Matrix

Minfa Lin, Gregory B. Olson and Morris Cohen

The martensitic transformation on subambient cooling has been monitored in defect-free nanocrystalline fcc Fe-Co particles that have been coherently precipitated in a Cu matrix. Transformation is found to occur at a driving force of ~ 10 kJ/mole, a factor of 7 higher than the known critical driving forces for heterogeneous nucleation in bulk alloys. The observed transformation characteristics are entirely consistent with classical homogeneous coherent nucleation, whereas heterogeneous nucleation and homogeneous semicoherent nucleation can be ruled out in this case. An observed variation in transformation temperatures is explained by the experimentally-determined differences in Co content (and, hence, in transformational driving force) among the Fe-Co precipitates in relation to their distribution of particle sizes. The role of thermal activation in the homogeneous nucleation process is demonstrated by applying a high magnetic field to impose an increment of driving force at low temperatures.

29. Theoretical Calculation of the Transformation of Austenite into Ferrite

Zi-Kui Liu and John Agren

The decomposition of austenite into ferrite is one of the main research topics in steels. It has been known for many decades that various types of plate-shaped ferrite may form if the supersaturation is large enough. The transformation features seem to change dramatically as the supersaturation increases and consequently, the various types of ferrite have been given different names, i.e. Widmanstätten ferrite, bainite and martensite, respectively. There has been much emphasis on the dissimilarities among the different types rather than their strong similarities. Thus the continuous change of the transformation characteristics has only rarely been considered until quite recently.

In the present calculation of the transformation, the effects of surface tension, diffusion in austenite and the phase interface, the elastic contribution due to the coherent interface, relaxation of the elastic strain by dislocations in the interface and the finite mobility of the phase interface are taken into account simultaneously and consistently. The transition from a partially coherent interface to a coherent interface is considered to occur gradually and the misfit between the two phases may be stored as elastic distortion of the lattice instead of misfit dislocations. The transformation in a number of alloy systems is calculated with the present model and compared with available experimental results in the literature.

30. On the Nucleation and Growth of Ferrous Martensites

Xiumu Zhang and YiYi Li

The nucleation and growth of ferrous martensites, including ϵ , butterfly, lenticular, thin plate and self-accommodating plate ones, have been investigated using optical and electron microscopy equipped with cooling device. The results for ϵ -martensite are in agreement with the faulting model proposed by Olson and Cohen. The formation courses of the thin plate, butterfly and lenticular martensites were recorded using a video camera. It was found that the twin and grain boundaries, especially their triple point are the favourable sites for the thin plate and lenticular martensites, but not for butterfly martensite which occurred inside austenite grains. The lenticular martensite grown along grain boundary and from thin plates was also found. It was proposed that the dislocations ($b = 1/2[111]_b = 1/2[110]_b$) emitted from incoherent twin boundaries of transformation twins in thin plate can provide the dislocation source for the transition of lattice invariant shear model from twinning to slip for the formation of lenticular martensite.

31. Decomposition of Homogeneous Unstable States with Conservation of Energy

Alexander Umantsev and Gregaory B. Olson

The effect of energy conservation on the decomposition dynamics of unstable states is considered for systems with nonconserved order parameters. We demonstrate that close to the critical point of instability the dynamics of the order parameter field is described by the nonlinear Cahn-Hilliard equation, leading to evolution by heat-transfer-controlled modulation. The results are applied to first-order displacive transitions predicting a new mechanism which follows a path of continuous strain modulation with finite wavelength.

32. Reverse Transformation of Aged Cu-Zn-Al Martensite: The Mechanism of Stabilisation

Muthuswamy Chandrasekaran, Eduard Cesari and Jan Van Humbeeck

In Cu-Zn-Al alloys which normally transform to martensite at room temperature or above it, quenching through and/or ageing in the martensite condition shifts the retransformation of martensite to higher temperatures. Diffusion processes occurring during ageing are responsible for such stabilisation. What is less clear, however, is the primary reason for the stabilisation as several mechanisms have been proposed in the literature to explain the same. The mechanisms can broadly be divided into two groups: one in which configuration changes in martensite with ageing are considered responsible and the other comprising of mechanisms unrelated to such configuration changes within the martensite. The purpose of the present work is to show that these two broad approaches can be differentiated by well designed experiments as well as to report and to discuss the results of such experiments.

33. Site Determination of Mn Atom in Cu-Al-Mn Alloys by Alchemi

Norihiko Nakanishi, Toshihiko Shigematsu, N. Machida, K. Ueda, Ken'ichi Shimizu and Yoshiyuki Nakata

The authors tried to study the fundamental mechanism of the shape memory character having ferromagnetic property due to the Mn-Mn atom interaction in Cu-Al-Mn alloys. This mechanism is based upon the phase separation between the ordered structure, Cu_3Al , and the Heusler one (L_{21}), Cu_2MnAl ; the former plays a role of the function of thermoelastic martensitic transformation and the latter covers that of ferromagnetism. The Cu based alloys consisted of several Mn contents between 6-15 at% and Al content of 23 at%, which is almost constant. After the necessary heat treatment, the alloys were isothermally held at 433 and 473 K for several hours up to 432 ks, and followed by TEM observation, XRD, DSC, electrical resistivity and magnetic measurements. The following experimental results are dominant: (i) The increase in the M_s and A_s temperatures during the aging was rather small; about 10 and 35 K at 433 and 473 K, respectively, in the specimen having 8.0 at% Mn. (ii) After the determination of Mn atom site in the DO_3 lattice by the method of Atom Location by Channelling Enhanced Microanalysis (ALCHEMI), it was made clear that Mn atoms behaved to preferentially occupy the Heusler position. (iii) As a result of the gradual growth of the Heusler domain caused by the alternate diffusion of Mn and Cu atoms, an endothermic peak was observed at the temperature range 503-533 K, which is the Curie temperature associated with the transition from Heusler to DO_3 lattice. The phase diagrams obtained by G. Thomas and T. Nishizawa were discussed.

34. Atom Location of the Third Element in Ti-Ni-X Shape Memory Alloys
Yoshiyuki Nakata, Tsugio Tadaki and Ken'ichi Shimizu

The atom location of the third element X in Ti-Ni-X shape memory alloys have been studied by the electron channelling enhanced microanalysis. The studies were carried out for three kinds of compositions, that is, $Ti_{50-x}Ni_{50}X_x$, $Ti_{50-x/2}Ni_{50-x/2}X_x$ and $Ti_{50}Ni_{50-x}X_x$, where X is Cr, Mn, Fe, Co or Cu. As a result, it turned out that Mn and Cu atoms showed a tendency to occupy the Ti atom site in $Ti_{50-x}Ni_{50}X_x$, the Ni atom site in $Ti_{50}Ni_{50-x}X_x$ and both the sites in $Ti_{50-x/2}Ni_{50-x/2}X_x$. On the other hand, Co and Fe showed a preferential occupancy at the Ni atom site, irrespective of the alloy compositions. Preferential occupancy of Cr atoms at the Ni atom site was observed, but it was not so remarkable as that of Co and Fe atoms. These experimental results were compared with the theoretically calculated ones on the basis of the Bragg-Williams approximation. In the calculation, the atom locations were determined so as to minimize the free energy including the configurational entropy of the alloy systems. As a result, it was found that the atom location of X varied depending on the value of $D (= (H_{TiX} - H_{NiX})/H_{TiNi})$, where H_{AB} is the interaction energy between atom A and atom B). In the case of $D > 1$, which was satisfied in Ti-Ni-Co alloys, most of X atoms occupied the Ni atom sites preferentially, irrespective of the composition of alloys. On the other hand, in the case of $D < -1$, X atoms occupied the Ti atom site. In the case of $|D| < 1$, the atom site occupied by X atoms was dependent on compositions and temperature. If D was around zero, which was satisfied in Ti-Ni-Mn and Ti-Ni-Cu alloys, Ti and Ni atoms occupied their own right sites and X did the remaining atom sites. If D value was close to unity, which was satisfied in Ti-Ni-Fe alloys, X atoms occupied the Ni atom site even in the $Ti_{48}Ni_{50}Fe_2$ at some finite temperatures although they occupied the Ti atom site at 0 K. These calculated results were in good agreement with the experimental ones.

35. Effect of Aluminum Content on Precipitation in Cu-Zn-Al Shape Memory Alloys
Shyue-Shang Leu and Chen-Ti Hu

The study of the effect of aluminum content on the precipitation has been conducted on Cu-Zn-Al shape memory alloys (SMAs) after aging treated at various temperatures. It was observed that the α_1 precipitates with a structure similar to the quenched 9R martensite and the γ precipitates with a cube-cube orientation relationship to matrix exist in the aged specimens with aluminum content lower than 3.8wt% and higher than 6.9wt%, respectively. In addition, the length of the latent period of α_1 precipitation was shorten as the aluminum content decreased. However, the length of the latent period of the γ precipitation was shorten as the aluminum content increased.

36. Effects of Heat Treatment on Stabilization of Transformation Behavior in a Cu-Zn-Al Shape Memory Alloy
Jian-Pei Zhou, Horng-Show Koo and Ken'ichi Shimizu

The deterioration of the shape memory effect and the shift of the transformation temperature in CuZnAl Alloy are the pressing resolved problems in research and development. The influences on shape memory effect and transformation temperature of CuZnAl alloy have been investigated by means of four-probe electrical resistance method, differential scanning calorimetry, X-ray diffraction technique, scanning and transmission electron microscopes. It is shown that the cool-rolled and annealed specimens have no remarkable influence on the shape memory effect and transformation temperature of the alloys, but the step quenching, deformation training and aging in parent phase have a large effect. The sample treated at 800°C for 20min, and followed by 180°C for 10min aging treatment and slow cooling below M_s is the best condition for the heat treatment of the alloy, the specimen treated by this heat treatment has a better shape memory effect and a stable transformation temperature.

37. Structure and Morphology of Fe₆C and Fe₁₆N₂ Precipitates Obtained by Aging Martensites

Jean-Marie Robert Genin, I. Fall and Oswald N.C. Uwakweh

The clustering-ordering synergy which forms Fe₆C precipitates by aging Fe-C martensite is compared to the long range ordering which forms Fe₁₆N₂ in the nitrogen case. The two steps of aging as revealed by Mössbauer spectroscopy has a unique activation energy of 75 kJ/mol, both controlled by carbon diffusion. The small Fe₆C precipitates are plate-like with (023) habit plane made of alternating 1C-2Fe-1C-5Fe-1C-5Fe sequences of atoms along [001]₀, which gives rise to 12 a₀ superperiod antiphase domains where a₀ is the lattice parameter. On the contrary, the two steps of aging observed for nitrogen correspond respectively to about 95 and 126 kJ/mol, i.e. to nitrogen diffusion and iron pipe diffusion. The Fe₁₆N₂ precipitates with (001)₀ habit plane, first coherent with the matrix, become semi-coherent with a misfit dislocation every 11 atomic spacings along [001]₀. A complete comparison is drawn between the two systems reviewing all experimental methods, e.g. calorimetry, dilatometry, X-ray diffraction, resistivity ... Another step which marks when the martensite is rid of isolated carbon atoms is observed during aging just prior to the full development of the first stage of tempering by in-situ transformation with composition in the neighbourhood of Fe_{2.5}C, close to the ordered ε-η carbide Fe₉C₄ stoichiometry. The activation energy is then 122 kJ/mol. The homologous stage of tempering for Fe-N martensite is the formation of Fe₄N with its nitrogen diffusion controlled as testified by an activation energy of about 94 kJ/mol. Finally, the same Mössbauer spectra are used to determine the interstitials distribution into the retained austenite. An ordered Fe₆C phase can explain the three observed Fe environments whereas a random distribution occurs among nitrogen atoms.

38. Low Temperature Ageing of Iron-Based Martensites

Kari Ullakko, V.G. Gavriljuk and Vladimir M. Nadutov

Ageing of the freshly formed iron based carbon and nitrogen martensites at temperatures below room temperature was studied by means of X-ray and neutron diffraction, Mössbauer spectroscopy, positron life time, internal friction, dilatometric, electrical resistivity and magnetic susceptibility measurements. The nature of abnormal tetragonality, stresses, redistribution of carbon atoms and their interaction with dislocations were the topic of the studies. The second stage of the decrease of tetragonality in the Fe-Ni-C martensite during heating at 200 - 300K is attributed to the decomposition of solid solution with clustering of carbon atoms. The results obtained do not confirm the idea of Taylor *et al.* about the isomorphness of the carbon rich regions in the aged Fe-C martensite to the α''-phase Fe₁₆N₂ in the aged Fe-N martensite. Along with clustering in solid solution strong interaction of carbon atoms with dislocations occurs causing the pinning of the carbon atoms and the formation of the Snoeck atmospheres.

Unlike in Fe-Ni-C martensites tetragonality increases during heating of the virgin Fe-C and Fe-Mn-C martensites at temperatures below the region where carbon atoms become mobile. The results obtained are consistent with the idea about the main contribution of twins (110) into low tetragonality and its increase during ageing but in a way which is different from the hypothesis proposed by Roitburd and Khachaturjan. Unlike Fe-Ni-C martensite the ageing of the virgin Fe-Mn-C martensite above 200K is not accompanied with a decrease of tetragonality, which can be explained by the retarding effect of manganese on the mobility of carbon atoms in α-iron. Redistribution of nitrogen atoms during ageing at low temperatures differs significantly from that of carbon atoms. Mössbauer measurements revealed that no clustering occurs. In addition, some new magnetic effects were observed in binary Fe-2.4wt%N martensite.

39. Tempering of Cold-Deformed Fe-Ni-C Thin-Plate Martensite

Marku Nieminen and Juhani Pietikainen

Heavily cold deformed Fe-25Ni-0.7C thin plate martensite was aged and tempered at various temperatures up to the temperature of reverse transformation α→γ. During the ageing stage no sign of the normal increase in electrical resistivity was detected. This indicates that the usual clustering process has been prevented. At the later stage of ageing anomalies were found in the dilatometric curve. Around 80 °C a clear decrease in the sample length was recorded. Also, at the tempering stage an abnormal high decrease in the dilatometric curve was found after 300 °C. This change was explained by increase of the amount of austenite despite the fact that the normal A_s-temperature for this material is only reached at 500 °C. The change in the amount of austenite was confirmed with the X-ray measurements. A strong precipitation of carbon to lattice defects during tempering was also detected in austenite. Changes in the materials structure were also studied by cooling tempered samples from room temperature to 30 K and measuring the change of magnetic susceptibility and electrical resistivity during cooling and heating. In addition, results of transmission electron microscopy studies, Mössbauer measurements and some rapid heating experiments are presented.

40. Internal Friction Behaviour of Virgin Dislocated Martensite
Yong Liu and Juhani Pietikainen

The internal friction behaviour of two morphological type of virgin martensite has been studied systematically. In the case of lenticular martensite the internal friction exhibits a kind of four-peak curve from 80 to 350 K. Two peaks in the case of lenticular martensite were due to the interaction between carbon atoms and dislocations at temperatures between 170 and 270 K. From the computer simulation of the internal friction curves the peak position of the component peaks could be determined precisely. The activation energies were calculated to be 0.79 eV for the 210 K peak and 1.3 eV for the 255 K peak. These values suggested that the process at temperatures from 170 to 220 K is related to the diffusion of carbon atoms and the process at temperatures from about 230 to 270 K is related with carbon atoms clustering. In the case of thin plate martensite an two-peak internal friction behaviour has been found. The mechanism of the this behaviour is discussed.

41. Ti-Ni Shape Memory Alloys and Martensitic Transformations
Toshio Saburi

Recent development of investigations on the martensitic transformations of TiNi shape memory alloys is reviewed. Nucleation and growth processes and self-accommodation mechanisms of the three kinds of martensitic phases in Ti-Ni alloys, i.e., the R-phase and B19' martensites which form from the B2 parent of the binary Ti-Ni alloys and the B19 martensite which forms from the B2 parent of Ti-Ni-Cu alloys are now being clarified. While the R-phase martensite which has a relatively small shape strain can nucleate from stress centers of relatively small intensity, such as single dislocations, the orthorhombic B19 and the monoclinic B19' martensites which have a larger shape strain can not nucleate from single dislocations and nucleate from larger stress centers. Self-accommodation of the R-phase is characterized by four twin-related variants arranged around each of $\langle 100 \rangle$ axes resulting herring-bone type and parallel-band type appearance on the surface. The B19 and B19' martensites, on the other hand, are characterized by triangular morphology. Self-accommodation of the B19' martensite is still not well understood. Cu substitution for Ni in near equiatomic Ti-Ni alloys affects in many respects on the transformation behavior and related shape memory characteristics (reduction of shape memory hysteresis, of composition sensitivity of the transformation temperatures, and of the flow stress level in the martensite state). The effects are now being practically utilized. Transformations and mechanical properties of rapidly solidified TiNi shape memory alloys are now being investigated and possibilities of improving the properties in many respects have been shown.

42. Martensitic Transformation and Shape Memory in Ti-Ni-Zr Alloys
Jan H. Mulder, Jan H. Maas and Jeno Beyer

Within the framework of the development of high temperature shape memory alloys TiNiZr is investigated. In a Ni-TiZr diffusion couple a broad diffusion layer of TiNi solid solution containing 23 at% Zr has been observed, showing a martensitically transformed region on the Ni-poor side. Therefore, alloys $Ti_{31.5-x}Ni_{48.5}Zr_x$ with x ranging from 0 to 20 at% were arc-melted and heat treated at 880 °C/48 h. The transformation temperatures show an increase of about 18 °C/at% Zr above 10 at% Zr. These results indicate that transformation temperatures depend strongly on the Ni-content in alloys with a Zr-content above 10 at%. The decrease of transformation temperatures on thermal cycling in $Ti_{31.5}Ni_{48.5}Zr_{20}$ heat treated at 880 °C/48 h has a thermal cause, and is thought to be due to precipitation of the Laves phase.

43. A Study of the Martensitic Transformation in Ti-Rich TiNi Alloys

H.C. Lin, Shyi-Kaan Wu and J.C. Lin

The martensitic transformations in Ti-rich TiNi alloys were studied by DSC, hardness and microstructure observation. Transformation temperatures and ΔH values of Ti-rich alloys are higher than those of equiatomic or Ni-rich alloys. There exists a lot of second phase Ti_2Ni around B_2 grain boundaries. The martensite stabilization in $Ti_{61}Ni_{39}$ alloy is found to be induced by cold rolling at room temperature. The ΔH value of the first reverse martensitic transformation of the cold-rolled specimen is found to decrease quickly with the increasing degree of cold rolling. The release of accumulated elastic energy, the smaller transformation volume and the reduce of degree of order are proposed to correspond to this characteristic. Transformation temperatures decrease, but hardness increases, with the increasing thermal cycling N. These effects come from the introduction of dislocations during the thermal cycling. The R-phase transformation can be promoted both by cold rolling and by thermal cycling in Ti-rich TiNi alloys due to the introduced dislocations depressing the M^* temperature.

44. Internal Structures of Triangular Self-Accommodating Martensite in Ti-Ni Shape Memory Alloy

Minoru Nishida, Kiyoshi Yamauchi, A. Chiba and Y. Higashi

Internal structures of martensite in Ti-50.1 at.%Ni shape memory alloy have been studied by transmission electron microscopy (TEM). Microstructural aspects in the specimen were remarkably changed by electropolishing conditions, especially with temperatures of the electrolyte. A stress induced product with orthorhombic unit cell and (001) compound twinning of B19 structure were observed in the thin foil electropolished at relatively high temperatures around M_f . A hydride was formed by hydrogen absorption in the specimen prepared at relatively low temperatures below M_f . A sound martensite with B19 structure was observed in the thin foil electropolished at intermediate temperatures between above conditions. Internal defect of martensite was confirmed to be $\langle 011 \rangle$ Type II twinning by electron diffraction. $\langle 011 \rangle$ Type II twinning planes were converted to (111) Type I twinning planes in many of junction planes between martensite variants. It suggested that (111) Type I twinning was variant accommodation twinning which is introduced as a means of mutual accommodation of shear strains between variants.

45. Shape Memory and Superelasticity in Powder Metallurgy TiNi Alloys

Sei Miura, Hiroyuki Kato, T. Koyari, K. Isonishi and Masaharu Tokizane

Shape memory properties of powder metallurgy TiNi alloys produced by Plasma-Rotating Electrode Process (P-REP) were examined. Using a prealloyed ingot of Ti-50.7at.%Ni, TiNi powder was produced by P-REP. The consolidation by Hot Isostatic Pressing (HIP) attained to obtain the compact having a relative density of 99.6%. The P/M alloy showed not only shape memory effect but also superelasticity, as the typical melted alloy having of this composition shows. The comparison of the martensitic transformation and mechanical properties between the P/M and of a typical melted alloy showed that the former alloy have almost identical characteristics to those of the latter. In particular, superelastic strain of 4.8% will be first reported for the powder metallurgy TiNi alloy.

46. Shape Memory Characteristics of Ti-Ni Thin Films Formed by Sputtering

Shuichi Miyazaki, Akira Ishida and A. Takei

Ti-Ni shape memory alloy thin films have been made by sputter-deposition technique. As-sputtered films were amorphous and the crystallization temperature was determined to be 756K by DSC measurement. After heat treatment, the shape memory characteristics and crystal structures have been investigated using DSC, thermomechanical tests and X-ray diffractometry. The crystal structures were determined to be B2 and monoclinic for the high and low temperature phases, respectively, which are the same as those of bulk specimens. Two types of thin films with different alloy compositions were prepared. Ti-50.4at%Ni alloy showed a single peak in the DSC curve indicating a single stage of transformation occurring from B2 to the martensitic phase, while Ti-51.4at%Ni alloy showed double peaks indicating the R-phase transformation occurring prior to the martensitic transformation. The transformation peak temperatures are as follows; M^* and A^* are 275K and 320K for the former alloy, while R_s^* , M^* , A^* and R_f^* are 289K, 230K, 288K, and 290K, respectively. It is shown that the perfect shape memory effect was achieved in sputter-deposited Ti-Ni thin films in association both with the martensitic and R-phase transformations, and it was characterized quantitatively for the first time. The stresses for inducing the martensitic and R-phase transformations vs. temperature curves showed the Clausius-Clapeyron relationships, which are almost quantitatively same as that of bulk specimen with similar alloy composition.

47. The Effect of Cold Work and Heat Treatment on the R-Phase to Austenite and Martensite to Austenite Transformation of a Near-Equiatomic Ni-Ti Shape Memory Alloy

Paul E. Thoma, Ming-Yuan Kao, Sepehr Fariabi and D.N. AbuJudom

The influence of cold work and heat treatment on the R-Phase to austenite and martensite to austenite transformation temperature of a near equiatomic NiTi shape memory alloy has been examined. For the same cold work, the R-Phase to austenite transformation temperature increases with decreasing heat treat temperature. At heat treat temperatures of 500, 525, and 550°C, the amount of cold work has little influence on the R-Phase to austenite transformation temperature. For heat treat temperatures of 425, 450, and 475°C, the R-Phase to austenite transformation temperature increases significantly with increasing amounts of cold work and the greatest increase occurs at low heat treat temperatures. At heat treat temperatures of 575 and 600°C, stable R-Phase does not form from austenite on cooling. The martensite to austenite transformation temperature is constant for all cold works and heat treat temperatures when the temperature is 575°C and higher. In general, for a particular heat treatment, the martensite to austenite transformation temperature decreases with increasing cold work. For cold works greater than 31% with heat treat temperatures of 450°C and lower, the martensite to austenite transformation temperature increases slightly with increasing cold work and coincides with the R-Phase to austenite transformation temperature. Coincident with merging of the martensite to austenite transformation temperature and R-Phase to austenite transformation temperature is the emergence of a stable R-Phase from martensite on heating. The behavior of the austenite transformation temperature and the emergence of a stable R-Phase from martensite are attributed to the level of internal stress.

48. Influence of Heat Treatment on the Internal Resistance to the Martensitic Transformation in NiTi

Yinong Liu and Paul G. McCormick

It is known that the phase boundary motion accompanying the martensitic transformation in shape memory alloys requires irreversible frictional work against an internal resistance. A study has been carried out to investigate the influence of heat treatment on the internal resistance in a NiTi alloy. The resistance was determined from measurements of the heat loss during a thermal cycle through the forward and reverse transformations and transformation hysteresis. The mechanical work dissipated during a deformation cycle of pseudoelasticity was also measured. The results show that heat treatment influences not only the internal resistance, but interalia also the transformation behaviour.

49. Electrical Resistance Change in a Ti-Ni Alloy During a Thermal Cycle Under Constant Load

Shuichi Miyazaki, Yinong Liu, Kazuhiro Otsuka and Paul G. McCormick

The martensitic transformation is accompanied by an electrical resistance change as well as a shape change. In the present paper, both the strain and electrical resistance (ER) in a Ti-49.5at%Ni alloy have been measured simultaneously during cooling and heating under a variety of constant stresses between zero and 250 MPa. Two stages of strain change were observed upon cooling, the first stage being associated with the R-phase transformation and the second one with the martensitic transformation. The corresponding ER showed an increase due to the first transformation and a decrease due to the second one. Since the martensitic phase reversed directly to the parent phase upon heating, the ER during cooling was always higher than that during heating under no stress. However, by applying a stress, the ER during the martensitic transformation increased and the ER-temperature curves during cooling and heating crossed each other under a constant stress less than 147MPa. By applying a stress higher than 147MPa, the ER during heating became higher than that during cooling at any temperatures. The ER of the martensitic phase under a stress of 196MPa was about 30% higher than that under no stress. This change in ER originates from specimen shape change, change in the density of lattice defects such as dislocations and twin boundaries, and reorientation of martensite variants.

50. Effects of Neutron Irradiation on the Transformation Behavior in Ti-Ni

Akihiro Kimura, Shuichi Miyazaki, Hiroshi Horikawa and Kiyoshi Yamauchi

The effects of neutron irradiation and post-irradiation annealing on the martensitic transformation behavior of Ti-50.0, 50.5 and 51.0at%Ni alloys were investigated by means of the differential scanning calorimetric (DSC) measurement and transmission electron microscope (TEM) observation. The neutron irradiation up to the fluence of $1.2 \times 10^{24} \text{ n/m}^2$ at 333K suppressed the martensitic transformation of these alloys, resulting in the absence of the transformation above 150K. TEM observations at room temperature revealed that high density of black dot type radiation damage structures were formed in the neutron irradiated Ti-51.0at%Ni alloy. Diffraction patterns taken from this area showed the superimposition of diffused halo rings on the matrix spot pattern, indicating multi-scattering caused by radiation damage structure. Post-irradiation annealing caused the recovery of the transformation behavior of which the progress depended on the annealing temperature and period. From the dependence of the transformation temperature on the annealing condition, an activation energy of the recovery of the transformation behavior in a neutron irradiated Ti-50.0at%Ni alloy was estimated to be 1.2eV by cross-cut method.

51. Comparison of Homogeneous Shear and Tensile Tests on a NiTi Shape Memory Alloy

Pierre-Yves Manach and Denis Favier

For classical isotropic materials, the push-pull tests are often used as identification tests, if equivalent stress and strain can be defined. In fact, these push-pull tests imply only one diagonal component of the stress tensor; moreover, in the cases of the torsion of a thin tube or of the simple shear of a sheet, a non-diagonal component of both stress and strain tensors is principally concerned in constitutive equations. Therefore these two kinds of homogeneous tests are complementary in order to develop constitutive laws applied to alloys including shape memory alloys. Isothermal and non-isothermal tensile and shear tests are performed on sheet samples of different shape memory alloys. First results on Cu-Zn-Al and Ni-Ti alloys are presented.

For different alloys, superelastic and pseudoelastic behaviour have been observed and compared for both types of test; the anisotropy of the materials (in the plane of the sheet) has been tested. Assuming an isovolume deformation, equivalent stress and strain are obtained for two particular Cu-Zn-Al alloys; for superelastic alloy, the behaviour is closed to Von-Mises type whereas rubberlike material shows a typical Tresca behaviour. For a given Ni-Ti alloy, for which isotropy in the plane of the sheet has been tested, it seems not possible to define equivalent stress and strain.

The previous studies are necessary to achieve a tensorial scheme allowing the description of the thermomechanical behaviour of shape memory alloys. A continuum mechanics description of the combined elastic and hysteresis effects has been proposed ("Thermomechanics of Hysteresis Effects in Shape Memory Alloys", Favier et al, ICOMAT 1989); it appears to be a general and versatile basis for future design of shape memory elements. This scheme is identified and compared with previous experimental results.

52. Stability of Deformed Martensite in Ni₄₇Ti₄₄Nb₉ Shape Memory Alloy

Lian-Cheng Zhao and C.S. Zhang

The stability of deformed martensite in Ni₄₇Ti₄₄Nb₉ alloy has been studied by means of transmission electron microscopy and diffraction, electrical resistance measurements and tensile tests at various temperatures. The experimental results indicate that the stability of deformed martensite depends strongly upon deformation conditions. In general, the stability of the thermal martensite and stress-induced martensite formed at temperatures a little higher than M_s under small strain is low, while the strain-induced martensite formed at temperatures above M_s^0 possesses high stability, but does not exhibit shape memory effect. It is noteworthy that the stress-induced martensite formed at $M_s+30^\circ\text{C}$ under large strain (16~20%) not only possesses high stability, but also exhibit good shape memory effect. Microstructural analysis shows that a large amount of (001)_M twins and some of dislocations are generated in the stress-induced martensite formed under large strain which is different from that formed under small strain. Based on the present results, the concept of deformed stress-induced martensite is proposed and the reasons for the high stability and good shape memory effect of the deformed stress-induced martensite are discussed.

53. Martensitic Transformations- A Structural Classification

John W. Christian

The choice of a deformation twinning mode frequently involves a conflict between small shears and shuffles of small magnitudes. Modes of large shear are generally found only in single lattice structures which twin without any shuffling. Similar rules may be deduced for martensite formation, and are used to derive a new structural classification for martensitic and related transformations. A critical consideration is whether or not any necessary change in the stacking sequence of close-packed planes may be achieved by shuffling alone. Comparison is made with previous classifications of martensite.

54. S.O.S.- Shears or Shuffles in Martensitic Transformations

John W. Christian

In the conventional crystallographic theory, the atomic displacements at the martensite interface are regarded as the net effects of a lattice deformation and a lattice invariant deformation, both of which contribute to the macroscopic shape change, and of shuffles which have no macroscopic effects. There are nevertheless possible ambiguities in this factorization of the displacements, and the shear or shuffle division may depend on the scale of observation. Ambiguities also occur in the distinction between the lattice and lattice invariant deformations, as exemplified by Khachaturyan's recent description of the martensitic structure as an "adaptive phase". The implications for interface structure and growth mechanisms will be examined.

55. Crystallography of Hierarchical Structures of (Ti,Nb)₃Al Alloys Involving Both Displacive and Chemical Ordering

Leonid A. Bendersky, W.J. Boettinger and Alexander L. Roytburd

In the present work the microstructure of rotational domains of the orthorhombic O phase in continuously cooled Ti-25Al-12.5Nb (at%) and Ti-25Al-25Nb (at%) alloys were investigated. For the Ti-25Al-25Nb alloy the domains form from the B2 phase through a transient B19 structure and have a strain accommodating polytwin structure. For the Ti-25Al-12.5Nb alloy the domains form from the disordered BCC phase by (1) the formation of hexagonal phase domains and subsequently (2) their transition to the O phase by ordering. The strain accommodating morphology occurs in the second step. The configuration of the domain interfaces can be understood on the basis of strain energy minimization.

56. Martensite Group Morphology and Relative Frequencies of the Crystallographically Different Junction Planes in β_1' Martensite

L. Chen, Druce P. Dunne and Noel F. Kennon

A common feature of martensite plates in β_1' (9R or 18R) shape memory alloys is self-accommodating plate units, which consist of four martensite variants with habit plane normals clustered about one of the six $\{110\}$ poles of the parent phase. However, some uncertainty exists about the dominant morphology of the plate groups which form on cooling: a diamond shaped four plate cluster and a spear or chevron shaped grouping have both been suggested as the characteristic group morphology. A potential means of resolving these conflicting proposals is by measurement of the relative frequencies of the three major martensite plate junction planes: $\{110\}_{\beta_1}$, $\{100\}_{\beta_1}$ and the $\{155\}_{\beta_1}$ habit plane junction.

In the present work, the relative frequencies of the crystallographically different kinds of junction planes have been determined for β_1' martensite in a Cu-Al-Ni-Mn shape memory alloy by using quantitative metallography. The experimental results indicate that the main arrangement of the four martensite variants in a group is an extended chevron type morphology which is repeated in a "zig-zag" pattern on a larger scale. As a consequence, the dominant junction plane interface is the habit plane junction, which is about 8 times more common than the $\{110\}_{\beta_1}$ junction plane. The frequency of $\{100\}_{\beta_1}$ junction planes was found to be so low that it can be disregarded as a significant microstructural feature of thermally produced β_1' martensite.

57. Self-Accommodation in Martensites

Kaushik Bhattacharya

Shape-memory alloys are able to transform from the austenite to the martensite phase without any apparent change in shape. This is known as self-accommodation. Though there is a change of shape at the microscopic level, the martensitic variants arrange themselves in such a microstructure that there is no macroscopic change in shape. Wayman and others have emphasized the importance of self-accommodation in the shape-memory effect. Apart from being an inherent part of the one-way shape-memory effect, it can be argued that self-accommodation is also important for the reversibility of transformation in polycrystals and for easy nucleation of martensite during cooling. Using a theory of thermoelasticity, we investigate which materials can form a self-accommodating microstructure. This approach is significantly different from the previous studies because it makes no a priori assumption on the microstructure. We find that if the austenite is cubic, the material is self-accommodating if and only if the transformation is volume preserving. On the other hand, if the symmetry of the austenite is not cubic, it is not possible to construct any microstructure that is self-accommodating unless the transformation strain or the Bain strain has to satisfy additional, rather strict conditions. We shall discuss the implications of these results on potential candidates for new and improved shape-memory alloys.

58. Shape Memory Effect and Superelasticity Effect Associated With β_2 to ξ_2' Martensitic Transformation in a Au-49.5 at.% Cd Alloy

Koichi Morii, Shuichi Miyazaki and Kazuhiro Otsuka

The Au-Cd alloy at or very close to Au-50at%Cd composition exhibits $\beta_2 \rightarrow \xi_2'$ (trigonal) martensitic transformation. Since neither the stress-induced transformation from β_2 to ξ_2' nor the reorientation of ξ_2' martensite variants under stress have been observed yet, they were explored in the present work. By tensile testing single crystals of a Au-49.5at%Cd alloy, the $\beta_2 \rightarrow \xi_2'$ stress-induced transformation was found only in orientation near $\langle 111 \rangle_{\beta_2}$ in a very narrow temperature range, and the reorientation of the ξ_2' martensite was also observed. This orientation dependence was clarified. Associated with the transformation, superelasticity and the shape memory effect were found for the first time. The observed transformation strains agreed well with the calculated values from the lattice deformation. The entropy of transformation and the enthalpy of transformation were calculated to be $\Delta S = -1.34(\text{J/mol}\cdot\text{K})$ and $\Delta H^* = -407(\text{J/mol})$ respectively from the Clausius-Clapeyron relationship.

59. High Resolution Electron Microscopy Observation of Twin Interfaces in γ_1' Cu-Al-Ni and γ_2' Au-Cd Martensites

Toru Hara, Takuya Ohba, Kazuhiro Otsuka Y. Bando and S. Nenno

Twins in martensites play an important role. Type I twins in γ_2' Au-Cd and Type II twins in γ_1' Cu-Al-Ni martensite are introduced as the lattice invariant shear. The twinning plane of Type I in Au-Cd has rational indices {111}, and that of the Type II twin in Cu-Al-Ni has irrational indices {1, 1.5036, 0.5036}. In general, an irrational plane such as in Cu-Al-Ni martensite is believed to consist of steps and ledges. The purpose of this paper is to clarify the structure of Type I and Type II twin interface by electron microscopy. Single crystals of Cu-Al-Ni were prepared by the Bridgman method whose surface is parallel to (011) to observe the Type II twin from the η_1 direction. Type I twins which are not the lattice invariant shear were also observed. Images of the Type II twin from the η_1 direction were obtained for the first time. Observations from various directions were also made and confirmed that the Type II twin interfaces are broad in contrast to sharp interfaces of the Type I twins. These images suggest that the Type II twin interface is diffuse rather than steps and ledges. Structural consideration was made on the interface of the Type II twin. The most possible model has been constructed which explains the characteristics of the observations. The Type I interface of Au-Cd alloy will be also discussed at the presentation.

60. Limitations of Phenomenological Theories of Martensitic Transformations

Sol Mendelson

Phenomenological theories of martensitic transformations include Landau theory in the "physical" camp, and the WLR and BM theories in the "metallurgical" camp. By their nature, phenomenological theories lend themselves to applications which ignore experimental data and the physics involved. For example a solitary wave (soliton) model for motion of incoherent interfaces created by the Bain distortion is meaningless. In addition to this, the formulation of Landau theory is sometimes misrepresented in order to make the problem tractable. Contradictions arise when Landau theory is applied to the non-degenerate displacements of the Bain distortion. The essential feature of mean field second order displacive phase transitions in Landau theory is that both positive and negative order parameter displacements (electric, magnetic, elastic) are equally favorable. These "degenerate" displacements are represented by setting to zero all odd powers of the order parameter in the free energy expansion. An odd power of an additional order parameter, such as for a volume change relaxation, can be included for the first order aspect of a weakly first order transition. Since the Bain distortion is non-degenerate, its displacements are purely first order and cannot be represented by even power terms (the essence of Landau theory) which represent degenerate displacements. In this paper we characterize Landau, and the WLR and BM phenomenological theories, and summarize their limitations. We show that Landau theory and the degenerate order parameter displacements in the scenario of the lattice-variant-shear-theory (LVST) are complementary, in contrast to the incompatible non-degenerate Bain distortion.

61. Fluctuationless Mechanism for Martensitic Transformation

David A. Vul

Classical mechanism of first order transformations supposes the possibility of fluctuation formation (homogeneous or heterogeneous) of critical nuclei of a new phase. Different models of nucleation of a martensite make use the same ideology. In the case when such heterophase fluctuations are blocked by kinetic reasons, there is another alternative mechanism for structural transformations that does not require fluctuations at all. This type of transformation arises as a result of defect-driven instability in a strong anharmonic crystal. The transformation begins near a defect, spreads out similar to an elastic wave and stops when the boundary between transformed and untransformed regions is in mechanical equilibrium. As the first example of a fluctuationless transformation, the theory of the displacive β - ω transformation is developed. It is shown that this transformation is triggered by interstitial impurities. The proposed theory enables one to construct a phase diagram and to describe kinetics and morphology of the β - ω transformation in Zr and Ti alloys.

62. The Lattice Distribution of Alloying Elements and Martensite Nucleation in Steels

Yuri N. Petrov

The structural imperfections and alloying elements distribution in high alloyed Cr-Ni and Mn austenites with different carbon contents has been investigated. It is pointed out that substitution and interstitial alloying elements distribution strongly depend on the nature of defect and the austenite heat treatment. The structural imperfections are considered as F.C.C.-structure unsteadiness regions which under appropriate strain and elements concentration conditions may be transformed into the B.C.C. and H.C.P. martensite nucleus. The alloying elements distribution between the austenite matrix and martensite phases are considered.

63. OPEN

64. Thermodynamics and Kinetics of Martensitic Transformations

Jordi Ortin

This lecture reviews our current knowledge of the thermodynamics and kinetics of martensitic transformations. Since these transformations are diffusionless in nature, the suitable thermodynamics is that of a single-component system undergoing a first-order phase transition. In principle, all intensive quantities coupled to extensive variables that suffer a discontinuity in the transition play the role of external fields capable of driving the transition. Reference is made to available experimental examples: temperature, uniaxial stress, hydrostatic pressure and magnetic field. Regarding kinetics, distinction is made between athermal (driven by a change of external fields) and isothermal transformations. Thermoelastic transitions, undergone by most shape-memory alloys, belong to the first category: shape changes associated with the transformation are fully accommodated elastically, and the transformation proceeds through a sequence of metastable states. Characteristic relaxation times between thermoelastic equilibrium states are comparatively negligible, and for this reason the transformation can be studied in a continuous formalism. In this framework, the classical description of transformation in ideal equilibrium is improved to consider the role of elastic strain energy and energy dissipation in the transformation, and to provide quantitative methods for their determination. Particular attention is dedicated to hysteresis, a macroscopic evidence of energy dissipation in the transformation, and to the thermodynamic information contained in the characteristic subloop behaviour of hysteretic thermodynamic trajectories. Possibilities of extending this formalism to non-thermoelastic, athermal transformations (typically found in ferrous alloys) are also discussed. The lecture concludes by establishing a comparison between athermal transformations and the less frequent category of isothermal transformations, exhibited by a number of ferrous alloys, and by suggesting directions of interest for further research.

65. Thermodynamics of Martensitic Transformations

T.Y. Hsu (Xu Zuyao)

A summary of the calculation of the driving force for the martensitic transformation and M_s in ferrous alloys and thermoelastic Cu-based alloys is given, including the results of the application of the Central Atomic Model, the confirmation of the formula expressing the non-chemical free energy for ferrous alloys suggested by the present author and the effect of various orderings of the parent phase on M_s in Cu-Zn-Al alloys. In addition, an approach for expression of the size effect on M_s in ceramics containing ZrO_2 is briefly suggested.

66. On Some Features of Martensitic Transformation

E.I. Estrin

This report summarizes the results of numerous researches of the martensitic transformation (MT) in different kinds of solids (ionic crystals, semiconductors, metals) carried out under ambient and high pressures. It has been found that MT in all solids are characterized by common features. Neither athermal nature of MT nor the M_s temperature is connected directly with the loss of the parent phase stability. The M_s point occurs at a temperature where the thermodynamic driving force is equal to the energy needed to produce the shape deformation. The MT's failure to come to the completion at isothermal conditions and spreading it onto a range of temperatures is not caused by exhausting of the preexisting embryos. It is an effect of a change of the parent phase during MT and the increase in the shape deformation work. The M_f point results from the fact that below some temperature the thermodynamic driving force of MT ceases to grow with undercooling but the work of shape deformation continues to increase. MT initiated by loading (both in elastic and plastic fields) starts when the critical external stress is achieved. According to Clapeyron-Clausius equation, the critical stress is determined by the MT shape deformation, the MT heat effect and the difference between temperatures at which the sample is loaded and the M_s point of the retained parent phase.

67. On Thermodynamics of Shape Memory Alloys in the Pseudoelastic Range

Ingo Muller

Materials undergoing phase transitions are characterized thermodynamically by non-convex free energies. Such is the case in the austenitic-martensitic phase transition in shape memory alloys in the pseudoelastic range. In such a solid-solid phase transition the coherency energy must be considered; in fact that energy accounts for the hysteresis and determines its size, see [1].

A thermodynamic theory has been developed that is based on the concept of the non-convex free energy and that accounts for sound emission as a loss mechanism. The theory permits the calculation of the coherency energy and of the coefficient of sound emission from calorimetric measurements and stress-strain measurements.

This theory is akin to ordinary thermostatics except that it must account for the fact that even quasistatic processes are irreversible because of coherency and sound emission. The theory is compared with the theory of Ortin & Planes [2]. Differences are explained and discussed.

[1] Müller, I., Xu, H. On the pseudoelastic hysteresis. *Acta metall. mater.* **39** (1991)

[2] Ortin, J., Planes, A. Thermodynamic Analysis of Thermal Measurements in Thermoelastic Martensitic Transformations. *Acta metall.* **36** (1988)

68. Thermodynamics of the R-Phase Transformation in NiTi Shape Memory Alloys

Graziella Airoidi, Guido Riva, Giordano Carcano and A. Sciacca

The presence of the R phase in NiTi alloys is related not only to the chemical composition of the alloy, but can be connected with a strain state, generated by the introduction of linear defects as dislocations, or by precipitates.

Attention is here focussed on the key characters of the R phase depending upon the way adopted to introduce constraint. To reach this goal investigations have been performed on polycrystalline NiTi wires, with the same composition, submitted to different thermal treatments of annealing or ageing. Results show that R-phase transformation settled by the introduction of dislocations, as during thermal cycling P-M, has a low heat of transformation and can easily be removed by a very short annealing (e.g. 1' at 400°C). R-phase transformation, settled by aging at intermediate temperatures (300°C-500°C), involves a higher enthalpy change and modifies its kinetics with ageing time.

69. Solid Solution Strengthening and Kinetics of Martensitic Transformation in Fe-Base Alloys

Gautam Ghosh and Gregory B. Olson

A large body of experimental data for athermal martensitic transformation in binary, and ternary Fe-base alloys; and the experimental data for the activation energy for fcc \rightarrow bcc martensitic nucleation in Fe-Ni, Fe-Ni-C, and Fe-Ni-Mn alloys have been analyzed. By incorporating the theory of solid solution hardening, we have modelled the composition and temperature dependences of the frictional for a martensitic interface in multicomponent alloys. The available data suggests that the composition dependence of the athermal frictional work for the martensitic interface is the same as that for the conventional slip deformation. The normalized activation energy $Q(T)/\mu(T)$ vs normalized driving force $(\Delta g_n / \Delta \hat{g})$ data in isothermal martensitic nucleation is found to follow the general $Q-\Delta g$ relationship proposed by Kocks et al [26] in connection with the kinetics of conventional slip deformation of solid solution strengthened alloys. The temperature dependence of the activation volume and the "stress equivalency" phenomena are also found to exist in the case of isothermal martensitic nucleation. The present analysis suggests that the individual solute atoms act as barrier to the martensitic interfacial motion.

70. Some Remarks on the Thermodynamical Description of the Hysteretic Behaviour in Martensitic Transformations

Antoni Isalgue, Antoni Amengual, Francisco C. Lovey, J.L. Pelegrina and Vicenc Torra

An elementary thermodynamical treatment for the martensitic transformation in SMA is developed in order to estimate the thermodynamic reliability of the measurements. See, for instance, the entropy production due to the hysteresis width. It is found that the driving force ΔG associated to the changes in the entropy production is coherent with the dislocations creation.

71. The Thermodynamic Properties of the Martensitic Phases in a Cu-Al-Ni Alloy

Clifford M. Friend, Ll. Mafiosa, Jordi Ortin and Antoni Planes

This paper presents the results from a calorimetric study on a Cu-Al-Ni single crystal alloy. The work has used a novel microcalorimeter which is capable of carrying out measurements on samples subjected to uniaxial tensile stress. This device has allowed the direct determination of the enthalpy and entropy changes during both $\beta \rightarrow \gamma'$ and $\beta \rightarrow \beta'$ martensitic transformation. This data has been used to produce a thermodynamic characterisation of the β -phase/martensite σ/T phase equilibria in this alloy.

72. Subloop Behaviour in Thermoelastic Martensitic Transformation

Antoni Amengual, Eduard Cesari and Concepcio Segui

The martensitic transformation in shape memory alloys can proceed through different paths inside the two-phase (β -m) coexistence region due to irreversible processes producing hysteresis. Partial transformation cycles of Cu-based alloys are studied in this work by means of calorimetry and resistance changes. Attention is paid to the uniqueness and to the location of the start temperatures of the forward and reverse partial transformations.

73. Calorimetric Study of the Martensitic Transformation in Cu-Al-Be Shape Memory Alloys

David Rios-Jara, Jordi Ortin, Ll. Manosa, Antoni Planes, S. Belkahlia and Michel Morin

The thermodynamic properties associated with the martensitic transition of a family of composition related Cu-Al-Be alloys have been measured by differential scanning calorimetry. Enthalpy and entropy changes, transformation temperatures, elastic and dissipated energies and changes in specific heat between the austenite and martensite phases have been evaluated. These measurements have shown the entropy change of the transition to be independent on the composition; this finding is in concordance with recent measurements for Cu-Zn-Al alloys.

74. A Simple Mathematical Model of Two-Way Memory Effect

Yefim Ivshin and Thomas J. Pence

A constitutive model for shape memory alloys, which incorporates evolution equations describing phase transitions between austenite and two variants of martensite, is used to model the two-way memory effect. The underlying phase transitions are triggered both mechanically and thermally on the basis of changes in material stability; consequently both stress and temperature are treated as thermodynamical driving forces. A numerical simulation using this model for treating a bar with a nonuniform residual stress distribution demonstrates cyclic length changes upon heating and cooling. This two-way memory behavior stems from the ability of the model to account for asymmetry in transitions between austenite and the two variants of martensite owing to the nonuniform nature of a residual stress distribution.

75. Micromechanical Aspects of the Shape Memory Behaviour

Etienne Patoor, M.O. Bensalah, A. Eberhardt and Marcel Berveiller

In this contribution, some micromechanical aspects of the phase transformation mechanisms in shape memory alloys are presented through the influence of stored energy in the transformation thermodynamical potential. The thermomechanical behaviour of these materials is obtained by minimizing this potential in presence of kinematical constraints. Special attention is given to the internal stress state associated with variant and grain interactions.

76. The Connection of Martensitic and Bainitic Transformations in Carbon and Alloyed Steels

Vadim M. Schastlivtsev, D.A. Mirzayev, A.I. Baev, S.Ye. Karzunov and I.L. Yakovleva

The temperature dependence of phase γ - α transformation on the cooling rate has four steps. Transformation, occurring at II-IV steps, has martensite character. Increasing of carbon or nitrogen contents lowers the temperature of transformations but with different intensity, because of that steps intersect. In proeutectoid steels martensitic transformation has two steps, which differ by the structure of transformation products. Step-wise kinetics of martensitic transformation is explained.

Formation of bainite for chromium and nickel steels is directly connected with martensitic transformation. Growth of crystals of upper bainite is considered as realisation of martensite step II under diffusion control at interphase boundary. Formation of lower bainite is considered as diffusion-controlled growth under constant driving force equal 1250 J/mole, the same as for martensitic transformation. In terms of this supposition and Trivedi-Ivantsov model of growth the quantitative theory of bainite's growth was developed. It predicts two maxima of bainite crystals growth rate. Data on martensitic points for Fe-Cr-N alloys are represented as well.

77. The Crystallography of the $(225)_F$ Martensite Transformation in Steels

Patrick M. Kelly

Despite its success in accounting for the crystallographic features of the $(259)_F$ transformation in steels and of martensitic transformations in numerous other alloy systems, the phenomenological theory has never been able to provide a satisfactory, comprehensive explanation for the ferrous martensite with a $(225)_F$ habit plane. Multiple lattice invariant shears on irrational systems, plastic accommodation, and an arbitrary dilatation parameter have all been introduced in an attempt to explain $(225)_F$ martensite, but without complete success. When the habit plane is right, the orientation relationship is not correct. Getting the orientation relationship right leads to the wrong shape strain direction, and so on. The present paper shows that by systematically varying the lattice invariant shear systems in a double lattice invariant shear version of the theory it is possible to account for ALL the crystallographic features of the $(225)_F$ transformation, including the reported spread in the direction and magnitude of the shape strain. The theoretical predictions are based on the major component of the lattice invariant shear being $(112) [111]_B$ twinning, but additional shears are required, some of which are on irrational deformation systems.

78. The Crystallography of Lath Martensite in Steels

Patrick M. Kelly

From a technological point of view lath martensite is the most important type of martensite formed in steels. Because of the difficulties of obtaining lath martensite in the presence of significant quantities of retained austenite, the experimental data on lath martensite is not as comprehensive as that available for the plate-like (225)_F or (259)_F martensite. Nevertheless sufficient information now exists on the habit plane (close to (557)_F) and the orientation relationship (midway between the Kurdjumow-Sachs and Nishiyama-Wasserman orientation relationships) to test the predictions of the phenomenological theories. Unfortunately, to date, the theoretical predictions have not been entirely consistent with the observations. The present paper shows that with a double lattice invariant shear version of the theory and an appropriate choice of rational shear systems it is possible to account for ALL the known features of the (557)_F lath martensite using the conventional correspondence. The values of the shape strain are larger (0.25-0.45) than in the case of plate martensite, but are not excessive. In addition this theoretical treatment can account for many of the characteristics of bainite and of Widmanstätten ferrite.

79. The Formation of Widmanstätten Cementite Plates in Alloy Steels

F.A. Khalid, M. Farooque and David V. Edmonds

The characteristics of proeutectoid phases and bainite in hypoeutectoid steels are very similar to those in hypereutectoid steels. The features of Widmanstätten cementite precipitation in particular appear identical to Widmanstätten ferrite. There is now support for the view that Widmanstätten ferrite and bainite in hypoeutectoid steels form by a displacive shear mechanism. However, because the residual parent austenite phase in hypoeutectoid steels decomposes to martensite on cooling to room temperature, destroying itself and the transformation interface in the process, complete metallographic observation of the decomposition product is not possible. This is found not to be the case in highly alloyed hypereutectoid steels. A high-Mn hypereutectoid alloy in which Widmanstätten cementite plates can be formed and examined in parent austenite is used in the present investigation to study basic features of morphology, substructure and crystallography, which may help to clarify the formation mechanism. Further deliberate additions of Si and Cu are made to the basic high-Mn alloy composition, and the partitioning and precipitation behaviour of these elements during plate cementite formation is studied in order to give further information on the transformation reaction. The experimental evidence observed is not inconsistent with a displacive mechanism.

80. Acicular Ferrite Formation at Inclusions in Low-Carbon Steels

Peter Krauklis, F.J. Barbaro and Kenneth E. Easterling

Experimental low carbon steels with a high density of inclusions were prepared by hot rolling weld metal deposits, and acicular ferrite formation was studied under simulated and actual weld heat affected zone conditions by means of quantitative metallography and other techniques. It was found that the formation of acicular ferrite is enhanced by the presence of a suitable distribution of inclusions above 0.4 μm in size. The characteristics and amount of acicular ferrite in the microstructure also depend on the prior austenite grain size and cooling rate. The relationship between these factors and welding trial data is considered in terms of a simplified quantitative model, and some thermodynamic implications of acicular ferrite formation are discussed. Observations are also made concerning the mechanism of acicular ferrite formation, which appears to involve intragranular nucleation of primary acicular ferrite plates at inclusions, and subsequent nucleation and growth of smaller secondary acicular ferrite grains.

81. Transformation Kinetics in Superhardenable Steels

John B. Breedis and Lee J. Cuddy

The ability to harden steels to depths greater than would be predicted can result from a number of phenomena such as secondary hardening at the relatively slow cooling rates in the work-piece interior, bainite hardening, or excessively deep martensite formation. The latter phenomenon, the formation of martensite at unusually slow cooling rates, results from extra suppression of the higher-temperature transformation products, and is true superhardenability. A necessary condition for superhardenability in alloy steels with moderate hardenabilities (i.e., steels in which ferrite formation is already suppressed) is the suppression of bainite. Bainite transformation kinetics were examined by means of Jominy tests, isothermal-transformation studies, and controlled-cooling dilatometry coupled with electron microscopy. Results of studies of a series of Cr-Mo steels indicate that by careful control of steel composition, steelmaking practice, and heat treatment, a delay in the isothermal bainite start time by a factor of at least four can be realized. These observations are discussed in terms of the current models of bainite formation.

82. Serrated Plastic Flow in the Martensite of a Low-Carbon Steel

Shoji Okamoto, David K. Matlock and George Krauss

Sheet tensile specimens of a 0.14 pct C-1.48 pct Mn-0.27 pct Si steel were austenitized and quenched to martensite, and tested between room temperature and 150°C at strain rates between $8.3 \times 10^{-4} \text{ s}^{-1}$ and $1.7 \times 10^{-2} \text{ s}^{-1}$. Serrated flow, characterized by localized plastic strain and stress drops, developed after various critical uniform strains were attained in specimens tested above room temperature. An activation energy for the initiation of serrated flow for specimens with a critical strain of 1.8 pct was calculated to be 77 kJ/mol (18 kcal/mol), in good agreement for the diffusion of carbon in bcc iron. The serrated flow is described and the initiation of the serrated flow is attributed to the elimination of mobile dislocations and segregation of carbon atoms to screw dislocations during straining prior to the onset of serrated flow. At the critical strain for serrated flow within the gauge length of a tensile specimen, all mobile dislocations are eliminated and the screw dislocations rendered unable to cross slip, necessitating all subsequent plastic deformation to be accomplished by dislocation multiplication and motion in localized deformation bands.

83. Effects of Magnetic Fields on Martensitic Transformation of Austenitic Fe-Ni and Fe-Ni-Cr Steels at Cryogenic Temperatures

Yasushi Karita, S. Emura, K. Fujita, K. Nagai, K. Ishikawa and Koji Shibata

Effects of magnetic fields up to 8 Tesla (T), applied elastic stress and plastic deformation on martensitic transformation at 4K have been investigated in an Fe-37.4wt%Ni alloy, Type 304L and Type 316LN stainless steels. Isothermal transformation was enhanced with an increase in applied stress and magnetic fields. In Type 304L steel, ϵ' martensite seemed to be induced by an 8T magnetic field from γ phase but not from ϵ martensite. An additional effect of the duplex application of elastic stress and an 8T magnetic field was small. The amount of deformation-induced α' martensite was increased by the magnetic field and was larger in Type 304L steel than in Type 316LN steel. The deformation-induced increment in the amount of α' martensite varied with plastic strain in Type 304L and 316LN steels, which was attributed to the $\epsilon \rightarrow \alpha'$ transformation enhanced by the magnetic field. In an Fe-37wt%Ni alloy, the amount of deformation-induced α' martensite was small and almost constant independent of the amount of plastic strain.

84. Mobility of Coherent Interfaces in Twinned Fe-Ni and Fe-Ni-C Martensites

Kari Martti Ullakko and V.G. Gavriljuk

Tetragonality of the virgin Fe-Ni-C martensite is abnormally high. Using different experimental methods the authors came to the conclusion that coherency at the interphase between martensite and retained austenite is a reason for high tetragonality in Fe-Ni-C martensites. The existence of stresses caused by the coherent bond was proved by neutron diffraction measurements. During heating between 110K-170K the coherency was broken, which was evidenced by a decrease of tetragonality and a new internal friction peak at 150K. Simultaneous electrical resistivity and magnetic susceptibility measurements made it possible to distinguish the partially overlapping effects of reheat martensite formation and the break of coherency. In experiments with deformation in situ during X-ray diffraction and internal friction measurements the evidence was obtained for the coherency at the interphase between martensite and retained austenite as a reason for high tetragonality in Fe-Ni-C martensites. Using a special two-stage cooling method it is possible to lower M_s temperature of the dislocation martensite near 100 K. Measurements made on these samples revealed no coherency effects, which means that the twinned structure is a necessary condition for these effects, not the low M_s temperature itself. However, it is not a sufficient condition, because coherency was not observed in low- M_s Fe-Mn-C martensites although they are twinned. A model in which the ordering of nickel atoms in the initial austenite plays an important role of the coherency effects was proposed.

85. Effect of Hydrostatic Pressure on Isothermal Martensitic Transformation in an Fe-Ni-C Alloy at Low Temperatures

Z.L. Xie, H. Hanninen and Juhani Pietikainen

The effect of hydrostatic pressure on isothermal martensitic transformation has been investigated with an Fe-21.5Ni-0.95C alloy single crystal by electrical resistivity, magnetic susceptibility, X-ray diffraction, optical microscopy and transmission electron microscopy. The martensitic transformation starting temperature is lowered by applied hydrostatic pressure. The isothermal martensitic transformation occurs first as a burst under a critical pressure and is continued by further transformation with decreasing the hydrostatic pressure. The critical pressure, under which the isothermal martensitic transformation starts, changes curvilinearly with decreasing temperature. The morphology of the isothermal martensite formed under hydrostatic pressure is similar to that of athermal martensite. The quantitative calculation of the dependence of the applied hydrostatic pressure on the martensitic transformation starting temperature based on the proposal of Fisher and Turnbull (1953) is in good agreement with the experimental results.

86. Invar Effect on Martensitic Transformations Under Hydrostatic Pressure

Tomoyuki Kakeshita and Ken'ichi Shimizu

Martensitic transformation in an ordered Fe-24.0at%Pt invar alloy with $S = 0.8$ (degree of order) under hydrostatic pressures has been examined in the same way as in a disordered Fe-29.9at%Ni invar alloy previously examined. That is, hydrostatic pressure dependence of transformation temperatures in the Fe-Pt alloy has first been examined by measuring electrical resistivity under hydrostatic pressures up to 1.5GPa. Then, the atomic volume of the austenite and martensite phases and the spontaneous volume magnetostriction, ω_s , of the alloy have been measured by X-ray diffractions at sub-zero temperatures and by magnetization measurements, respectively, under hydrostatic pressures. The hydrostatic pressure dependence of transformation temperature has then been calculated by putting the measured atomic volume and ω_s and the bulk modulus so far known into a new equation previously derived by the authors, and compared with the experimentally examined one. As a result, the calculated dependence was in good agreement with the experimental one in the applied hydrostatic pressure range, as in the previous Fe-29.9at%Ni alloy, and thus the previously proposed effect of spontaneous volume magnetostriction on martensitic transformations and the newly derived equation were confirmed to be appropriate for more wide range of invar alloys.

87. Copper-Based Shape Memory Alloys and Martensitic Transformation

Jan Van Humbeeck, Muthuswamy Chandrasekaran and Rudy Stalmans

The requirements and problems in selecting Cu-based shape memory alloys are reviewed. Alloys in current use and the factors which influence their transformation temperatures are described. The influence of chemical factors, such as composition and the order of state of beta and martensite are explained. The influence of a number of other factors such as non-equilibrium precipitation, grain refining elements, grain size and defects are also reviewed.

Improved physical stability can now be obtained by proper thermomechanical processing and by alloying other elements such as Ni, Mn. Better mechanical properties are obtained by the addition of grain refining precipitate forming elements (B, Co, Ti, Zr), in combination with proper thermomechanical processing.

One should however take into account that the above mentioned instabilities and the solutions to avoid them have a great influence on the martensitic transformation characteristics and thus on the global shape memory behaviour too. In addition, some important new findings about the two way shape memory effect in Cu-Zn-Al alloys will also be discussed.

88. Modelisation of the Influence of Order-Disorder State on Hysteresis of Martensitic Transformation in a Cu-Zn-Al-Ni Shape Memory Alloy

Laurent Buffard, Pierre Charbonnier, A. Delon, C. Roucau, J. Jaud and Bernard Dubois

A modelisation of the influence of microstructural parameters on transformation temperatures in a Cu-Zn-Al alloy leads to a better mastery of the hysteresis. The ordering is one of the most important of these parameters.

We study the long distance ordering A2-B2 and B2-L21 in a Cu25%wtZn9%wtAl alloy by transmission electron microscopy and X-ray diffraction. The characteristic transformation temperatures are determined by differential scanning calorimetry and resistivity.

For a long time these temperatures have been correlated with ordering of the alloy and we put in evidence the influence of the size of ordered domains.

89. Parameter Determination for the Thermodynamic Model of Shape Memory Cu-Zn-Al Polycrystal by Resistivity and Infra-Red Thermography

Cecile Rogueda, Christian LExcellent, Bogdan Raniecki and A. Chrysochoos

The possible simplest thermodynamic model of pseudoelasticity has been developed. It approximately accounts for the basic features of the behaviour of shape memory alloys at temperature range $T > A_f$. Two entirely independent techniques are applied during loading-unloading tensile tests to determine the whole set of model parameters for Cu Zn Al polycrystals, i.e., resistivity and infrared thermography measurements.

90. The Effect of Load-Cycling on the Psuedoelastic Behavior in a Polycrystalline Cu-Zn-Al Shape Memory Alloy

Noboru Ono

Polycrystal specimens of a Cu-14.3(at.) % Zn-17.0 % Al-0.14 % B alloy with $M_s=270K$ and grain size about $120\mu m$ were subjected to pseudoelastic cycling at $40K$ above M_s with constant plastic strain ranges until the pseudoelastic loop had become nearly stable. The pseudoelastic behavior of these specimens, as well as virgin specimens, was examined in the temperature range from 5 to $40K$ above M_s where the change in electric resistivity with strain was monitored. The yield stress for the virgin specimens was in fair agreement with the prediction made through the modified Taylor model assuming the formation of β_1' -martensite but that in the higher temperature range was far smaller than the expectation. In the cycled specimens, the temperature dependence of yield stress was linear in the whole test temperature range but smaller in comparison with that for the virgin specimens. Corresponding to this, the resistivity-plastic strain relation showed small but definite dependence on test tempretature in the virgin specimens, but it did not in the cycled specimens. These results suggests that the contents of martensites changes with temperature in virgin specimen. The cycled specimens are so trained that they are the same independent of temperature.

91. Ductility and TWME Associated With Stress-Induced Martensite Stability Produced by Deformation of Cu-Al-Ni Alloys

Maria A. Morris and T. Lipe

A Cu-Al-Ni alloy with manganese and boron additions has been used to induce a two way memory effect (TWME) by thermal cycling under constant load. The total TWME obtained has been related to the strain produced by the internal stresses created by the formation of stress-induced martensite that oppose the applied stress. The existence of these internal stresses in the trained material has been confirmed by the larger A_s-A_f and M_s-M_f temperature intervals measured during the transformation.

92. Prediction of Reversion Stress of Shape Memory Alloys During Martensitic Transformation

Li Lu, Etienne Aernoudt, Patrick Wollants, Jan Van Humbeeck and Luc Delaey

Reversion stresses are generated in constrained shape memory alloys (SMA), which are heated above A_s after having been deformed and unloaded at a temperature below M_s . The reversion stress increases with increasing heating temperature. How the reversion stress changes on heating can be predicted by using a multi-element displacement model[1]. According to this model the maximum reversion stress σ_r equals σ^{P-M} at which the martensitic transformation proceeds at the corresponding strain. The reversion stress is not affected by the strain level once the pre-loading strain exceeds a certain value. The predictions are in good agreement with Madangopal's observations [2].

93. The Two-Way Memory Effect of a Cu-Al-Be Alloy:

General Characteristics and Ageing

H. Flores Zuniga, S. Belkahla, Francisco C. Lovey and Gerard Guenin

The ability of the Cu-Al-Be alloy to exhibit the two way memory effect (TWME) is demonstrated. The obtained results concerning the strain amplitude, the dependence with the training stress is similar to those of Cu-Zn-Al and Cu-Al-Ni alloys. A remarkable thermal stability of this TWME is demonstrated and is quantitatively measured at different temperatures ranging from 150°C to 300°C. The thermal decrease of TWME is attributed to localized precipitation on training dislocations which occurs well before the generalized precipitation leading to the martensitic transformation degradation.

94. Acoustic Emission Study of Thermoelastic Martensitic Transformation in Cu-Al-Ni Alloys

Katsuro Oda, I. Takahashi, S. Tamaki, Kazuhiro Otsuka and Tetsuro Suzuki

The thermoelastic martensitic transformation between the parent (β_1) phase and martensite (γ_1') phase of Cu-13.7wt%Al-4.0wt%Ni and Cu-14.0wt%Al-4.0wt%Ni single crystals were investigated by acoustic emission (AE) measurements. When cooling the solution treated specimen, weak AEs were observed at temperatures 20-30K above the M_s temperatures. In order to clarify whether these emissions are due to transformations from β_1 to β_1' phase or to precursor phenomena for the martensitic transformation, AE measurements were performed on the tempered specimens in which no transformation from β_1 phase to γ_1' phase takes place. No AEs were observed above the M_s temperatures. From these results, it is concluded that these AEs are due to the β_1 to β_1' transformation, and consequently it is presumed that no precursor phenomena exist for the Cu-Al-Ni alloy.

95. The Reverse Martensitic Transformation in Cu-Al-Ni Shape Memory Alloys

Aaron D. Cockerill, Noel F. Kennon and Druce P. Dunne

In situ optical microscopical investigations were carried out to observe the reverse γ_1 martensitic transformation in Cu-Al-Ni shape memory alloys. The most significant of these observations showed that the path of the reverse transformation frequently differed from the path for the forward transformation and that, the reverse transformation always regenerated the original parent phase. An effective method for elevated temperature polishing of the alloys was developed to facilitate the study.

96. Shape Memory Characteristics in P/M Cu-Al-Mn-Ni Alloys

Norihiko Nakanishi, Toshihiko Shigematsu, N. Machida, K. Ueda, H. Tanaka, T. Inaba and O. Iwatsu

Shape memory characters with ferromagnetic property were studied in Cu-Al-Mn-Ni alloys fabricated by the powder metallurgical method. The results obtained are: (i) M_s , M_f , A_s and A_f behaved linearly against the aging time at 433 K and the increased range was up to about 15 K. (ii) A simultaneous measurement was made between the stress-strain relation and acoustic emission (AE) counts. (iii) The critical temperature corresponding to a reaction, DO₃-rich phase + L2₁-rich phase \rightarrow a single phase, was moved from 525 to 540 K associated with the increase in aging time at 433 K and a gradual increase in the enthalpy value was observed. (iv) Shape memory behavior in the stress-strain curve was confirmed.

97. **Training of Copper Based Shape Memory Alloys**
Rudy Stalmans, Jan Van Humbeeck and Luc Delaey

The development of the two way memory effect (TWME) during training is accompanied by concomitant effects such as residual strains of the hot shape (either due to plastic deformation or due to local martensite stabilization), and shifts of the transformation temperatures. In the present study, the relationships between the training procedures, the TWME and the concomitant effects are quantitatively determined. Although plastic deformation and local martensite stabilization are frequently mentioned as necessary prerequisites to the TWME, the results show that those effects have to be considered as side-effects of "overtraining". By the proper choice of the training parameters those side-effects can be minimized. It was also found that the stability of the TWME increases with the number of training cycles, that the TWME can withstand considerable forces during cooling, and that thermal cycling, when preceding the training, diminishes the maximum attainable TWME. Those results indicate that transformation cycling stabilizes a martensite formation path. In contrast with the path stabilized by thermal cycling, the martensite formation path stabilized by thermomechanical cycling (training) corresponds with a macroscopic shape change and thus a TWME. This mechanism of path stabilization suggests that the TWME is directly determined by the shape change induced during training. This suggestion was confirmed by experimental results for several kinds of training procedures.

98. **Effect of Thermal Cycling on Transformation Behavior of Rapidly Solidified Cu-Al-Ni-Cr Shape Memory Alloy Ribbons**
Hong-Show Koo

In academic terminology, shape memory effect which existed in certain specialty alloys is a reversible thermoelastic martensitic transformation. The occurrence of this transformation is activated by applying thermal energy. Thermal cycling is a deserved attention problem for practical device application. The effect of thermal cycling on the shape memory behavior and microstructure of rapidly solidified Cu-Al-Ni-Cr alloy have been examined by means of the four-probe resistivity measurement and scanning and transmission electron microscope. Cu-11.7 wt%Al-3.78wt%Ni-0.15wt%Cr alloy ribbon was produced by the meltspinning technique. The width and thickness of the shape memory ribbons are about 15 mm and 65 μm . It was found that as the number of thermal cycling increased, the transformation temperature of M_s and M_f shifted to higher temperature and the temperature of A_s and A_f decreased to the lower temperature range. On the other hand, when the shape memory alloy ribbon was thermally cycled between 77 and 350K, the amount of dislocation in the alloy ribbon increased with increasing the number of thermal cycles.

99. **The Influence of Yttrium Additive on Shape Memory Behavior of Cu-Al-Ni Alloy**
Fu-Hsing Chen

Up to the present time, there have been three major types of copper-based shape memory alloy: Cu-Zn-Al, Cu-Al-Ni and their derivatives such as CuZnAlX or CuAlNiX (X: Ti, Zr, Mn, V, B etc.) for practical application. As compared with the nickel-titanium shape memory alloys, copper-based shape memory alloys exhibit feasible processing, excellent workability and economy, but its strength, anti-corrosion and fatigue is not so good that some of improvements for the mechanical properties must be performed. In general, some characteristics, strain-memory recovery, strength and resistance to thermal and corrosion, of the CuAlNi alloy have been confirmed to be better than the CuZnAl alloy. The factors which effected the mechanical properties of copper-based shape memory alloys are dominately the intrinsic properties of high elastic anisotropy and its large grain size. In this paper, we studied the effect of yttrium additive and heat treatment on the mechanical and transformation behavior of Cu-Al-Ni alloy. It was shown that the grain size decreased with increasing the addition of yttrium. Then, the transformation temperature slightly varied with increasing the content of dopant and aging treatment. The magnitude of strength and workability of quaternary CuAlNiY alloy is more than the ternary CuAlNi alloy. The crystal morphology and microstructure of CuAlNi and CuAlNiY alloys were also investigated.

100. Microstructural Development Related to Phonon Anomalies Leading to Displacive Transformations in Metallic Phases

Lee Tanner, Dominique Schryvers, Simon C. Moss, J.D. Axe, C. Marvin Wayman, Steven M. Shapiro, Y. Noda, Y. Yamada, Adam Schwartz and M. Wall

The phonons of crystalline phases (pure metal and alloyed) that undergo first-order displacive transformations on cooling exhibit anomalously low energies along those branch(es) related to the atomic displacements of the ensuing structural changes. Present at elevated temperature equilibrium, these effects become more pronounced as $T \rightarrow T_c$ (or M_s), the bulk transformation temperature, though the "softening" is never complete at T_c . The coupling between the softened phonons and local parent lattice distortions (defects) sets the stage for heterogeneous nucleation [Phys. Rev. B 44, 9301 (1991); Ultramicroscopy, 37, 241(1990)]. HRTEM and neutron scattering observations of Ni-Al, Ti-Ni-Fe, Ti-Pd-Fe, Ti-Pd-Cr, Ti-Mo and Zr-Nb transformations illustrate the foregoing and will be discussed in terms of nonclassical heterogeneous nucleation theory.

101. Heterophase Fluctuations and Exact Thermodynamics of a First-Order Structural Phase Transformation

James R. Morris and Robert J. Gooding

It has been well established that for some martensitic transformations (e.g., $bcc \rightarrow hcp$ in the Group IV metals) the dominant contribution to the latent heat at a first-order structural transformation is due to the change of phonon entropy. This change is due to the increase of elastic constants below the transformation temperature, i.e., from a β -cubic structure with a low c' elastic constant to the stiffer martensitic phase. We have studied the exact thermodynamics of a model which mimics these systems. Except for temperatures very near the transformation temperature, the system is described extremely accurately by a renormalized harmonic theory. The high-temperature phase is stabilized by the high phonon entropy owing to low-lying phonon branches. We show that for a defect-free system in equilibrium, heterophase fluctuations can only occur in small crystallites, in agreement with experiments in high-purity bulk samples. Dynamic structure factors calculated using molecular dynamics simulations of the model show sharp phonon peaks, as well as a central peak. Furthermore, in the coexistence regime, we see peaks corresponding to both high- and low-temperature phase phonons, in agreement with recent neutron scattering experiments on $Ni_{62.5}Al_{37.5}$.

102. A Thermodynamical Consideration of the Tweed Structure of Martensite

Francisco Eichi Fujita

The tweed structure, which appears in various materials as precursory electron microscopic image in the temperature range of some tens degrees above the M_s temperature of thermoelastic martensite transformation, is theoretically treated by a statistical thermodynamics taking account of the local medium range order structure. The result of calculation shows that the tweed structure rising from the martensite embryos of a few nanometer size can appear far above the M_s temperature and that the size and distribution of small static lattice distortions in and around the embryos revealed by ordinary electron microscopy, high resolution electron microscopy and X-ray diffraction can well be explained. The theory also shows that the precursor phenomenon in the thermoelastic martensite transformation is quite analogous in some respects to the medium range order clustering, that is the crystalline embryo formation, in liquid above the solidification temperature.

103. Pretransformation Twinning in Indium Based Alloys

Manfred Wunig

104. Modulated Structure and Martensitic Transformation in Fe-28.10 Ni-5.19 Al-0.36 C Alloy

J.S. Lee and Woong-Kil Choo

The tweed microstructure changes of Fe-28.10wt%Ni-5.19wt%Al-0.36wt%C alloy have been investigated after aging at 973K. Both the transmission electron and the high resolution microscopes have been employed as investigation tools. The development of the diffuse scattering in diffraction patterns and the accompanying modulated images above the martensitic starting temperature is intimately related to the premartensitic phenomena.

105. The Origin of Martensitic Transition in TiNi

Frederick E. Wang

It was shown in 1965 [1] that the unique martensitic transition with 'memory' effect occurring in TiNi is expandable linearly into TiCo and TiFe. Further, it was demonstrated through X-ray that this linear relationship for the 3-d transition elements existing in TiNi (Co, Fe) actually extend into 4-d [2] and 5-d [3] series of elements such as Zr-Ru (Rh, Pd) and Hf-Os (Ir, Pt). We show here that these relationships can all be reconciled by considering the d-orbital electronic configurations in these elements. In this manner, the fundamental cause for the unique martensitic transition in TiNi (Nitinol) may be understood.

106. Factors Determining B2 Phase Stability in Ti-Based Compounds

Svetlana A. Shabalovskaya

Binary or quasi-binary compounds TiMe (where Me stands for Fe, Co, Ni, Pd, Pt and Au, or Ni with one of the above metals) with the B2 (CsCl) structure are known to undergo martensitic transformation of two types: B2-B19'(B19) and B2-R, with an intermediate precursor charge-density-wave incommensurate phase IS. Analysis of both experimental and theoretical data enabled us to establish empirical relations between the transformation temperatures: M_s (B2-B19) and fundamental parameters of both electronic and crystal structures of the compound, such as the lattice parameters, the shift of the d-band in the compound with respect to the pure Me, the compounds d-band width, the Ti site-projected d-densities of states at the Fermi level in the compound and BCC Ti, and the temperature of $\beta - \alpha$ allotropic transformation in pure Ti. This correlation is based on localization of the Me d-bands in the compounds. As a result the Me-Me interaction becomes less important, and the interatomic interaction are controlled by d-d (Ti-Ti) and p-d (Me-Ti) bonds. The Fermi level are dominated by the Ti d-states, which control the lattice dynamic as well. The latter is also reflected in closeness of the C' moduli and similar values of the phonon frequencies in Ti and TiNi compound.

107. The Structure Factors, Charge Density and Debye-Waller Factors of Martensitic Ni-Rich β NiAl

Alan G. Fox and M.A. Tabbernor

The low-angle X-ray structure factors and Debye-Waller factors of a martensitic Ni-37.5 at.% Al alloy were accurately measured by the critical voltage technique in high energy electron diffraction at various temperatures. These measurements show that there is a large static contribution to the mean-square displacements of these alloys from both Ni antistructure atom defects and from the 'atomic shuffles' associated with the ω phase. In addition, the Debye-Waller factors of this alloy vary very slowly with temperature as many phonons have been trapped by the antistructure atom defects. The low-angle structure factors appear to be very little affected by changes in the charge density due to alloying except for the {200} reflections which are reduced by about 2%. A Fourier analysis of these reduced {200} structure factors indicated that bonding in this alloy arises as a result of depletion of electrons from both the nickel and aluminum atomic sites with large amounts of electron build-up in nearest-neighbor (n.n.) $\langle 111 \rangle$ directions. This suggests that bonding in this alloy is essentially covalent. Further analysis indicated large amounts of depletion of electrons between second n.n. atoms and thus significant ionic repulsion in $\langle 100 \rangle$ directions. These results show that the crystal potential in $\langle 111 \rangle$ is 'hard' and in $\langle 100 \rangle$ 'soft'; this explains why the anisotropy factor, $2C_{44}/(C_{11} - C_{12})$, for this alloy is very large (about 8.0) and the shear constant, $(C_{11} - C_{12})/2$, very small (near zero as M_s is approached). These results possibly represent the first experimental corroboration of the hypothesis that soft phonon modes associated with $[01\bar{1}](011)$ shear waves have their origins in ionic repulsion effects of the sort first proposed by Zener in 1947.

108. NMR Study of the Martensitic Transformation in Ni-Al and Ag-Cd Alloys

Silvia Rubini, C. Dimitropoulos, F. Borsa, D.R. Torgeson and Rolf Gotthardt

^{27}Al Nuclear magnetic resonance and relaxation measurements are presented for Ni-Al alloys of different composition (from 37at.% Al to 38at.% Al) in samples of different particle sizes and subjected to different thermomechanical treatment. The ^{27}Al Knight shift changes by about 10% on going from the austenite to the martensite. In the temperature interval between M_s and M_f the NMR spectrum is analyzed in terms of the superposition of two resonance lines belonging to the two coexisting phases. The temperature dependence of the ^{27}Al spin lattice relaxation rate follows a Korringa-like behavior. Measurements of magnetic susceptibility and of low temperature specific heat are also presented and analyzed together with the NMR results to gain information about the electronic structure of the alloy and its changes at the martensitic transformation. An analogous investigation is presented based on $^{113,111}\text{Cd}$ NMR in a Ag-47at.% Cd alloy. The present results in the binary alloys are discussed and compared with the previous investigation in a ternary Cu-Zn-Al alloy [1]

[1] S. Rubini, C. Dimitropoulos, R. Gotthardt and F. Borsa, Phys. Rev. B 44, Aug. 91

109. Neutron Scattering Studies of the Structures and Lattice Dynamics of the Alkali Metals

Harold G. Smith, R. Berliner and J. Trivisonno

The crystal structures, phonon behavior, and pre-martensitic behavior of Li, Na, K, Rb, and Cs as a function of temperature and pressure (Li, Na, Rb, and Cs) are reviewed. Li has been shown to partially transform to the 9R (Sm-type) structure in the vicinity of 75 K and then partially to fcc on annealing. Its T_c increases with applied pressure. Na, on the other hand, partially transforms to a mixture of 9R and nearly hexagonal R-polytypes, which approach hcp on annealing. Its T_c is rapidly suppressed by application of modest pressures. No martensitic or pre-martensitic phenomenon, or phonon anomaly, has been observed in K down to 5 K. Also, a search for CDWs in the vicinity of (110) has been inconclusive. Similar negative results have been obtained for Rb.

110A. Pre-Martensite Observations Using Thermal Expansion

Trevor R. Finlayson and T.F. Smith

Measurement of the thermal expansion coefficient using capacitance dilatometry has proved to be a most convenient method with which to observe pre-transformation phenomena. In this paper a summary of results found for single-crystals of In-Tl and Ni-Al, and for polycrystalline A15-structure compounds, V_3Si , Nb_3Sn and V_3Ge are described. Anisotropies in expansions within the cubic phases for these materials are interpreted as pre-transformation departures from cubic symmetry which are influenced by stresses, either applied externally or, as are the cases for V_3Si and Nb_3Sn , present as residual stresses in the materials. A small degree of anisotropy found for non-transforming V_3Ge , indicates some departure from cubic symmetry on a microscopic scale.

110. Dynamic and Static Precursors of Displacive Transformations

Winfried Petry

In spite of the dominating first-order character of martensitic transformations recent neutron scattering experiments show a variety of precursor phenomena of static, as well as dynamic nature. In *pure* metals like those of Group 3 and 4, viz., Sc, Y, La, Ti, Zr and Hf, the bcc parent phase is characterized by a valley of low-energy phonons, the displacements of which correspond to the very ones needed for the transformations into the low-temperature or high-pressure product phases. In *alloys*, e.g. $Ni(1-x)Ti_x$ ($x=0.5$) and $Ni(1-x)Al_x$ ($x = 0.32-0.40$), similar transformation-related low-energy or large-amplitude phonons are found as well. In addition, and *different* from the pure elements, increasing elastic diffuse scattering is observed in the alloys on approaching the transformation from high temperatures. This diffuse scattering is located in Q-space where the soft phonons are observed and is directly related to the product phase structure. Information that this elastic precursor scattering is possibly defect-driven comes from experiments with dilute alloys of Zr with solutes of Co, Nb, etc. A review of recent neutrons scattering experiments will be presented: i) emphasizing the role of low-energy phonons in stabilizing the parent phase by *increasing entropy*, ii) revealing the importance of low-energy phonons at *large q* in driving the transformation, and iii) demonstrating the role of defects as centers of *strained domains* which are embryos of product-like distortions within the parent phase. Finally, a comparison with new first-principle calculations of the phonon softening at martensitic transformations will be presented.

111. Martensitic Transformations in Ceramics

Barry C. Muddle and Geoffrey R. Hugo

Although the occurrence of martensitic transformations in ceramic materials has been well recognised for many years, it is only in the last decade that they have achieved prominence. This recent interest has arisen primarily from the recognition of the technological importance of the stress-activated tetragonal (t) to monoclinic (m) transformation in zirconia-based ceramics and its role in affording useful plasticity and toughness to an important range of engineering ceramics. Attention has also been drawn to suggestions that the twinned orthorhombic superconducting phase in the high T_c superconductor $YBa_2Cu_3O_{7-x}$ may be the product of a martensitic transformation. The present review will thus focus on these systems, beginning with an assessment of developments in understanding of the tetragonal to monoclinic transformation in zirconia and zirconia-containing alloys. The applicability of the crystallographic theory to the t to m transformation will be examined critically and the results interpreted in terms of their significance for models of transformation plasticity and transformation toughening. Progress in the investigation of other ceramic systems with potential for transformation toughening through stress-activated martensitic transformation will also be discussed. The characteristics and crystallography of the tetragonal to orthorhombic transformation in the superconducting oxide $YBa_2Cu_3O_{7-x}$ will be critically assessed and evaluated in terms of their compatibility with those criteria normally considered indicative of a martensitic transformation.

112. Neutron Diffraction Study of the Martensitic Monoclinic-to-Tetragonal Phase Transformation in Zirconia ZrO_2

Friedrich Frey and H. Boysen

The importance of structure refinements in the study of martensitic transformations is emphasized. Corresponding neutron powder measurements were evaluated for the m-t and the t-m transformations in pure ZrO_2 . From the evolution of the structural parameters with temperature we conclude a displacive precursor of the martensitic m-t transformation with likewise different lattice correspondence. An equivalent two-stage process is absent in the reverse direction. The transformation intervals in the forward and reverse direction are 600 and 150 K, respectively. Overall microstrains are present in both phases with a minimum in the coexistence region. These are traced back to subgrain structures consistent with disordering in both phases. Remarkable macrostraining was only observed during the m-t transition.

113. Application of the Crystallographic Theory to the Tetragonal-to-Monoclinic Transformation in Ceria-Zirconia

Geoffrey R. Hugo and Barry C. Muddle

The single shear crystallographic theory has been applied to the tetragonal (t) \rightarrow monoclinic (m) transformation in ZrO_2 -12 mole% CeO_2 using a lattice correspondence (LCB) for which $c_t \rightarrow b_m$. The solutions to the theory are characterised by very small magnitudes (0.003-0.006) of lattice invariant strain (LIS) and almost identical predictions of habit plane and orientation relationship for a range of possible LIS systems. The solutions for the habit planes cluster about rational poles of the form $(130)_t$ and $(11,1,0)_t$ and are consistent with those observed experimentally. The predicted orientation relationships are significantly closer to the exact rational relationships reported than those predicted for a previous application of the crystallographic theory to t \rightarrow m transformation in a ZrO_2 -MgO alloy. The very small magnitudes of LIS predicted for the present system suggest the possibility that the LIS could be accommodated elastically, rather than by slip or twinning, and the implications of this possibility are discussed.

114. The Diffusionless Cubic-to-Tetragonal Transition in ZrO_2 -R₂O₃ Systems (R: Rare Earths)

Taketa Sakuma, T. Seki and T. Yamamoto

It has originally been proposed that the diffusionless cubic-to-tetragonal (c-t) transition in zirconia is of martensitic type. Present authors' group has later pointed out from microstructural examinations in ZrO_2 -Y₂O₃ that this transition is not a simple martensitic transformation as has generally been accepted, but has a nature of second-order phase transition. The nature of this transition, however, is still in controversy. In this study, the microstructure formed by this transition were examined in several ZrO_2 -R₂O₃, where R is trivalent cations of rare earths. The principle interest was to survey whether or not the microstructural features and the nature of diffusionless c-t transition are different with the type of trivalent cations. This transition accompanied the initial generation of domain structures and subsequent twin formation in some ZrO_2 -R₂O₃ as well as ZrO_2 -Y₂O₃. On the basis of microstructural examinations, the nature of this transition will be discussed in this paper. The discussion will also be made on the relationship between the nature of this transition and the c-t equilibrium.

115. Effect of Grain Size on the Martensitic Transformation in CeO_2 -TZP (Tetragonal Zirconia Polycrystals)

Motozo Hayakawa, H. Shinmen and Muneo Oka

Grain size dependence of martensitic transformation was studied using 12mol% CeO_2 -TZP (Tetragonal Zirconia Polycrystals) with the grain sizes between 1.3 and 14 μm . In addition to the usual M_s and A_s , M_s^0 (the critical temperature where transformation yielding starts) were measured through bending tests. The stability of the parent phase as measured by these characteristic temperatures decreased significantly with the increase of grain size. Apart from the characteristic temperatures, the most significant change with the increase of grain size was a decrease in the hardness. Correlation between the average strength and the stability against the martensitic transformation was suggested.

116. Morphology and Crystallography of Martensitic Product in a Ceria-Zirconia Alloy

Xiuhua Zheng and Ron Stevens

The martensitic transformation in tetragonal grains in a ceria-zirconia alloy has been studied using transmission electron microscopy. Two distinct morphologies of monoclinic product and the corresponding orientation relationships between the tetragonal and monoclinic phases are observed in the transformed grains. The first morphology is such that comprising parallel-sided monoclinic plates which are twin related on $(110)_m$. In this case, the transformation occurs by the alternative re-nucleation and growth of two twin-related variants parallel to a $(110)_m$ twinning plane. The orientation relationship between the two phases is given by $(110)_t // (110)_m$ and $[1\bar{1}0]_t // [1\bar{1}0]_m$. In the second case, the monoclinic phase takes the form of needle-like plates which form by single plate growth but in a twinned relationship. The monoclinic variants with approximate $(401)_t$ and $(40\bar{1})_t$ habit planes have a $(100)_m$ conjunction twinning plane. The orientation relationship obtained is $(100)_t // (100)_m$ and $[010]_t // [010]_m$. The influence of the tetragonal grain size on the martensitic transformation in this material is briefly discussed.

117. Transformation Mechanisms in Dicalcium Silicate and in Other Ceramics

Y.J. Kim and Waltraud M. Kriven

Five polymorphs have been reported for the pure dicalcium silicate (Ca_2SiO_4)--- α , α'_H , α'_L , β and γ . From structural and microstructural characterizations of polycrystalline samples of pure Ca_2SiO_4 , Ba-stabilized Ca_2SiO_4 and Ca_2SiO_4 -dispersed in ceramic matrices, transformation mechanisms of these polymorphs were studied by XRD and TEM. Throughout the whole transformation sequence, a symmetry element of 2/m were conserved. The $\alpha \rightarrow \alpha'_H$ (Pmcn?) transformation generated three rotation-related domains, which suggested the existence of a 6/m symmetry element for α , with a space group of $\text{P6}_3/\text{mmc}$ as among three possible space groups ($\text{P6}_3/\text{mmc}$, $\text{P6}_3\text{mc}$ or P3m1). In this case, the $\alpha \rightarrow \alpha'_H$ transformation is ferroelastic. The $\alpha'_H \rightarrow \alpha'_L$ (Pmcn?) transformation is known to be related to the ordering of Ca^{2+} ions or rigid SiO_4 tetrahedra. Two superlattice structures of α'_L have been observed in this study: the $x2a, 2b$ -type and the $x3c$ -type. The $\alpha'_L \rightarrow \beta$ ($\text{P2}_1/\text{n}$) transformation also generated two twinned domains, (on $\{100\}$ and $\{001\}$), and is also possibly ferroelastic. The $\beta \rightarrow \gamma$ (Pcnn) transformation, accompanied by a large volume increase ($\sim 12\%$), was stress induced. The strains built into β by the previous ferroelastic transformations, as well as the strong repulsive forces between Si^{4+} and Ca^{2+} ions are suggested to be the major driving forces for the $\beta \rightarrow \gamma$ transformation.

118. Analysis of Creep-in-Tension Data on Mg-PSZ

W.J. Batchelor and Trevor R. Finlayson

Mg-PSZ has been observed to creep at room temperature in uniaxial tension. The measured plastic deformation contains contributions from both phase transformation and microcracking, the latter being in evidence through a reduction in Young's modulus. A method is outlined which enables the measured strain to be separated into contributions from phase transformation and microcracking. Comparison is made with the predictions of the shear dilatation model of Chen and Reyes-Morel (1986) for plastic deformation. Relatively poor agreement with this model, has prompted the proposal of an alternative, based on the crystallography of the tetragonal \rightarrow monoclinic transformation given by Muddle and Hannink (1986), and extended to include some stress-induced, tetragonal \rightarrow orthorhombic transformation.

119. Martensitic Transformation in Twinned Tetragonal ZrO₂ Precipitates in Y₂O₃ Partially-Stabilized ZrO₂ (Y-PSZ) Single Crystals

Julian Martinez-Fernandez, M. Jimenez-Melondo, A. Dominguez-Rodriguez and Arthur H. Heuer

Mosaic-like monoclinic ZrO₂ particles have been found by TEM in 3.4 m/o Y₂O₃ partially-stabilized ZrO₂ (Y-PSZ) single crystals aged for 150 hours at 1600 °C. These particles transformed from tetragonal symmetry during TEM examination; the parent phase existed as internally-twinned precipitates which had formed during aging. Those monoclinic particles show {100} and {110} transformation twins, and the twin variants have uniform thickness. The lattice correspondence and transformation modes operating are discussed.

120. Crystallography of the Cubic to Tetragonal Transformation in Lead Titanate Single Crystals

Chen-Chia Chou, Kunio Wakasa and C. Marvin Wayman

The cubic to tetragonal (C/T) transformation of flux-grown lead titanate single crystals has been investigated using optical microscopy (OM), transmission electron microscopy (TEM) and electron and X-ray diffraction. Theoretical calculations on transformation characteristics based upon the martensitic crystallographic theory of Bowles and Mackenzie were also carried out. Habit plane between the parent and the product phases were studied by "freezing" the two phases during transformation using in-situ hot-stage OM. The habit planes vary within a certain range. Not only different specimens show this real variation, but also the same specimen under different transformations follows this, indicating the importance of local arrangements near the habit plane interfaces. With only a minute change of lattice parameters in calculations, it is shown that experimental data appear to be consistent with calculated results, if one considers lattice parameter variation. The results imply that the martensitic crystallographic theory applies. Discussions on the microstructural features as well as previous work on perovskite materials are presented.

121. The Alpha to Beta Transformation in Stoichiometric Nickel Sulfide

B. Kim, Chen-Chia Chou and C. Marvin Wayman

The forward (alpha to beta) and reverse transformation characteristics of NiS have been studied using the hot-stage x-ray diffraction, hot stage optical microscopy, dilatometry, and electrical resistivity measurements. The hot-stage x-ray diffraction patterns confirmed the structural change from beta to alpha during the heating cycle and alpha to beta during the cooling cycle. The structural change of NiS was observed as surface relief through hot stage optical microscopy. Both the dilatometry and resistivity measurements revealed a large hysteresis, spanning a temperature range of approximately 200° C. The shape of the hysteresis resembled those found in martensitic materials and shape memory alloys. Also, from the dilatometry measurements, the volume change associated with the transformation was calculated to be approximately 4.7%. All experimental results appear to fit the characteristics of a martensitic transformation.

122. Effect of Stress on Bainitic Transformation in Fe-Si-Mn-C Steel

Akihiro Matsuzaki, Harshad K.D.H. Bhadeshia and H. Harada

The effect of uniaxial stress on bainitic transformation is investigated in a Fe-C-Si-Mn steel. A technique has been developed to simultaneously monitor the longitudinal and transverse strains that arise during the isothermal formation of bainitic ferrite. The measurement of more than one strain has permitted the deconvolution of the volume change due to bainite transformation, and transformation plasticity components thereby permitting the crystallographic or stress-induced anisotropy of the microstructure to be evaluated. The experiments have been conducted using a silicon-rich steel in which bainitic reaction is not accompanied by the formation of carbides, which can in principle complicate the interpretation of data. It is demonstrated that the transformation behaviour is strongly affected by compressive stress. It is also observed that bainite microstructure of the steel transformed under stress is much more strongly aligned than that transformed without stress, which implies that the stress can enhance and/or suppress the formation of specific crystallographic variants. These results are discussed in terms of the thermodynamics and mechanism of the bainite reaction in steels.

123. Effects of Elastic Stress on Bainitic Transformation in a 0.4C-2Mo Steel
Koji Shibata, Toshifumi Hori, K. Asakura and A. Ohmori

Effects of elastic tensile and compressive stresses on B_s of upper bainite were examined and compared with effects on $\gamma \rightarrow \alpha$ transformation start temperature (F_s) and with expected effects on M_s using a 0.4C-0.5Mn-2Mo-0.0008B steel. The B_s and F_s were measured during cooling at 10°C/min and at 2°C/min, respectively, in a furnace attached to a single specimen double lever creep testing machine. Tensile and compressive stresses of 4kgf/mm² and 2kgf/mm² were applied on specimens from 650°C for B_s measurements and from 770°C for F_s measurements during cooling, respectively. Effects of the stresses on B_s and F_s were examined by dilatometry and optical microscopy. Although it was observed that the tensile stress increased B_s , a clear increase in B_s by the compressive stress has not been detected. From the viewpoint of thinking that the nucleation of bainite is martensitic, this fact is difficult to be interpreted at the present stage. Effects of the stresses on F_s were similar to those on B_s . However, a fairly large creep deformation was measured at 800°C under 2kgf/mm². Hence, such a creep deformation or certain accompanying phenomena might affect the $\gamma \rightarrow \alpha$ transformation.

124. Upper Bainite Transformation in an Fe-2%Si-0.6%C Alloy
Kaneaki Tsuzaki, Aki Kodai and Tadashi Maki

In order to clarify the growth mechanism of the ferritic component of bainite, the bainite transformation during isothermal holding at 723K in an Fe-2.01%Si-0.59%C alloy (mass%) has been investigated by means of transmission electron microscopy. Carbide-free bainitic ferrite forms in the initial stage of transformation. Laths of the bainitic ferrite are in parallel one another and separated by carbon-enriched retained austenite. Both the bainitic ferrite and retained austenite involve a large number of dislocations. The orientation of the bainitic ferrite laths is identical within a bainitic packet consisting of parallel laths. The lath width does not change during the subsequent isothermal holding. In the later stage of transformation, carbide plates form in the austenite between bainite laths in a bainitic packet and the carbon content of the austenite is decreased. Subsequently, dislocated bainitic ferrite laths form in the austenite and the transformation is completed. The orientation of the bainite laths formed in the later stage of transformation is different from that of the initially formed bainite laths in a bainitic packet. The present results strongly suggest that the bainitic ferrite develops by a displacive mechanism rather than by the diffusional mechanism.

125. Bainitic Intermediate Microstructures of Very Low-C Steels
Toru Araki, Koji Shibata and Hirooki Nakajima

The complicated intermediate microstructures (Z_w), transformed in the temperature range between the typical reconstructive/diffusional ferrite, α_p , and the bcc lath martensite, α'_m , of very low carbon low alloy steels were reexamined as an activity of the Bainite Committee in Japan, in particular focusing on the continuously cooled microstructures. After investigating a large number of micrographs of such steels together with various influencing factors the obtained knowledge was analyzed: 1) With the carbon content below 0.02%, i.e. solubility of C in α of 2%Mn-Fe, the matrix Z_w -phases formed below T_0 temperature by a C-invariant manner are reasonably classified into three wide categories: massive(-like) α_q , Widmanstätten α_w and bainitic α'_b/α_b . 2) By continuous cooling, α allotriomorph can successively grow as α_q , α_w , afterward leading to α'_b being effected by recovery phenomena. 3) Inheritance of the prior γ -grain boundaries to the α phases is an information to discriminate the nature of various Z_w s. 4) Deformed and unrecrystallized γ gives rise to a more variety of combination of Z_w - α phases due to enhanced nucleation sites for varied modes of formation. 5) An atomistic model of semi-displacive/diffusional transformation for Z_w was proposed. The interface of transforming γ - α phases postulated as a lattice junction region of γ -bcc to α -bcc with the mutual {101} plane will trap C-atoms in the straining and defected lattice and influence the transformation behaviors and partitioning of carbon into γ .

126. Relationship of Bainitic Microstructure to Impact Toughness in Cr-Mo and Cr-W Steels

Ronald L. Klueh and D.J. Alexander

Habraken and Economopoulos (H&E) demonstrated that bainite microstructures developed during continuous cooling of low-carbon alloy steels were different from upper and lower bainite developed by isothermal transformation. Two of H&Es non-classical bainitic microstructures have been produced in a 3Cr-1.5Mo-0.25V-0.1C steel by using different cooling rates from the austenitization temperature: when quenched, a carbide-free acicular bainite formed, and when air cooled, granular bainite formed. Charpy impact properties were determined on the quenched and air-cooled steels and after they were tempered. Before tempering, the quenched steel had the lower ductile-brittle transition temperature (DBTT). After tempering, the DBTT of both the quenched and air-cooled steels decreased and approached a common value. However, the final value was obtained with a much less severe temper for the quenched steel than the air-cooled steel. A similar observation was made with respect to upper-shelf energy for the different cooling rates. This behavior for carbide-free acicular bainite and granular bainite was also observed for several Cr-W steels. These results indicate that by the proper choice of bainitic microstructure, it is possible to develop steels with optimized strength and toughness.

127. Theoretical Investigation of the Bainitic Transformation in Copper-Based Alloys

Kanzaburo Marukawa

The atomic mechanism of the bainitic transformation in Cu alloy has been studied theoretically with the intention to solve the apparent dual nature of this transformation, i.e., features of shear transformation and diffusional phase decomposition. The results are as follows. (1) Bainitic precipitates in this alloy can be taken as coherent precipitates, so that their growth can be described in terms of the motion of transformation dislocations. (2) The dislocation motion is coupled with the solute re-distribution through the concentration fluctuation. It is to be noted that the lattice shearing and the solute diffusion are compatible with each other in the course of the bainitic reaction. (3) Transformation by lattice shearing takes place even at a temperature above the equilibrium temperature T_0 of the two phases, if it is coupled with the solute re-distribution. (4) A situation may happen in which shear transformation is controlled by the atomic diffusion. (5) A high stress concentration arises at the edge of a coherent precipitate as a result of pile-up of transformation dislocations, so that the lengthwise growth of a precipitate may attain quite a high growth rate.

128. Composition Dependence of the Bainitic Transformation in β Phase Cu-Zn-Au Alloys

Tsugio Tadaki, Cai Jing-Qiang, Ken'ichi Shimizu, Yin Fuxing and Gu Nanju

The composition dependence of the bainitic transformation in β phase $\text{Cu}_{60-x}\text{Zn}_{40}\text{Au}_x$ ($x=4, 9, 15$; nominal) alloys has been studied by means of analytical electron microscopy and optical microscopy. The bainite plates in the 4%, 9% and 15% Au alloys were observed to form upon isothermal aging at 473K for about 5h, 1.5h and 15min, respectively. The amount of bainite plates increased, while the size of them decreased remarkably with increasing Au content. The composition differences in Cu concentration between matrix and bainite were 5.8, 4.4 and 1.5 at.% on the average for the bainite plates about 100nm thick in the 4%, 9% and 15% Au alloys, respectively. A certain difference in composition was also found even for a bainite plate whose width was comparable to the size of the next nearest neighbor type antiphase domains (30nm on the average) in the matrix of the 15% Au alloy. These results suggest that the bainitic transformation is essentially accompanied by diffusion.

129. The β_3 to α_1 Transformation in a Cu-Zn-Al Alloy

Y. Hamada, Ming-Hsiung Wu and C.M. Wayman

The 18R ordered α_1 plate that forms during isothermal aging of an L2₁ ordered Cu-26.7wt.%Zn-4.0wt.%Al alloy at 475°K has a composition lean in both Zn and Al concentrations. Solute depletion at parent phase dislocations was also observed, suggesting the possibility of shear nucleation of the plate at these defects. Lattice coherency and strain field are present at early stage interfaces. Misfits and ledges appear at later stages when diffusion dominates and controls the plate growth.

130. Observation of Bainite Shear in a Cu-Zn-Al-Mn Alloy

Fu-Min Chen, M. Han, Y.R. Chen, W.X. Liu and Tsun Ko

Two sets of dislocation contrast on the interfaces of bainite - matrix in a Cu-Zn-Al-Mn alloy have been observed with TEM. One set is the Schockley dislocation at the boundaries of stacking fault substructure, and the other is the interfacial micro-ledge, the arrangement of which forms the apparent curvature of the interface. The shear bands were found during bainite reaction, and the shear bands in the bainite plate are strictly parallel to the stacking faults plane. These shear bands relatively deviated from those caused by deformation in matrices, and the deviation angle equals the shear angle of the lattice during transformation.

131. TEM Study of Bainite in Copper Alloys

D.L. Liu, Q.H. Li and Tsun Ko

Bainite formed in Cu-38.98 Zn, Cu-12.15%Al, Cu-30.4%Zn-1.25%Al and Cu-11.2%Al-2.9%Ni has been examined and compared. Difference in morphology of bainite plates formed from virgin β phase and the β phase formed by reverse transformation of martensite, midrib and regions formed from intersection of two bainite plates crossing each other have been examined and interpreted as further evidence of the shear nature of the transformation. Fine structure and electron diffraction revealed the presence of stacking faults formed across a bainite plate with steps on the plate edge: resembling the "ledges" and "superledges", occasionally observed in steel.

132. OPEN

133. Transformation Behavior of ϵ -Martensite in Fe-Mn-Si Shape Memory Alloys

Tadashi Maki and Kaneaki Tsuzaki

The shape memory effect in Fe-Mn-Si alloys occurs by the reverse transformation of stress-induced ϵ (hcp) martensite. In this paper, the experimental results on the behavior of $\gamma \rightarrow \epsilon$ transformation, $\epsilon \rightarrow \gamma$ reverse transformation, and $\gamma \leftrightarrow \epsilon$ cyclic transformation in Fe-24-33Mn-6Si alloys (shape memory alloys) and Fe-24Mn alloy (not a shape memory alloy) will be presented, and the mechanism of shape memory effect in Fe-Mn-Si alloys will be discussed. The ϵ martensite is formed by the movement of Shockley partial dislocations on every two adjoining {111} austenite plane. In the case of thermally-transformed martensite, ϵ plates generally consist of the three variants with different shift vectors (i.e., the movement of three kinds of partial dislocations on the given {111} austenite plane) in order to reduce the total transformation strain. On the other hand, the stress-induced ϵ plate is formed by the movement of one kind of partial dislocations, resulting in the large transformation strain compared with thermally-transformed ϵ . A significant difference between Fe-Mn and Fe-Mn-Si alloys can be seen in the behavior of $\epsilon \rightarrow \gamma$ reverse transformation. Although the reversed austenite in the Fe-24Mn alloy contains a high density of dislocations, dislocations are scarcely observed in the reversed austenite in the case of Fe-24Mn-6Si alloy. This indicates that the addition of Si plays an important role in the appearance of crystallographic reversibility during reverse transformation of ϵ martensite. The Fe-Mn-Si alloy also exhibits a microstructure memory during $\gamma \leftrightarrow \epsilon$ cyclic transformation unlike the Fe-Mn alloy.

134. Shape Memory Behaviour in Fe-Mn-Co-Ni-Si Alloys

Manijeh M. Reyhani, X. Chen and Paul G. McCormick

A new series of Fe-Mn-Co-Ni-Si alloys has been found to exhibit a martensitic transformation and shape memory behaviour similar to that observed in Fe-Mn-Si and Fe-Mn-Cr-Ni-Si alloys. This paper will report the effect of composition, heat treatment and repeated thermomechanical cycling on the transformation characteristics and shape memory behaviour.

135. Cyclic γ to ϵ Transformation Behavior and its Effect on the Shape Memory Characteristics in Fe-Mn-Si-Cr-Ni Alloy

Hideyuki Ohtsuka, S. Kajiwara and T. Ishihara

The effect of $\gamma \leftrightarrow \epsilon$ cyclic transformation on the shape memory characteristics has been studied in Fe-14Mn-6Si-9Cr-5Ni (wt%) alloy. The effect of cyclic transformation on the transformation temperatures for thermally formed and stress induced martensites were investigated by DSC. The A_f temperature of stress induced martensite and the amount of thermally formed martensite remarkably increases with increasing number of cyclic transformation. ϵ martensites were stress-induced by tensile deformation at room temperature, and they were reverse transformed by heating under various stresses. The recovery stress was measured after the $\gamma \leftrightarrow \epsilon$ cyclic transformation was repeated various times. As the $\gamma \leftrightarrow \epsilon$ cyclic transformation was repeated, the recovery stress remarkably increased at first, and then gradually decreased. This rapid increase of recovery stress is attributed to not only the increase of elongation when specimen is deformed but also the increase of stacking faults which act as nucleation sites of martensite. The decrease of recovery stress is attributed to the decrease of elongation.

136. Study of Thermal ϵ -Phase Martensite in a Fe-Mn-Si-Cr-Ni Shape Memory Alloy by X-Ray Diffraction and Thermoelectric Power

Luc Federzoni, D. Gex, Q. Gu, Gerard Guenin, D. Labrosse, Marc Mantel and Jan Van Humbeeck

The influence of the grain size, the dislocation density and the 'restauration process, on the thermal ϵ -martensite, created by cooling at liquid nitrogen temperature in a Fe-Mn-Cr-Si-Ni shape memory alloy, has been investigated. It appears that these parameters have a strong influence on the thermal ϵ -phase volume fraction, which can vary from 2% to more than 50%, with an appropriate thermomechanical treatment. An easy technique, the ThermoElectric Power has been standardized, to allow measurements of ϵ -phase quantities at room temperature.

137. In Situ Experiments During a Thermal Cycle in an Fe-Mn-Si Shape Memory Alloy

K. Tamarat, G. Andre and Bernard Dubois

A biphased γ - ϵ structure of an Fe-Mn-Si S.M.A. was obtained at room temperature. During heating until 479K, X ray diffraction analysis detected ϵ martensite lines whereas A_f would be 450K from internal friction measurements. By cooling until 1.7K, neutron diffraction showed an antiferromagnetic phenomenon, the hysteresis of which is not exactly the same as those observed in the shear modulus variations.

138. Reversible Martensite Transformation and Shape Memory Effect in Fe-Ni-Nb Alloys

Yuri N. Koval and G.E. Monastyrsky

Perfect shape memory effect due to ausaging has been discovered in Fe-Ni-Nb alloys. These alloys near the chemical composition range 30-31 at.% Ni and 3-4.5 at.% Nb exhibited a wide temperature hysteresis (500-550 K) and a partial SME in the homogeneous state. To modify the transformation the ausaging at 923 K for different time has been applied. By ausaging during certain times, hysteresis reduced to about 230 K, the drop of M_s temperature and the perfect SME was observed. It was found that the martensite in the specimen aged at 6-25 hours was of bcc-structure with small tetragonality distortion (2.5%) which vanished for more long period of thermal treatment. Ausaging produces in austenite two phases: fine coherent γ'' -particles of the type Ni_3Nb in the volume of grains and greater particles of Fe_2Nb Laves phase at the boundaries of grains. By transmission electron microscopy, it was confirmed that the particles of γ'' -phase inherited by the martensite have been plastically sheared, but retained their structure. The lattice of the particles undergoes some misorientation between both the lattices of the untransformed austenite and the surrounding martensite. It is assumed that the rotation and the deformation of the particles accommodate the shear of the martensitic matrix. The elastic fields produced by these particles appear to be the reasonable factor to improve the shape recovery.

139. Some New Aspects of Shape Memory Behavior of ϵ -Martensites

Jian-Hua Yang, H. Chen and C. Marvin Wayman

Shape memory behavior and phase transformation characteristics of newly developed ϵ -martensite-related shape memory alloys have been investigated utilizing a combination of bend tests, dilatometry, electrical resistance, DSC, magnetic susceptibility and microstructural analysis. It is shown that the alloys studied exhibit a good SME without special training. The SME is significantly improved by prestraining at low temperatures. A higher net reversible strain is made available by over-prestraining at lower temperatures or other training processes, although the fully reversible prestrain usually does not exceed 2%. Superelasticity, the two-way shape memory and a softening effect of the matrix at low temperatures are also briefly discussed based on the preliminary results. The variations of shape memory properties with different alloying and prestraining temperatures are interpreted in terms of the transformation characteristics. It is shown that the ϵ -martensite can be readily strain-induced under the stabilization effect of the antiferromagnetism which strongly suppresses the thermally-induced transformation. The strain-induced transformation of ϵ -martensite is more preferred as a predominant deformation mechanism at low temperatures under a combined influence of the antiferromagnetism and other physical factors, whereas the irreversible deformation mode is more likely with prestrain at relatively high temperature. The transformation characteristics can be significantly changed by alloying and mechanical/thermal treatments. This offers a possibility of developing new practical Fe-based shape memory alloys with a wide range of mechanical and physical properties.

140. Secondary Variants, Self-Accommodation and Shape Memory Mechanism of ϵ -Martensite

Jian-Hua Yang and C. Marvin Wayman

Transmission electron microscopy and crystallographic analysis on the orientation relationships of various ϵ - martensite variants have been carried out in the ϵ - martensite-related shape memory alloys. Some new ϵ variants, which do not originate directly from the matrix by the well-known $\{111\}\langle 112 \rangle$ simple shear process for the FCC to HCP transformation, have been observed and distinguished as secondary variants. Formation mechanisms and corresponding hard-sphere models of these variants are proposed based on the intersecting shears associated with intersecting initial variants. The reorientation features of various secondary ϵ - martensite variants and intervariant relationships predicted by these models are in good agreement with experimental observations. Experimental aspects of the self-accommodation of ϵ - martensite variants have also been clarified in connection with the formation of various secondary ϵ variants. Characterization of the faulting configuration of martensitic substructures confirms that the spontaneous FCC - HCP martensitic transformation is generally self-accommodating, although involving localized homogeneous shears which often result in the formation of secondary variants at intersections. Stress-induced transformation promotes the growth of a single preferred variant, either at the expense of others within a band or by the formation of secondary variants at intersections between different bands. Theoretical aspects of the self-accommodation and shape memory mechanism of ϵ - martensite are thus discussed in comparison with the well-known and widely studied Cu-based shape memory alloys. It follows that the FCC - HCP martensitic transformation and its related shape memory behavior share some similarities in self-accommodation of the transformation and variant reorientation upon deformation. Therefore, the basic processes involved in the shape memory behavior of ϵ -martensite can be similarly generalized in terms of the model established for the Cu-based SMAs, although some details are significantly different.

141. Transformation Behaviour and Shape Memory Effects in Melt Spun Ni-Al Alloys

J.H. Zhu, Druce P. Dunne, G.W. Delamore and Noel F. Kennon

The shape memory effect (SME) has been previously demonstrated in nickel rich Ni-Al intermetallic alloys produced by conventional methods such as casting and hot working. The current investigation was carried out on rapidly solidified Ni-Al alloys with nickel concentrations in the range 63 - 66 at.% Ni. Ribbons with a very fine grain size and a thickness of 25-50 μ m were successfully produced by melt spinning. Transformation temperatures were determined using differential scanning calorimetry (DSC) for both the forward and reverse transformations. The DSC results clearly indicated that the $M(s)$ temperatures in the 63 and 64 at.%Ni alloys were lower than those reported in previous investigations of conventionally processed bulk alloys. However, the transformation temperatures in the 63 and 64 at.% alloys increased on aging at $-0.3T(m)$ for 5 minutes. Thermoelastic transformation was demonstrated for up to 6 thermal cycles in melt spun ribbon samples with a composition of 64 at.% Ni, and the shape memory effect was confirmed by repeated bend tests.

142. Mechanical Properties and Microstructure of Rapidly Solidified TiNiCu Alloy

Yasubumi Furuya, Minoru Matsumoto and T. Matsumoto

Several properties of rapidly solidified TiNiCu alloys, i.e., thermoelastic transformation temperature, behaviors of transformation strain vs. temperature hysteresis and stress vs. strain hysteresis curves at various temperatures were investigated. Specimens of thin plate were prepared by using melt-spinning machine with single or twin Cu rolls by changing the cooling rate from 1m/sec to 40m/sec. From optical and SEM observations, metallurgical microstructure changed from dendritic grain to very fine columnar grain texture along the direction of width with increasing the cooling rate. It was confirmed that transformation strain clearly increased with cooling rate, moreover, from the stress vs. strain hysteresis curve, superelasticity (i.e., ability of recovery strain energy) and damping capacity (i.e. dispersion strain energy) improved very much by rapidly solidification. The reasons of these characteristic material properties of rapidly solidified TiNiCu alloys will be discussed by relating with the observed unique microstructures.

143. First Order Phase Transition of Fe-Rh Alloys

Ryuichiro Oshima, M. Takahashi, A. Taniyama and Yorihiro Tsunoda

Near equiatomic FeRh alloys which undergo a first order phase transition from the high temperature ferromagnetic (B2) to the low temperature anti-ferromagnetic (Heusler type) phase have been examined by electric resistance and magnetic measurements, neutron diffraction and transmission electron microscopy. It was found that remarkable changes in thermal hysteresis of the transition with heat treatments were caused by phase boundary pinning at unidentified annealing products, the formation of which was not expected by previous phase diagrams. Neutron diffraction experiments suggested a premonitory effect in the magnetic peaks before the transition from the anti-ferromagnetic to the ferromagnetic phase on heating.

144. OPEN

145. Phase Transformations in Superconducting and Non-Superconducting Perovskites

Terrence E. Mitchell

Most of the high T_c superconductors and other perovskite-related cuprates exhibit some kind of structural instability. For example, structures in the Bi-Ca-Sr-Cu-O and Tl-Ba-Ca-Cu-O systems have incommensurate periodicities associated with displacements of the heavy cations, while tetragonal-to-orthorhombic phases transformations occur in the Y-Ba-Cu-O and La-Sr-Cu-O systems. In $\text{YBa}_2\text{Cu}_3\text{O}_{7-x}$, the transformation is due to the ordering of oxygen vacancies while in $\text{La}_{2-x}\text{Sr}_x\text{CuO}_4$ the transformation is accompanied by rotation of the CuO_6 octahedra. Such rotations and distortions of the co-ordination octahedra commonly occur in perovskite-related compounds and transformations between the structures are frequently martensitic. Transmission electron microscopy observations on the microstructures due to phase transformation in the superconducting cuprates will be compared with those on other perovskites. In particular the accompanying twin configurations will be compared and used to calculate twin boundary energies.

146. Diffuse X-Ray Scattering Study of Oxygen-Disordered Tetragonal $\text{YBa}_2(\text{Cu}_x\text{Al}_{1-x})_3\text{O}_7$ Crystals

X. Jiang, P. Wochner, Simon C. Moss and P. Zachack

X-ray scattering from tetragonal single crystals of $\text{YBa}_2(\text{Cu}_{1-x}\text{Al}_x)_3\text{O}_7$ ($x=0.045, 0.055$) shows pronounced diffuse streaking in $[110]$ directions about the Bragg peaks. This diffuse scattering bears a remarkable resemblance to the $[110]:\langle 1\bar{1}0 \rangle$ streaking above certain martensitic transformations and there exists considerable TEM evidence for a twinned microstructure in these doped superconductors. There is, however, no evidence for soft $[110]:\langle 1\bar{1}0 \rangle$ phonons. Through a quantitative calculation using a coupled concentration wave/static displacement wave approach, we show that this diffuse scattering is essentially attributable to the shear displacement field produced by a disordered oxygen array on the $\text{Cu}(1)\text{-O}$ "chain" plane. In addition we observe pronounced short-range chain order (local orthorhombic fluctuations) whose correlation range is considerably greater than the superconducting coherence length but which decreases with increasing x . This suggests that on a scale relevant for superconductivity the (local) orthorhombicity remains important in this tetragonal structure. While the correlated chains are a distinctive feature there is no evidence, or need, of a micro-domain description of the disordered state. In fact, our Monte Carlo calculations of the undistorted disordered state show no distinct microtwins but only patches of local order correlated over $\sim 30\text{\AA}$ for $x=0.045$.

147. Oxygen Ordering and Strain-Related Morphology in $\text{YBa}_2\text{Cu}_3\text{O}_{7-x}\text{M}_x\text{O}_7$ Systems

Zhi-Xiong Cai, Yimei Zhu and David O. Welch

Monte Carlo simulations of an anisotropic lattice gas model which represents well the interaction between oxygen atoms in $\text{YBa}_2\text{Cu}_3\text{O}_7$ systems doped with trivalent impurity atoms M such as Fe or Al were performed in order to study the nature of oxygen ordering in these materials. Using the concentration wave/displacement wave approach the concentration wave amplitudes c_q obtained from these simulations were used to calculate the diffuse X-ray scattering intensity caused by the displacement field. The results suggest that the small orthorhombic domains associated with the oxygen "cross-link" around impurity atoms M cause the diffuse intensity to fall off with increasing magnitude of the oxygen concentration wave vector q as $1/q^2$ for small q and as $1/q^4$ for larger q . We also show that the size of such domains depends on the dopant concentration and can be obtained from diffuse X-ray scattering data. The calculated diffuse x-ray scattering will be compared with the experimental data of Jiang, Wochner, Moss, and Zschack (presented at this conference).

148. Study of Structural Phase Transition and Superconductivity in Quenched $\text{YBa}_2\text{Cu}_3\text{O}_x$

Shoichi Edo

The orthorhombic-tetragonal phase transition and its relation to superconductivity in quenched $\text{YBa}_2\text{Cu}_3\text{O}_x$ have been investigated by means of x-ray diffraction, dc resistivity and ac susceptibility measurements. Samples were prepared from the orthorhombic $\text{YBa}_2\text{Cu}_3\text{O}_x$ with the diameter of 15 mm and the thickness of 2 mm by annealing for 6 hours at temperatures between 450 and 900 °C in air, followed by quenching in liquid nitrogen. The lattice parameters of the quenched samples at room temperature were determined as a function of annealing temperature based on the x-ray diffraction patterns. In as-quenched bulk surfaces, parameter a exhibits the plateau between 600 and 700 °C. Above 700 °C, parameters a and c markedly increase and the phase change from orthorhombic to tetragonal is completed at 735 °C. However, in the powder samples prepared by milling the quenched bulk samples, parameters a and c increase, while parameter b decreases monotonically with an increase in annealing temperature and the phase change occurs at 900 °C. The phase distributions are observed in the thickness direction in the quenched bulk samples. The phase distribution causes the above distinction in the lattice parameters between the bulk and the powdered samples. The annealing temperature at which the phase change occurs will vary widely depending on the quenching rate. Twin structures can be hardly formed at rapid quenching, and this results in unrelaxed strains and the plateau in parameter a . As a result, it is revealed that there is no direct relationship between the changes of the lattice parameters and those of the superconducting transition temperature in relatively slow cooled $\text{YBa}_2\text{Cu}_3\text{O}_x$ under constant oxygen concentration.

149. Discontinuous (Martensitic) and Continuous Displacive Transformations in High- T_c Superconductors and Other Solids

David S. Lieberman

A great many metallic and ceramic systems (including Hi T_c materials) exhibit one or more DISPLACIVE transformations on cooling in which: no long range diffusion of atoms occurs, i.e. all atoms move less than an interatomic distance (with the exception of O atoms in the oxide superconductors which may move in and out with changing T), nearest neighbors are maintained, the degree of order in the Parent persists in the product, etc. This transformation can be Discontinuous (martensitic) or Continuous. If \underline{D} , a sharp undistorted habit plane separates P and p, hysteresis on thermal cycling is always exhibited and hence p is metastable, all the crystal geometric features are accounted for by the W-L-R theory, and the phase change is 1st order with abrupt changes in lattice parameters at the transformation temperature (the Bain distortion). If \underline{C} , the structural change is continuous, no sharp interface has been observed between P and p, hysteresis has never been reported-hence p is stable, and the transformation is \geq 2nd order. Archetypes of \underline{D} ($\text{CsCl} \rightarrow$ twinned Orthorhombic in AuCd) and \underline{C} ($\text{CsCl} \rightarrow$ ~~tw~~ Tetragonal in VRu) are discussed to aid in examining similar transformations in Hi T_c materials. The $\underline{I} \rightarrow \underline{Q}$ transition at $\sim 700^\circ\text{C}$ in $\text{YBa}_2\text{Cu}_3\text{O}_{7-x}$ appears to be \underline{C} in some reports and \underline{D} in others; the lack of any definitive statement about hysteresis is not surprising since even if the transition is \underline{D} , the Bain distortions are so small-and hence also the expected hysteresis width-that its determination might be very difficult (and for other reasons to be discussed). $\text{La}_{2-x}\text{Ba}_x\text{CuO}_4$ and related compounds transform $\text{HTI} \rightarrow \text{LTQ}$; on further cooling, this superconducting Q phase transforms to a complex LTI. The 1st is \underline{C} , the 2nd is definitely \underline{D} -and was found to have "a profound effect on superconductivity in this material." Thus the salient differences in the properties of the phases resulting from \underline{C} and \underline{D} [stability, twins, defects, flux pinning (?), etc.] may be critical to understanding and exploiting these materials.

150. Internal Friction Study of Single Variant Transformations in Cu-Zn-Al Shape Memory Alloys

Johannes Stoiber, J.-E. Bidaux and Rolf Gotthardt

The internal friction (IF) has been measured during single variant transformation in Cu-Zn-Al single crystals. The results show that local interface displacements do not contribute significantly to the IF. In special specimen geometries, where global interface displacements are possible, the observed IF-peak is mainly due to the anelastic deformation produced in the habit plane system. A quantitative analysis of the observed IF-values suggests that the interface motion during IF is not completely irreversible as it is assumed in existing IF-models.

151. Role of Dislocations on the Properties of the Shape Memory Alloys

Francisco C. Lovey, Marcos Sade, Vicenc Torra and Antoni Amengual

The presence and production of dislocations are related to several characteristics and properties of shape memory alloys (SMA). Thus the intrinsic thermoelasticity, which was observed in single interface β -18R transformations, arises from the loss of translation symmetry of the Burgers vectors of the existing dislocations when they are absorbed by the martensite. This implies the progressive creation of faults and a continuous undercooling to compensate the energy of the faults. The intrinsic thermoelasticity prevents the growth of a plate and multivariants transformation normally occurs. Dislocations are formed from the interaction between variants leading to degradation of the SMA properties. Dislocations are also produced during pseudoelastic cycling in order to induce the two way shape memory effect (TWSM). These dislocations could be responsible of the TWSM according to the following two aspects. The stability of the variant where the dislocation energies are lower. The favorable effect for the nucleation and the initial growth of that specific martensite variant. The mechanisms associated to the influence of the dislocations on these aspects of the martensitic transformation will be analyzed in this work.

152. Study on the Mobility of Interfaces During the Martensitic Transformation of Cu-Al-Ni Shape Memory Alloy

Vicente Recarte, Maria Luisa No, J. Herreros and J. San Juan

In this work we have studied the mobility of the martensitic interphases, during and after the β -martensitic transformation, on the single crystal and polycrystal Cu-Al-Ni alloys.

The mobility of the interphases of the different martensitic phases β'_1 and γ'_1 has been characterized by internal friction and microdeformation. Depending on the concentration, we have observed one or two microdeformation stages, linked to the presence of the γ'_1 and β'_1 phases, or both, one after the other. The comparison between the electrical resistivity and microdeformation measurements, has allowed us to identify the stages in which the interphases move by nucleation of the martensitic variants on the β phase and also the stages in which the interphases move by the variants reorientation on martensitic phase.

153. Growth Kinetics During Thermoelastic Martensitic Transformations

Antoni Planes and Jordi Ortin

We consider the problem of growth during a thermoelastic martensitic transformation in both purely thermoelastic and non-equilibrium conditions. This second situation is associated with the possibility of local elastic instabilities which appear, for instance, as a result of shape change accommodation by simultaneous growth of different crystallographic variants. We predict scaling of the transformed fraction curves against temperature only in the case of purely thermoelastic growth. The analysis reveals that in the general case the energy dissipated has a double origin: release of elastic energy W , and entropy production S . The latter depends on both temperature rate and thermal conduction in the system. We finally discuss experimental results on the basis of the model presented before.

154. A Continuum Mechanical Approach to the Kinetics and Deformation of Alloys During Martensitic Transformations

Kikuaki Tanaka, Franz Dieter Fischer and E. Oberaigner

Thermomechanical and transformation behavior of polycrystalline alloys is studied in the process of martensitic transformation from the continuum mechanical point of view. The microscopic transformation/deformation is connected to the macroscopic behavior of alloys by introducing two different levels of microstructure in alloys; the microregion and the mesodomain. The driving force is derived as a transformation condition, and the constitutive equation and the transformation kinetics are discussed.

155. OPEN

156. Martensitic Transformation Plasticity Simulations by Finite Elements

J.F. Ganghoffer, K. Simonsson, S. Denis, Elisabeth Gautier, S. Sjostrom and A. Simon

The mechanical behaviour associated with the martensitic transformation has been modelled using a 2D FE description. The martensite variants are constituted of different elements of the mesh and four different variants are allowed to transform in the grain. The transformation progress is determined from a thermodynamical criterion based on the maximal work associated with the variant formation. Transformation plasticity deformation and plate orientation patterns are obtained for three stress levels. These results are discussed with regard to the model used and the physical parameters introduced in the model.

157. Thermal Fatigue of Shape Memory Alloys

Iain Le May, S.K.P. Cheung-Mak and P. Jacobsen

Thermal cycling has been conducted of Cu-Zn-Al shape memory springs under load. The test procedures are described and the spring characteristics are reported as a function of thermal cycles and load. The results indicate a strong dependence of changes in spring characteristics on both the number of cycles and on the load carried.

158. The Fatigue of Dual Phase Polycrystalline Cu-Zn-Al Shape Memory Alloy

W.G. Wu, X.Y. Wang, M. Zhu, Z.G. Wang and Dazhi Yang

In this work the fatigue properties of dual phase polycrystalline CuZnAl SMA have been investigated with respect to that of single phase alloy. By carefully controlled heat treatment three kinds of dual phase SMAs with a small amount of α phase ($<10\%$) showing different morphology and distribution, i. e. homogeneously distributed dot, block in grain boundaries and network along grain boundaries, can be obtained. The tension-tension fatigue tests are carried out both in martensitic and pseudoelastic state. Attention is paid to the effect of α phase on the fatigue life and fracture mechanisms. All alloys tested obey Coffin-Manson law and the fatigue life of dual phase alloys in martensitic state is longer than that of in pseudoelastic state regardless of the morphology and distribution of α phase. However, either in martensitic or pseudoelastic state the effect of α phase on fatigue life is obvious. Compared with single phase, the fatigue life of dual phase alloy with homogeneously distributed dot α phase is increased both in martensitic and pseudoelastic state and particularly in the latter. The network α along grain boundaries decreases fatigue life when the cycling stress is high but appears no evident effect at low stress level as far as that of single phase alloys be considered. But the block α in grain boundary shows no observable influence. Scanning electron micrographs suggest that the α phase can modify fracture features remarkably. This implies that the α phase plays an important role in fatigue crack nucleation and propagation. The effect of α phase on fracture mechanisms has been discussed for different cases.

159. Shock Damping in a Cu-Zn-Al Shape Memory Alloy

Jean Muller, Bernard Dubois, J. Condore and J.F. Fries

In order to precise high damping capacity of shape memory alloys (SMA), an extension from internal friction to shock damping capacity is proposed. For any metallic material submitted to a limited plastic deformation at high strain rates (from 10^{-3} to 5000 s^{-1}), a damping power concept Ω^{-1} is introduced and related to some aspects of the mechanical energy dissipation. Experiments were performed with a quadrant shock pendulum and Hopkinson split bars. In a Cu-27.6wt% Zn - 3.63wt% Al- 0.6wt% B SMA, adiabatic shear bands and shock induced martensites are observed. This would be an accommodation process for shock damping.

160. Restoration Phenomena and Deformation Behavior of Neutron Irradiated Ti-Ni Shape Memory Alloys

Tajii Hoshiya, Mitsuo Ohmi, I. Goto and Y. Ichihashi

Ti-Ni shape memory alloys are considered to be useful materials for fission and fusion reactor devices that may utilize shape memory capabilities or superelasticity. When Ti-Ni alloys are neutron irradiated, structural alterations can occur which may suppress the martensitic transformation. On the other hand, restoration (reverse) phenomena of an irradiated state to a normal one take place upon both high temperature irradiation and post-irradiation-annealing. In neutron irradiated Ti-Ni alloys, the relationships between the deformation behavior and radiation-induced structural alterations are not clear at the present stage. The purpose of this study is to clarify changes in deformation behavior of neutron irradiated Ti-Ni alloys before and after restoration.

Ti-Ni specimens were neutron irradiated in the Japan Materials Testing Reactors (JMTR). The irradiation conditions employed were temperatures of 323, 490, 520 and 620 in the fluence range between 1.3×10^{22} and $1.4 \times 10^{25} \text{ m}^{-2}$, which corresponds to the displacement damage range between 1.8×10^{-3} and 1.9 displacements per atom (dpa). Remote-controlled tensile tests were carried out in JMTR Hot Laboratory at various temperatures between 153 and 373K after post-irradiation-annealing at temperatures of 473, 523 and 573K. Young's moduli were obtained from their stress-strain curves. By neutron irradiation with $1.4 \times 10^{25} \text{ m}^{-2}$, the radiation-induced superelasticity, which was observed at the fluence level below 10^{23} m^{-2} , disappeared and the temperature dependence of Young's modulus was changed from positive (characteristic features of β phase alloys) into negative. It can be seen that the radiation-induced disordering may be abruptly brought about by heavy damage of 1.9dpa. Changes in deformation behavior of neutron irradiated Ti-Ni alloys are associated with the occurrence of back stress that may be produced by defects such as cascades.

161. OPEN

162. OPEN

163. Morphology Transitions of Deformation-Induced Martensites in Fe-Ni-C Alloys

Xiumu Zhang, D.F. Li, X. Zhao, Z.S. Xing, J.Z. Zhang, Elisabeth Gautier and A. Simon

Morphology transitions of deformation-induced martensites during isothermal tensile tests in the temperature range of M_s - M_d , have been studied in Fe-Ni-C alloys. With increase in strain the morphology transitions are as follows: lenticular \rightarrow butterfly \rightarrow $(111)_f$ massive martensite in Fe-30Ni; lenticular \rightarrow butterfly \rightarrow $(111)_f$ small butterfly martensite in Fe-30Ni-0.11C; thin plate \rightarrow lenticular \rightarrow $(3 \ 10 \ 15)_f$ massive martensite in Fe-25Ni-0.7C and thin plate \rightarrow couple-plate \rightarrow lenticular couple-plate martensite in Fe-30Ni-0.34C alloy. Some peculiar strain-induced martensites are reported for the first time.

164. Fracture of Cu-Al-Ni Shape Memory Alloy Single Crystals

A. Cherepin, S. Firstov, Yuri N. Koval and I. Lushankin

Fracture and related phenomena were studied in Cu-Al-Ni SMA single crystals tested in tension and bending. It is shown that irreversible deformation of the β_1 parent phase (ordered b.c.c. structure) and of the martensites (distorted f.c.c. ones) is localized at the interphase boundaries due to martensitic and martensite-to-martensite transformations. This deformation proceeds by multiple shears along the respective close-packed planes, all the latter being parallel to $\{110\}\beta_1$ due to lattice correspondence. Shear deformation during tension may lead to the formation of the V-shaped fracture surfaces composed of two parts, namely of a slip zone with shear traces and a take-off zone with ductile-like dimples. These dimples are observable even after fracture at 77K. Estimated fracture energy values and measured fracture toughness K_{Ic} ones were found to be in excellent agreement with one another for all temperatures, except those lying in M_s - A_f range. K_{Ic} values decrease on both heating or cooling toward the transformation temperature interval. Such trend in the K_{Ic} -vs- T behaviour is not observed in other materials (e.g. TRIP-steels or ceramics) also known to undergo martensitic transformations. The reason of the described effect is attributed to the strong localization of the deformation.

165. Tribology of Unlubricated Copper-Based Cu-Zn-Al Shape Memory Alloys

Hong Wei Wang, Dazhi Yang and Z.G. Wang

Experiments of unlubricated friction and wear have been carried out on nominal Cu-26Zn-4Al (wt. %) shape memory alloy (SMA) against steel using block-on-ring geometry with a sliding speed of $v=0.52 \text{ m s}^{-1}$, distance $S=93.4 \text{ m}$, and normal load $P=5-100 \text{ kg}$. SEM has been utilized to study worn surfaces and debris. It reveals that the wear of CuZnAl alloy was plasticity-dominated, with adhesion and delamination being the two main mechanisms. Wear results show that CuZnAl specimens in martensite exhibiting shape memory effect (SME) on average behave in a more wearproof manner than those in the β phase exhibiting superelasticity. However, both are more wear durable than the same materials in forged conditions. TEM observation of tensile tests on CuZnAl thin crystals in the β phase showed that stress-induced martensitic transformation occurred from the β phase in the vicinity of pre-existing microcracks on the foil during tensiling. The authors proposed the blunt mechanisms of crack tips due to preferential orientation reactions of variants in martensite and stress-induced martensitic transformation in the β phase to explain the nature of the wear of CuZnAl SMA.

166. The Tensile Properties of Grain Refined Copper-Based Shape Memory Alloys

D.N. Adnyana

Small addition of zirconium to Cu-Zn-Al alloys results in significant grain refinement with attendant improvement in strength and ductility. Stress-strain curves show significant changes with temperature and grain size. At or below A_f -temperature, there are four portions to the stress-strain curve with an initial region of higher slope, then a plateau of lower slope, followed by a second higher slope before the final region of low slope leading to fracture. Above A_f , only the first two or three portions of the stress-strain curve are visible. The alloys showed higher ultimate tensile strength and ductility in the martensitic state than in the pseudoelastic one. The ultimate tensile strengths as high as 815 MPa and fracture strains as high as 12 pct were obtained at the finest grain sizes. The transition stress σ_1 between stages 1 and 2 in the stress-strain curve was found to increase linearly with grain size according to a $(\text{grain size})^{-1/2}$ relationship indicating the linkage of σ_1 to a Hall-Petch type relationship. In addition, it was found that the pseudoelastic recovery was not affected significantly by decreasing grain size. The maximum recovery strains of 90 pct were generally obtained in fine grain samples.

167. Martensitic Transformations in Multiphase Stainless Steels

Fernando D.S. Marquis

Athermal, stress assisted and strain induced martensitic transformations have been studied in three low carbon multiphase stainless steels containing: Fe-Cr-Ni-Ti, Fe-Cr-Ni-Ti-Nb and Fe-Cr-Ni-Ti-Mo. The investigation focused on the morphology and substructure of the martensite and their relationships with physical and mechanical properties. Specimens were solution treated in the austenite phase field, quenched to 273 K and requenched to 77 K. The volume fraction of the athermal martensites were a function of the stability of the austenite, which was related to its composition and the dissolution of carbides during solution treatment, and the distribution of microstructural defects within the austenite. These multiphase microstructures were then deformed up to 1.6 true cumulative plastic strain at 293 K and 77 K, which resulted in very large volume fractions of deformation induced products. The roles of the athermal martensite were first to provide nucleation sites for the formation of deformation induced martensites and, secondly, together with the latter refine the microstructure upon further subsequent thermomechanical processing. This paper discusses the application of Quantitative Image Analysis, X-Ray Diffraction, Transmission Electron Microscopy, and Analytical Electron Microscopy in the study of these martensitic transformations.

168. The Influence of Impulsive Loading Temperature on the Martensitic Transformation and Abnormal Atoms Mobility

Yu.N. Petrov, V.F. Mazanko and I.A. Yakubtsov

The martensitic transformations and abnormal atoms mobility of F.C.C. iron-base alloys have been studied at impulsive loading temperatures of 300 and 77K. An increasing of H.C.P. and B.C.C. martensitic phases quantity with decreasing of loading temperature was obtained experimentally. The increasing of substitutional atoms (iron, nickel) mobility and decreasing of interstitial (carbon) atoms mobility has been detected also. It has been concluded that the martensitic transformation is an additional sources for interstitial atoms mobility.

169. OPEN

170. Systemizing the Use of TiNi Orthodontic Archwires

Rohit C.L. Sachdeva, Y. Oshida, Farrokh Farz-nia and Shuichi Miyazaki

SE NiTi alloys were recently introduced to the field of orthodontics. These alloys generates relatively constant stresses over large strains. Furthermore, the stresses generated by this alloy are temperature dependant. These unique characteristics are attributed to its ability to demonstrate reversible thermoelastic martensitic deformation to strains as high as 8%.[1] With appropriate annealing temperatures, cold work ratio and alloy composition, the thermomechanical characteristics of NiTi can be greatly varied.[2] This has resulted in the orthodontic market being inundated with a wide array of products that demonstrate great variation in their thermomechanical characteristics.[2] Established guidelines for the choice and selection of NiTi products are lacking. Traditional approaches for orthodontic wire selection are not applicable to the SE NiTi alloys. In the following discussion we present a rationale basis for the selection and use of SE NiTi orthodontic products from a clinical perspective.

171. Shape Memory Implants-Recent Developments

Seiko Fukuyo, Rohit C.L. Sachdeva, K. Suzuki and E. Sairenji

The purpose of this work is to present some of the developments that have occurred in shape memory dental implants in the past three years. Previous studies by Fukuyo et al. (1988) have shown that blade-type dental endosseous implants fabricated from nickel titanium alloy using the shape memory effect provide excellent fixation which may enhance osseous-integration. Studies in the past have shown that hydroxylapatite (HA) coating significantly enhances the bone-implant interface attachment of metallic implants. In view of these findings, a new generation of shape memory implants plasma sprayed with 50-70 μ layer of HA have been developed. Preliminary studies on these HA coated NiTi implants using the primate model demonstrate greater cortical bone ingrowth (average 90%) with the coated implant surface than with the uncoated (65%). Additional implant designs based upon the shape of the human root form using NiTi alloy have also been developed. These implants are best used in areas where single teeth have been lost. Our initial clinical studies using this implant system demonstrate a survival rate of 99% (2 year follow-up).

172. Bending and Whipping of TiNi Wires

Brian Berg, Richard D. James and Jim Stice

We present a model for the bending behavior of NiTi wires. The model predicts the shape of a pseudoelastic wire subject to terminal forces and moments. The input for the model is the stored energy as a function of curvature, which can be evaluated from experiments on the pure bending of the wires. Using the moment-curvature relation of dental arch wires measured on a machine developed by Berg, we evaluate the stored energy function of the model. We then predict the shape of the wire in a three point bend test and compare with experiments.

Wires that have been held in a bent shape for a long period experience changes of material properties. This gives rise to an interesting "whipping instability". We describe this instability and discuss its origins.

173. Mechanical Engineering for Shape Memory Alloys

Y. Gillet, Etienne Patoor and Marcel Berveiller

The use of Shape Memory Alloys in industrial applications make necessary to be able to describe their behavior, not only as tensile test specimen in which the stress is homogeneous but like mechanical elements (springs, bearings, beams...) where the stress distribution is, in many cases, inhomogeneous.

Because the Shape Memory behaviour is strongly dependant to the microstructural state inherited from the previous thermomechanical history it is of first importance to be able to determine in the most accurate way the level of stress and strain in every part of the structure considered, in order to avoid any local overloading which could be directly responsible for some dramatically change in the material response during the service life of the device. But due to their strongly inelastic and temperature dependant behaviour, the Classical Mechanical Engineering cannot afford it. This contribution presents Mechanical Engineering relations developed for SMA which are based on a phenomenological description of the SMA behaviour. In that way, the different parameters inherent to the material behavior are determined from measurement on uniaxial tension test. Results obtained with this pattern have been compared to experiments performed on copper based alloy elements and even with simplified flow rules, structure effects may be taken in evidence.

174. Application of Ni-Ti-Nb Shape Memory Alloy Pipe Couplings

Hiroshi Horikawa, Y. Suzuki, A. Horie, S. Yamamoto and Y. Yasuda

Ternary Ni-Ti-Nb alloys have about 50K wider transformation hysteresis than binary Ni-Ti alloy. Since ambient temperatures are located between the M_s and A_s temperatures of the former alloys, they are applicable to heat-to-shrink pipe couplings, which can be stored at ambient temperatures and installed by heating.

We prepared pipe coupling components from a 47at%Ni-Ti-9at%Nb alloy. Leak, pressure, tensile, tensile fatigue and bending fatigue tests were conducted to evaluate the performance of the components and joint systems, using nominal 1/4", 1/2" and 1" stainless steel (SUS316L) pipes which meet Japanese Industrial Standard (JIS) on nuclear power plants. As a result, we found the components applicable to pipe systems in the power plants. A ring-driver type heat-to-shrink pipe coupling was also made for a JIS-5" (SUS316L) pipe. We observed sufficient coupling force when heated, which indicates possible applications of Ni-Ti-Nb couplings to thicker pipe systems.

**175. Specific Manufacture of Copper Based Shape Memory Springs:
Thermomechanical Treatment and Working Test**

T. Lours, Michel Raymond and E. Weynant

The paper presents two very important posts of production of Cu-Zn-Al-Ni springs used in temperature control: thermomechanical treatments and working test of the finished articles, the thermomarkers. The paper will show the importance of these two posts of the production line which warrant the good working of the articles. First, the authors will describe the thermomechanical treatment machine, a specific one developed for the shape memory alloys manufacture, and which the productive capacity can reach 7000 pieces a day: its operating way, the more important parameters and the method to determine them. A good thermomechanical treatment is absolutely necessary to obtain a good working of the articles. Then, they will explain the method used to verify the good working of the thermomarkers: the test machine, the results and the conclusions to get on the choice of parameters of the thermomechanical treatment.

**176. Effects of Heat Treatment and Thermal Cycle on Helical Spring Properties in
NiTiCu Alloy**

Yoshiro Shugo, Takayoshi Shimizu, Koichi Morii, T. Yamada and K. Kusaka

In order to clarify the effects of heat treatment and thermal cycles on helical spring properties which are available for practical use, spring (force-temperature) test, differential scanning calorimetry and X-ray diffraction measurements have been performed on $\text{Ni}_{48.1}\text{Ti}_{39.2}\text{Cu}_{12.7}$ alloy. The force-temperature curves were measured in the temperature range from 293K to 363K at a constant height of the spring and the shear modulus $G_{\text{Austenite}}$ and $G_{\text{Martensite}}$ were calculated from the spring test at 303K and 363K. The $G_{\text{Martensite}}$ at the martensitic phase was 0GPa in either case of annealing temperature at 673K and 773K, having a tendency of increasing with rise in annealing at 873K and 973K. Meanwhile, the value of $G_{\text{Austenite}}$ was 20 to 30GPa at the parent phase. The $G_{\text{Austenite}}$ has little effect on annealing temperature. Transformation temperature was increased with rise in annealing temperature, but temperature difference (A_f-M_f) did not agree between the spring test and DSC measurement. The (A_f-M_f) was about 20K on the former and about 40K on the latter. The effects of thermal cycles resulted in decrease of the spring force and the ratio of the force after the 5000 cycles to 0th cycle at 363K, decreased with rise in annealing temperature. X-ray diffraction measurement made it clear the martensitic phase was monoclinic system in $X=7$ and orthorhombic system in $X=10, 12$ in all heat treatments.

**177. Static Rock Breaker Using TiNi Alloy With Reversible Shape Memory
Effect**

Minoru Nishida, K. Kaneko, K. Takashima, Kiyoshi Yamauchi and T. Inaba

A newly invented static rock breaker using TiNi shape memory alloy has been proposed by the present authors. The breaker consists of compressively prestrained TiNi rods of 15 mm in diameter and 29 mm in length and a pair of two-layered wedge type platens of steel, and requires no accessory equipments other than heating apparatus. The breaker is inserted into a borehole which is drilled the rock and rock-like objects of breaking. A distance between the breaker and the borehole wall is adjusted by sliding the inner platens. After this operation, TiNi elements recover their original length and generate the recovery force upon heating, associated with the reverse martensitic transformation. The total breaking force of the breaker is about 300 to 900 kN, depending on the number of TiNi elements used. The breaker is already applied practically to demolish concrete wall of building and natural boulder and shows its ability to the full. This fact demonstrates that TiNi shape memory alloy has a bright prospect as a solid pressure source. However, it is important to shorten the time of operation in practical use. The prestraining operation for TiNi rods is the most time-consumable. This problem must be solved by using TiNi alloy with reversible shape memory effect (RSME). A training of RSME is carried out by cyclically compressive deformation at various temperatures. The effects of deformation degrees, temperatures, alloy compositions and heat treatments on RSME behaviors are examined. AE monitoring during forward and reverse martensitic transformations in TiNi element and crack initiation around borehole has been also made. Then the performance of the breaker using TiNi alloys with RSME will be discussed on the basis of numerical analysis and laboratory tests.

178. The Dynamics of the Simple Pulley SMA Heat Engine

Brian Berg

A loop of shape memory alloy wire undergoing a bending-induced pseudoelastic phase transition is analyzed. The analysis is a simplification of the dynamics of the simple pulley heat engine that uses a shape memory alloy as the working medium. The engine's mechanical and thermal dynamics are considered.

179. Characterization of Nitinol Material for a Bending Application

Dennis N. Petrakis

NiTi alloy, in the form of a rod, purchased from two different suppliers has been characterized for a bending application. The design properties of the material have been determined and the engineering requirements to create a materials specification have been established. Material characterization includes physical, mechanical and shape recovery properties. Shape recovery is determined for tensile, compressive and bending modes within the transformation range. Relationships established include: Effect of strain (tensile and compressive) and heat treatment on the transformation temperature utilizing both Differential Scanning Calorimetry and Thermomechanical Analysis. Effect of heat treatment and thermomechanical cycling on tensile shape recovery. And finally, effect of thermomechanical cycling on bending shape recovery.

180. The Two-Way Effect in Homogeneous Alloys and Composites for Robotic Applications

Kurt Escher, Erhard Hornbogen and M. Mertmann

Three different ways are known to induce the two-way effect (TWE):

1. In one phase: The intrinsic effect is caused by lattice defects inside a single phase metallic material.
2. In two phase materials: A reverse shape change is realized by internal stresses which originate in a second phase added as component of a composite material.
3. In a system consisting of two separate parts: Two separated elements (SMA and non-SMA springs) are necessary for a biased TWE.

A comparison has been made for the unbiased effects using an NiTi-base alloy and a composite with a silicone elastomer. The two-way shape change achieved by a training process was analyzed. The relaxation of the effect by repeated thermo-mechanical cycling (fatigue) was also studied. Investigations have been made for unconstrained, constrained and mixed boundary conditions. The TWE was trained-in in longitudinal direction and determined by dilatometric measurements. During heating the specimens were allowed to contract freely for different fixed amounts until a base was reached which impeded the final shape change. The resulting force depends on the primary shape change. It was measured by a load cell. The thermo-mechanical fatigue behaviour of the specimens was investigated by dilatometry and microscopy. The results from the elements with the intrinsic TWE were compared with those of the composite materials. A systematic description is given for the microstructural causes of the effect. The experimental conditions correspond to the loading conditions in control elements or fingers of mechanical hands: 1. Closing (movement); 2. Gripping (force exertion); 3. Opening (reverse movement).

181. Stability of the Memory Effect and Mechanical Fatigue of NiTiCu and NiTi Elements

Peter Tautzenberger, Hans-Peter Kehrer, H. Nubkern and H.H. Kocher

The stability of the Memory-effect depends on a lot of parameters like magnitude of effect, stress, temperature range, overheating and design of device. The present contribution deals with the stability of the Memory-effect as a function of some of the above mentioned parameters for straight wires, helical springs and bending strips. It will be shown that the stability of the Memory-effect is severely influenced by the design of the device for a given application.

In most applications elements with a Memory-effect have to realize a certain magnitude of mechanical work. That means that they have to overcome a certain stress on heating for each thermal cycle. Therefore it is useful to know essential data on mechanical fatigue. The present work deals with some results of mechanical cycling of shape memory wires, helical springs and bending elements in the austenitic state. The tests have been extended to high strains so that one can see even some results referring to superelastic applications.

182. The Shape Memory Effect of Ni-Ti for Electrical Connectors

Heinrich Ehrenstein

Solderless electrical connections for Hf-radio-antenna applications using the SME of NiTi are produced. High reliable electrical connections which prevent transmission resistance for consumer applications need special tools in order to work with NiTi sheet. The one way SME is used in the design of different connections. The permanent elastic load of the NiTi part at the electric conducting areas of the wiresurface leads to well connections under difficult conditions. For heat treatment of the NiTi sheet while mechanical work Hf-induction and water cooling is used. A Discription of the Patent DE-GM 9012051 is given and the Tools for mass production of such plugs from NiTi sheet are expained.

183. Industrial Control of Transformation Temperature of Shape Memory Alloys: Comparison Between Ti-Ni and Copper-Based Alloys

Bernard Prandi

Thanks to their properties, the shape memory alloys are known as well by the research laboratories as by the consumers, even if all the possible industrial applications have not been developed yet, due to industrial difficulties in the control of the transformation temperatures (A_s and A_f on heating).

The purpose of this paper is to describe the experience of MEMOMETAL regarding the mastery of the A_s temperature in industrial applications of TiNi, CuZnAl and CuAlNi based shape memory alloys.

Using different methods of characterization as DSC, Thermoelectrical power, X-rays, tensile tests, ..., several factors like the basic chemical composition, the homogeneity, the impurities, the process route, the external stresses and the heat treatments are discussed.

With the industrial process developed by MEMOMETAL, the wanted A_s temperature is reached with a maximum variation of $\pm 3^\circ\text{C}$, depending on the alloy category.

184. A Tribute to Adolf Martens

Horst Czichos

Adolf Martens is considered together with personalities like Le Chatelier, Howe, Osmond, Roberts-Austen, Sorby, Stead and Tschernoff as one of the founders of metallography in the 19th century. In this tribute a short portrayal of his life and work is given.

Adolf Martens, born March 6, 1850 received an engineering education at the Royal Industrial Academy Berlin after a practical training at a machine factory, and joined in 1871 the engineering staff of the Royal Prussian Railways. There he worked in the fields of iron and steel structures and quality control of railway components. In 1884 he was appointed Head of a small Mechanical-Technical Testing Institute. This institute merged with a Chemical-Technical Testing Institute and a Test Office for Civil Engineering Materials to form in 1904 under the directorship of Adolf Martens the Royal Material Testing Office - a predecessor institute of the present Bundesanstalt für Materialforschung und -prüfung (BAM). Adolf Martens was appointed Professor in 1889, Member of the Royal Academy of Sciences Berlin in 1904 and received a honorary doctor's degree from the Technische Hochschule Dresden in 1905. After a life full of scientific-technological work and the successful establishment of the Royal Materials Testing Office, as one of the leading institutions of its kind worldwide, he died on July, 24, 1914. In appreciation of his important research work, Osmond termed the "martensitic" structure of steel after him.

185. A Tribute to Zenji Nishiyama
Shen'ichi Sato

Professor Zenji Nishiyama, one of the great leaders of the world-wide martensite community, passed away on March 12, 1991 at the age of 89. He had been eager to attend this conference, but unfortunately and regretfully, he could not make it. It is a great honor for me to recall his memory as one of his disciples at this conference, ICOMAT-92.



186. A Tribute to Vissarion Sadovsky
Alexander L. Roytburd

187. Materials Design: Building a Better Martensite
Gregory B. Olson

188. A Century of Martensite
Morris Cohen

189. A Phenomenological Model for Magnetically Driven Lattice-Distortive Transformations in Fe-Pd Alloys
Po Hong and Gregory B. Olson

A Landau model including both the magnetization vector \vec{M} and the two-dimensional deviatoric strain tensor (e_1, e_2) as order parameters has been developed and applied to Fe-Pd alloys in which a weakly first-order FCC-FCT phase transformation is known to occur after magnetic ordering. A set of model parameters pertaining to Fe-30Pd is determined from experimental data. In particular, the magneto-elastic coupling constant B_2 in the term $B_2 M^2 (e_1^2 + e_2^2)$ can be determined by the difference between values of the shear constant C' measured by ultrasonic and neutron scattering experiments. For the Fe-30Pd alloy, it is found that the appearance of deviatoric magnetostriction strain and a change of easy magnetization axis occur at a well-defined temperature above T_0 for the FCC-FCT structural phase transformation. The magneto-elastic coupling causes softening of the shear constant C' and defines a parent phase lattice instability temperature T_1^p at a critical magnetization.

190. Local Softening of Parent Phase Within the Incubation Period of Isothermal Martensite Transformation in an Fe-Ni-Mn Alloy

Zhang Jihua, Chen Shuchan, Xu Zuyao (T.Y. Hsu) and Chen Weizhong

The low frequency internal friction associated with the isothermal martensitic transformation in an Fe-23wt%Ni-3.5wt%Mn alloy at the temperature range of -20°C to -150°C has been measured by the use of an automatic inverted torsional pendulum. Under the condition of continuous cooling, the rise of internal friction begins within the incubation period and there appear two internal friction peaks at 0°C and -50°C respectively. The 0°C peak may be a pre-isothermal martensitic transformation and the -50°C peak shifts to a lower temperature, while the Q^{-1} value increases with the increase of cooling rate. During the isothermal holding, there appears a maximum internal friction value, corresponding to a minimum frequency at the very beginning. Between the temperature range of -20 and -70°C the maximum of the isothermal internal friction at the beginning increases with the decrease of the isothermal temperature. Consequently, it is suggested that there exists the nucleation process within the incubation period on the TTT-diagram, activated by local softening of the parent phase with an activation energy of only about 3925 J/mol .

191. A Lattice Dynamical Study of the Martensitic Tetragonal-Monoclinic Transformation of Zirconia

Sai-Kit Chan and C.H. Chen

A martensitic transformation usually consists of one or more shears accompanied by a volume change and some relative sublattice movements called shuffles. The question of whether the shears or the shuffles are driving the transformation is often controversial. To unravel the mechanism for the technologically important tetragonal-monoclinic transformation of zirconia, a lattice dynamical study has been carried out for the tetragonal phase at the temperature of transformation. By comparing the relative sublattice displacements so obtained with X-ray diffraction data on the atomic positions of both the tetragonal and the monoclinic phases, it is found that the shuffles correspond to five lattice modes of different frequencies and two symmetry types with wave vectors corresponding to the Brillouin zone boundary point M. These five zone boundary modes acting together effect the correct sublattice movements that double the period of the unit cell leading to the monoclinic phase. Since five modes of two symmetry types are activated simultaneously, it is suggested that these modes are secondary motions coupled via anharmonic interactions to the shear that drives the tetragonal-monoclinic transformation.

192. Nesting Features of Fermi Surfaces in β -Phase Shape Memory Alloys

I.I. Naumov, O.I. Velikokhatny, V.Z. Bashirova and Vladimir N. Khachin

In recent years the weighty evidence has been obtained to support the idea, that at least premartensitic phenomena in β -shape memory alloys are closely related to the nesting features of the Fermi surface (FS) and to the occurrence of Kohn-like anomalies. In order to investigate the FS nesting features in such system the generalized susceptibility $\chi(q,0)$ and different cross sections of FS were calculated for CuZn, NiAl, AuCuZn₂, TiNi, TiPd, TiPt alloys (the first principle LMTO method). The Ti-based and β -Hume-Rothery phases were found to exhibit similar behaviour, which was unexpected. Namely, the q -dependence of $\chi(q,0)$ in the two classes of materials were similar all over the Brillouin zone, except for q -areas adjacent to the $[111]$ -type directions. In all β -phases $\chi(q,0)$ shows the maximum along $[100]$, $[110]$ and $[112]$ directions at a distance of two-thirds to the Brillouin zone boundary (in NiAl this distance is some less). It's worth noticing, that the vectors $2/3[110]q_{\text{max}}$ and $2/3[112]q_{\text{max}}$ characterize a number of structural anomalies, in particular, phonon ones, X-ray and electron diffuse scattering.

193. Elastic Properties of Single Crystals of $\text{Ti}_{50}\text{Ni}_{50-x}\text{Fe}_x$ Alloys

Vladimir N. Khachin and S.A. Muslov

Elastic properties of single crystals $\text{Ti}_{50}\text{Ni}_{50-x}\text{Fe}_x$ ($0 < x < 50$) were investigated. It was found that the behavior of elastic constants C_{44} and $C' = \frac{1}{2}(C_{11} - C_{12})$ are normal ($dC_{44}/dT < 0$, $dC'/dT < 0$) in $\text{Ti}_{50}\text{Fe}_{50}$, $\text{Ti}_{50}\text{Ni}_{25}\text{Fe}_{25}$, where martensitic transformations (MT) are absent. With the increase of nickel content and implementation of MT B2 \rightarrow R, ($x=5$), B2 \rightarrow R \rightarrow B19' ($x=2$) in the alloy the behavior of elastic constants changes gradually: $dC_{44}/dT \approx 0$ and $dC'/dT \approx 0$ ($x=15$), then $dC_{44}/dT > 0$ and $dC'/dT > 0$ ($0 < x < 5$). Thus, lattice "softening" precedes implementation of MT in B2 intermetallic compounds of titanium. Moreover, the lattice "softening" takes place in all crystallographic directions simultaneously.

194. Landau Theory of Premartensitic Transformations in TiNi Alloys

Yu.S. Zolotukhin and Vladimir N. Khachin

Landau theory is used for description of structural phase transformations in TiNi alloys which are realized in two-channel scheme $B_2 \rightarrow (\text{ISS } 1,2) \rightarrow (\text{R}, \text{B19}) \rightarrow \text{B19}'$. Intermediate structures of shear (ISS) are formed in the result of atom displacement with wave vector k and polarization e_k $1/3\langle 110 \rangle_k$ $1/3\langle 110 \rangle_{e_k}$.

$1/3\langle 112 \rangle_k$ $\langle 11\bar{1} \rangle_{e_k}$ and $1/2\langle 110 \rangle_k$ $\langle 1\bar{1}0 \rangle_{e_k}$. For all stages of structural transformations the changes of symmetry are determined, are realized the parameters of order, obtained induced representation compositions in the space of atom displacements. Also irreducible representations responsible for structural phase transformations are determined. Thermodynamic potential are constructed also tensor of spontaneous deformation, elastic constants and some other physical properties are calculated.

195. Strain-Induced Interaction and Blocking Effects of Nitrogen Atoms in Fe-N Austenite and Martensite

V.G. Gavriljuk, Vladimir N. Nadutov, Valentine A. Tatarenko & C.L. Tsynman

The model is considered, in which an influence of impurity N-atoms and of the temperature change on the lattice periods of the elastically-anisotropic crystal of Fe with the initial cubic symmetry. It was shown by the numerical analysis for Fourier components of the energy of the long-range indirect (strain-induced) interaction of N-atoms in their interstitial solid solution based on the f.c.c. crystal of Fe that the total energy of such interaction of a single selected N-atom with the other ones is equal to -2.1eV at 1428K and does not exceed the total energy value for the short-range direct ("electrochemical") N-atoms repulsion (3.5eV). The own introduction energy of each N-atom within the octahedral interstices was estimated as 2.53eV at 1428 . Values of the corresponding energy parameters for N-atoms in the b.c.c. crystal of Fe are changed greatly at the temperature (T) increase. Within the nearest and next-nearest interstitial coordinational spheres the N-N electrochemical repulsion dominates over the N-N strain-induced attraction. The correlation between the interaction character and N-atoms distribution in austenite was determined.

196. The "Premartensitic" Superstructures of Trigonal Symmetry

B.B. Khaimson, A.I. Potekaev and Yu.I. Paskal

There are some evidences in the literature that martensitic transformation in TiNi based alloys places not in B2 structure, but in the more complicated superstructures. In order to explain the experimental data, a peculiar superstructure with spatial group $P\bar{3}m1$ was supposed by Wang et al. The Wang's hypothesis remained nondeveloped, however. Our analysis has shown that a great number of superstructures with the spatial group $P\bar{3}m1$ and trebling of translation vector in cubic axes are found to be feasibly existed. These superstructures are very similar to each other in the energetic and thermodynamic sense. They can be simultaneously realized in a wide range of interatomic interaction parameters or replace each other while changing alloy composition and temperature. These superstructures may be treated as superpositions of plane static concentration waves with the wave vector $1/3 [111]$, $2/3 [111]$ and $[111]$. The concentration waves are accompanied by plane longitudinal static displacement waves of the same symmetry. Proceeding from the symmetry considerations, the displacement waves must be accompanied by atomic ordering when the atom mobility is sufficient. Each differential effect to be treated as a displacement mode can be compared with concentration mode of the type under consideration. It enables some experimental results to be explained, in particular, the small value of order parameter in nighitemperature phase to be treated as B2 structure and evidences of the role of concentration inhomogeneities in R(w)-phase formation

197. Pretransition Phenomena, Nucleation and Martensitic Crystal Growth in Alloys and Compounds with Martensitic Transformations

V.G. Pushin, V.V. Kondratyev and Vladimir N. Khachin

The mono- and polycrystals of various alloys and compounds with thermoelastic and unthermoelastic martensitic transitions were studied by in situ HREM, electron and X-ray scattering, measurements of elastic constants and mechanical tests. Evolution of parent crystal structure before martensitic transition, nucleation and growth of martensitic nuclei and properties were investigated in wide temperature and composition intervals. It is shown that premartensitic instability are accompanied by dynamical and then quasistatic and static displacements of atoms together with softening of elastic constants and phonon modes. Displacements of atoms are increased to approach to martensitic point and form special microdomains with short order of displacements (SOD) and intermediate local substructures of shear (ISS) by type of martensitic phases. It is found that SOD or ISS domains are the real nuclei of martensite crystals. Microtwins and antiphase domains inside martensite could be described in terms of combined mechanism of crystal growth from many nuclei of SOD and/or ISS and long-period elastic accommodation of spontaneous strain. A new "nonclassical" mechanism of nucleation is observed by in situ HREM in different materials.

198. Process of the Phase Structure Formation with the Properties of the Hologram Memory in Materials with the Stress-Induced Martensite: Mathematical Model

E.N. Bondaryev and V.V. Doudoukalenko

Oscillations of the solids with the stress-induced martensitic transformation are studied. External action is supposed to be stable and to have a constant oscillation frequency. The material is brought to the premartensitic state by means of static external stresses or by cooling. The vibrations cause the martensitic transformation and form an inhomogeneous phase structure that corresponds to the wave field and changes the natural frequencies and oscillation modes. Thus the dynamic process forms an attractor corresponding to the structure for which the frequency and the mode of the forced oscillation becomes natural and resonant. Due to the hysteresis in the material with the stress-induced transformation the above attractor will not be destroyed when the external dynamic forces cease their action. So the oscillation record takes place. When the vibration is applied again the material "responds" only to the frequency resonant for the structure formed. A mathematical model of this process is constructed. Analogies with a hologram associative memory are investigated. Possibilities of the repeated oscillation records are shown and the conditions of their reproduction are formulated.

199. Molecular Dynamics Study of Martensitic Transformations in B2 Phases with Defects

V.V. Kulagina and M.F. Zhorovkov

Using the Parrinello-Rahman Lagrangian, molecular dynamics computer simulations of the martensitic transformations in B2 phases containing simple defects have been performed. Our study is based on idea of the modulated lattice relaxation model regarding defects as a possible embryos of the low temperature martensitic structure in the parent phase. We considered substitutional defects caused by deviation from the stoichiometric concentration or/and defects caused by atomic disordering. It has been shown that the static lattice distortions around defect can both stabilize B2 structure and stimulate martensitic transformation in dependence of defect type and orientation. Two structures having an inessential energy difference were obtained in a process of the dynamics computations. Basic cell of the metastable phase contains 18 atoms and has R-phase symmetry, but the final structure is hexagonal one. In the martensitic phase, the strain fields have been localized in the vicinity of structural defects. The defects harmonize well with the formed martensitic structure. The effect of the periodic boundary conditions on the results of the computer simulations is also discussed.

200. Mobility and Structure of FCC-HCP Martensite-Austenite Interfaces

S. Chen, Philip C. Clapp and Jonathan A. Rifkin

The structure of the lowest energy interface between an hcp austenite phase and an fcc martensite phase of similar atomic volumes has been simulated by annealing a disordered region between the two perfect lattices until semi-coherent intergrowth occurred. The two structures were oriented so that the close packed planes were parallel. The dynamics of this interface and the structure which it evolved as it moved was then studied and analyzed. Embedded Atom Method many body potentials and Molecular Dynamics simulations at different temperatures were utilized. The results will be displayed with the help of computer movies.

201. The Effect of Rapid Solidification on Shape Memory Behaviour of a Copper-Based Shape Memory Alloy

J.H. Zhu, Druce P. Dunne, G.W. Delamore and Noel F. Kennon

CANTIM 125 is a Cu-Al-Ni-Ti-Mn alloy which is commercially produced as a high strength, high temperature shape memory (SM) alloy. Although some grain refinement is achieved through the presence of coarse X-phase $[(\text{CuNi})_2\text{TiAl}]$ particles, the grains in hot rolled strip are still relatively large ($\sim 200 \mu\text{m}$) and the ductility remains limited. In the current investigation, a rapid solidification technique - planar flow casting - was employed to form thin strip directly from the molten state, and to produce marked refinement of the parent β grain size. An average grain size of $2.4 \mu\text{m}$ was obtained and the formation of both coarse and fine X-phase precipitates was suppressed. Using DSC thermal cycling and repeated bend tests, the transformation behaviour and shape memory effect in rapidly solidified ribbons were examined. A reproducible shape memory effect was clearly shown in the ribbon samples. The transformation temperatures for both forward and reverse transformations were much lower than those of bulk material formed conventionally. However, melt spun material which was reheated to 900°C then quenched in 5% KOH solution showed neither reproducible transformation characteristics nor shape memory effect on thermal cycling, as the martensite started to decompose by tempering rather than reverting to parent phase. It is concluded that the type and distribution of X-phase precipitates, formed in the melt spun ribbon at 900°C and on quenching, adversely affected the reversibility of the martensitic transformation, which is highly sensitive to the state of X-phase precipitation.

202. The Crystallographic Analysis of WLR Method on BCC to 9R or 18R Transformations in Cu-Base SMA

Wang Baoqi, Gu Nanju, Yin Fuxing, Wang Ruixiang and Zhang Jianxin

Using WLR method a crystallographic analysis on BCC to monoclinic structure transformations has been developed. With the aid of computer the habit planes, the magnitudes of the invariant lattice shear, and the rotation matrices, the shape deformation directions, the total transformation relationships between martensite and parent phase have been calculated for five alloys and are in good agreement with the observed results.

203. Twinned Structures in Terfenol

Richard D. James and David Kinderlehrer

Terfenol-D, $Tb_xDy_{1-x}Fe_2$, with $x \approx .3$, is an iron/rare earth alloy which is particularly attractive for actuator applications owing to its huge magnetostriction and small magnetomechanical losses. Like many martensitic and shape memory materials, it exhibits a complex highly mobile domain structure consisting of structural domains, although magnetic domains play a role as well. Typical growth habits result in configurations with parallel twinned layers. These layers persist in the magnetostrictive process. We describe here a theory based on our work related to martensite and apply it to accurately account for the observed microstructure of Terfenol-D¹.

204. The Atomistic Processes of the Martensitic Transformation of Fine Iron Precipitates in Copper Alloys by Cold-Rolling

Iwao Ishida (WITHDRAWN FROM THE ORAL PROGRAM DUE TO ILLNESS)

The $\gamma \rightarrow \alpha$ transformation of fine, coherent iron precipitates in single crystal copper alloy by cold-rolling has been investigated by the electron microscopy and the magnetic method. Cold-rolled along the $(101)_f[010]_f$, the transformed α -iron particles had the Pitsch orientation relationship with the matrix and the shape expected from the Pitsch transformation mechanism, and the magnetic anisotropy expected from the coercive force also corresponded to the oblate spheroidal α -iron particles expected from the Pitsch mechanism. Cold-rolled along the $(101)_f[101]_f$, the α -iron particles with the same orientation relationship and shape were also observed. Thus, it was concluded that the atomistic processes of the $\gamma \rightarrow \alpha$ transformation of fine γ -iron particles are those proposed by Pitsch.

205. Discussion on Invariant Habit Planes of Martensites

Gu Nanju, Wang Ruixiang, Yin Fuxing and Zhang Jianxin

Using vector algebra, the strain tensor and the vector displacement in lattice deformation of martensitic transformations have been deduced and used to analyse the crystallographic features for martensitic transformations. It was found that the strain tensors of twin and matrix in a twinned martensitic plate are different for which the shear components are opposite roughly, so that the strain energy would reduce and the growth of twinned martensitic plates may be with the aid of the self-accommodation for twin and matrix, along the normals of the twinned planes. According to the analysis upon the vector displacements of the normals for different habit planes, the $\{10,3,15\}_f$ plane could make up a macro-invariant habit plane, since the effect of the self-accommodation. But the $\{575\}_f$, $\{111\}_f$, $\{252\}_f$ habit planes would be very difficult to make up the invariant planes, since their normal's displacements being larger and without any variants in a martensite as well as the self-accommodation. In addition, if the plastic-accommodation of parent phase could take place completely, the $\{575\}_f$ habit plane could make up, however it may not be a invariant plane.

206. Conjugation of Lattices at Martensitic Transformation in TiNi

Vladimir N. Khachin, V.P. Sivokha and Yu.S. Zolotukhin

Regularities of martensitic transformations in $Ti_{0.5}Ni_{0.5-x}Me_x$ ($x=0.4-0.5$), $Me=Fe, Co, Pd, Pt, Au, Cu$) alloys are determined. In the above mentioned alloys (depending on the composition) there are realized four consequences martensitic transformations: $B2 \rightarrow B19$, $B2 \rightarrow B19 \rightarrow B19'$, $B2 \rightarrow R \rightarrow B19'$, $B2 \rightarrow B19'$. Using geometrically non-linear tensor of deformation the value of lattice deformation and directions of its main axes for each transformation consequence are calculated. It is detected that in martensitic transformation $B2 \rightarrow B19 \rightarrow B19'$, the lattice deformation is realized with microscopic invariant plane-ideal coherency crystallographic orientation and phases turn angles relatively to each other are calculated.

207. Possible Mechanism of Polymorphic Transformation in Interstitial Alloy
Vladimir N. Bugaev, V.G. Gavriljuk and Vladimir N. Nadutov

The injection of the impurity interstitial atoms into the host crystal lattice and their redistribution among the interstices can be the reason of the production of the large numbers of vacancies due to the interaction between the interstitial and matrix subsystems. Consequently, the interstitial alloy can become unstable and the transformation of matrix into another polymorphic modification with the less amount of structural vacancies which is energetically more preferably can take place. This idea is improved in the case of f.c.c.-h.c.p. transformation in Fe-N austenite. Statistical-thermodynamical calculations were carried out within the theory of the strain-induced interaction in interstitial alloy.

208. Nucleation and Growth of Butterfly Martensite in Vanadium and Carbon Bearing Iron-Nickel Alloys
Q.Z. Chen, X.F. Wu and Tsun Ko

The effect of inhomogeneities formed on ageing in an Iron-Nickel alloy containing approximately 27% Ni, 1% V and 0.05% C on the formation of butterfly martensite and its fine structure have been examined by TEM and interpreted from the viewpoint of the nucleation effect of the strain field of carbon clustering or V-C precipitates and their retarding effect on the growth of nucleated martensite. The interplay between the stress field, spontaneous deformation of austenite and the formation of the martensite wings and then subunits is discussed. Martensite nuclei consisting of regions enveloped by dislocations with Burgers vector $1/2 [011]_{f.c.c}$ with piled up dislocations with Burgers vector $1/2 [110]_{f.c.c}$ within have been observed, with a structure lying between f.c.c and b.c.c due to the dislocation distortion. In situ observation of their transformation to martensite by cooling and stressing showed that further cooling to a certain temperature and stress field introduced by the formation of a nearly martensite plate cause the nuclei to develop into martensite. Tensile stress also caused new nuclei to form and grow. The result of transformation developed from the dislocation structure is a butterfly martensite wing with a Kurdjumov-Sachs relation.

209. Computer Simulation of Phase Transition Process
J.Q. Zhou and Jianxi Rao

This paper discusses the martensitic transition process simulated on a computer. Based on the experimented fact that the habit plane in crystal is an invariant plane when the phase transition is developing, the phase transition process can be simulated. In terms of measured data that indicate habit relationship between the initial phase and the martensitic phase, this paper gives the more reasonable transition mechanism of the proposed. It settles the problem in Solid Physics that the phase transition can only be imagined but can't be observed.

210. Shear-Rotation Mechanism of Martensite and IPS Crystallographic Theory
Shidao Wang, Xiumu Zhang and L.F. Wang

A semi-twin shear combined a rotation strain mechanism of martensitic transformation has been proposed. The shear-rotation mechanism not only results in the required structure of α' or ϵ martensite, but also may be used to formulate a quantitative crystallographic theory. The results predicted by the present theory are in good agreement with the experiments and the ones calculated from the phenomenological crystallographic theory.

211. Crystallographic Analysis of Martensites Throughout an Austenite Grain

Fugao Wei, X.Y. Huang, J.Z. Wu, B.Z. Lou and F.S. Shen

The SEM examination of the fracture of 300M steel prepared by quenching and tempering found that the rather "random" martensite structure transforming from an austenite grain seemed to have a nearly-parallel lower index crystallographic plane along which cleavage was able to propagate through a martensite packet or the whole austenite grain smoothly because it was found that cleavage facet was nearly flat and was of a size equivalent to a packet or even the whole prior austenite grain. Results of crystallographic analysis indicate that if consider all the martensites obey K-S orientation relationship (O.R.) and hence have 24 different martensite variants within the same parent phase, there exists a phenomenon termed "martensitic transformation orientation concentration (MTOC)" that 24 $\{100\}_m$ or $\{110\}_m$ planes from each of the 24 variants orient closely together with a mutual deviation of less than 25 degrees. There are at least three MTOC's in an austenite grain and at least seven within a packet whose mutual deviation is less than 20 degrees. TEM observation confirms that most martensites in steel possess a K-S, N-W or G-T O.R. although a packet is not composed of all the six variants on the same $\{111\}_A$. MTOC is instructive of understanding the cleavage across a packet and the whole austenite grain.

212. Crystallography of Self-Accommodating Martensite Plates in Fe-Ni-C Alloys

Shidao Wang, Y.H. Wen and Xiumu Zhang

Habit plane, orientation relationship and shape strain of self-accommodated martensite in Fe-29.37Ni-0.34C alloy have been determined by means of transmission electron microscopy, optical interferometry and composite photomicrograph. The crystallographic parameters have also been calculated using a new quantitative crystallographic theory. The results are in agreement with those calculated from W-L-R theory and measured experimentally.

In the new theory, martensite lattice is considered to produce in austenite by two processes: one is a homogeneous semi-fault shear in $(111)_f [11\bar{2}]_f$ direction and the other is a rotation strain around the normal of the $(111)_f$ stacking fault plane. Since the shear and rotation strain in both matrix and twin of martensite are on the same $(111)_f$ stacking fault plane and the directions are opposite, the invariant plane strain in the $\{3\ 10\ 15\}_f$ martensite transformations could be kept. One advantage of the new theory is that one to one crystallographic correspondence among different variants could be revealed. So it is convenient to study morphology crystallography of self-accommodating martensite plates.

213. Crystallography of Martensitic Transformation in 50Ni-13Ni-37Pd High Temperature Memory Alloy

Yong-sen Li, Y.B. Jin and Xiumu Zhang

On the basis of the phenomenological theory, the crystallography of the martensitic transformation in Ti50Ni13Pd37 high temperature memory alloy has been studied. The lattice parameters of B2 parent and B19 martensite for the alloy have been determined using X-ray diffraction. The parameters, a_0 , a , b and c are equal to 3.132, 2.772, 4.526 and 4.772 respectively. The crystallographic features of the martensitic transformation for $\{111\}_m$ twinning models have been calculated with computer. The ratio of twin thickness is approximately 3:1. The habit plane corresponding with the models was also calculated. The results are in agreement with the experiments.

214. HREM Study of the Martensitic Phase Transformation in Strained Si/Ge Superlattices on Ge(001)

Werner Wegscheider and H. Cerva

The lattice mismatch of about 4% between Si and Ge causes a biaxial strain field in Si/Ge short-period superlattices pseudomorphic either to Si or Ge substrates. In particular for growth on [001] oriented Ge substrates due to the crystallographic relationship between the in plane tensile strain and the inclined {111} glide planes, strain relaxation occurs through the generation of twin bands as the critical thickness for lattice coherency is exceeded. We have recently identified the mechanism of microtwin formation in Si_3Ge_9 superlattices — an alternating sequence of 3 monolayers (ML) Si and 9 ML Ge — deposited on Ge(001) by molecular beam epitaxy as nucleation and glide of 90° $\langle a/6 \rangle \langle 112 \rangle$ Shockley partial dislocations on adjacent {111} planes. This material system provides therefore the unique possibility to artificially produce these planar defects in a well defined way. Based on high-resolution electron images of twin intersections in such samples, where the transformation from the diamond cubic phase to polytypic phases takes place, detailed dislocation reactions which have to occur at the twin boundaries can be formulated. Dislocation reactions which involve only 60° perfect as well as 30° and 90° Shockley partial dislocations describe successfully the martensitic transformation which leads to diamond hexagonal Si inclusions previously observed in low temperature chemical vapour deposited polycrystalline Si and in hot-indentated Si.

215. Hysteretic Behaviour in SMA: A Model Based on Intrinsic Parameters

Antoni Isalgue, Francisco C. Lovey and Vincenc Torra

Through high resolution automatised equipment (close to 1 mN, 0.1 μm and 5 mK) detailed observations of the stress, strain, temperature (σ , ϵ , T) surfaces of Cu-Zn-Al shape memory alloys can be performed and local minor evolutive phenomena (micromemory effects) can be observed. The analysis of the experimental curves (single crystal, single variant with one or more martensite plates) allows to build a model of the behaviour of the alloy.

216. Random Internal Stresses and Thermoelastic Equilibrium in Shape Memory Alloys

A.A. Likhachev and Yu.N. Koval

The possibility of thermodynamical balance between martensite and parent phase in the wide temperature region between M_s and M_f is one of the central problem in martensitic transformation physics. In general, thermoelastic equilibrium in Shape Memory Alloys (SMA) is supposed to be a result of the local balance between so called chemical driving force $g(T)$ and mechanical driving force $\tau(\vec{x}) = \hat{\epsilon} \hat{\sigma}(\vec{x})$, where $\hat{\epsilon}$ is a structure distortion matrix and $\hat{\sigma}(\vec{x})$ is an internal stress tensor. In general case, $\hat{\sigma}(\vec{x})$ may always be expressed as a superposition of the internal stress $\hat{\sigma}_m(\vec{x})$ produced by martensitic crystals system; and the stress $\hat{\sigma}_R(\vec{x})$ produced by randomly distributed system of crystal defects. The main aim of present paper is to develop a general method for theoretical analysis providing a successful description of the equilibrium microstructure of martensitic crystals ensemble and macroscopic properties of SMA in the thermoelastic equilibrium state. It is shown, that equilibrium conditions are satisfied if only the martensite is located in the region, where $g(T) < \tau(\vec{x})$ and $\tau(\vec{x})$ must satisfy a special nonlinear equation. To solve this equation, a convenient approximation method is proposed in present work.

217. On the Dynamics of Coherent Martensitic Phase Boundaries

A. Yu. Pasko and Yu. N. Koval

Kinetic features of diffusionless phase transformations in solids and dynamic properties of heterophase systems are largely governed by mobility of phase boundaries (PB). Coherent PBs can be treated as singular interfaces in terms of the theory of elastic physical continuum. Unlike [1], in the present work the complete set of evolution equations describing the self-consistent dynamics of PBs is derived immediately from balance relations of the non-equilibrium thermodynamics, which enables to take account of dissipative processes going on boundaries and within each phase. The uniform translational motion and small flexural vibrations of a single plane PB are considered. The free moving PB is shown to experience drag due to dynamic excitation of elastic and heat waves in the crystal. The total drag force is determined by the spontaneous strain and the entropy of the martensitic transformation, mechanical and thermal characteristics of the medium and depends on the velocity of the PB and its orientation with respect to the transformation invariant plane. Vibrations of the restricted PB are described in a linear approximation by the integro-differential equation of motion which corrects and generalizes the non-local membrane model [1].

[1] A.T.Kosilov, A.M.Perevoznikov, A.M.Roshchupkin: *Poverhnost* 10 (1983) 36; *Izv. Vuzov. Fiz.* 5 (1985) 54.

218. Thermodynamics of Acoustic Emission in Thermoelastic Martensite Transformations

V.A. Plotnikov, L.A. Monassevich and Yu.I. Pascal

The analysis of the acoustic emission contribution to a differential equation of the first principle of thermodynamics for the temperature cycle enables us to draw a conclusion, that a system involving a cyclic process, particularly, a cyclic martensite transformation, is an acoustic generator. In terms of the second principle of thermodynamics the acoustic emission is a channel of energy dissipation and entropy production, contributes slightly into the irreversibility of the system characterized by the area of the temperature hysteresis loop. The aggregate of experimental findings accumulated by now enables us to draw a conclusion, that generation of acoustic signals, different from the thermal noise in the martensite transformation, involves transformations of the "nonchemical" energy. The direct transformation of the lattice vibration energy into the "chemical" one, caused by alteration of the ideal crystal structure, gives a negligible contribution into the registered emission energy. In terms of quasiequilibrium description of the martensite transformation the acoustic radiation, accompanying the transformation, involves local instabilities that correspond to nonmonotonies of the quasiequilibrium state curve on the graph of the components of the process moving force against the portion of the martensitic phase. In such terms basic microscopic processes, responsible for emission during the martensite, may be described: the plastic relaxation of transformation stresses (accumulation of the phase cold hardening), the microexplosive generation - collapse of martensitic crystals, the relaxation in the reverse martensite transformation of the "nonchemical" energy, accumulated during the direct martensite transformation.

219. Mathematical Modelling for the Constitutive Behavior of Shape Memory Alloys

Sun Qing-ping and Hwang Keh-chih

In the present paper, by taking the constitutive element of material as the subject of study and applying the micromechanics, thermodynamics and internal variable constitutive theory, the macroscopic thermomechanical constitutive behavior of SMA at different temperatures is investigated quantitatively. The effect of microstructural physical mechanisms such as internal stress, elastic strain energy, twin boundary displacement and interface friction etc. upon the macroscopic behavior in the process of transformation or reorientation is taken into account in the present theory, making it possible to describe and to interpret the various phenomena by a unified interrelated model. The derived constitutive law is for the general complex loading paths, and it is simple in form and hence quite applicable. Various phenomena of SMA such as superelasticity, ferroelasticity, rubber-like elasticity and shape memory effect etc. are studied in detail by applying the theoretical model developed above. It is shown that the proposed theory can satisfactorily simulate the main features of the macroscopic behavior of SMA in the course of uniaxial mechanical loading as well as thermal cycling and acceptable agreement between theory and experiments is obtained. Finally, some theoretical predictions and discussions for the complex loading paths are also given which are yet subject to experimental verification.

220. Factors Influencing the Reverse Martensite Transformation in a Step-Quenched Cu-Zn-Al Alloy

Yin Fuxing, Wang Baoqi, Wang Ruixing and Gu Nanju

A martensite microstructure step-quenched to room temperature in Cu-24.97Zn-3.87Al(wt%) alloy was adopted for the study of the reverse martensite transformation. Electric resistivity measurement shows that ageing above A_f temperature or thermal cycling between M_f below and A_f above treating of the microstructure could prohibit the occurrence of parent phase with the increase of A_s temperatures. With X-ray diffraction and electron microscopy analysis, some discoveries were made on the martensite order degree and variant interface characteristics in microstructures corresponding to different treatments. It was concluded that among the factors influencing the reverse martensite transformation, such as martensite order degree, plane defects in martensite and the variants interface characteristics, the last one was considered to be predominant in influencing the nucleation of parent phase.

221. Thermodynamic Prediction of M_s Temperatures of Fe-Mn-Ni-C Alloys

Xu Binshi and Zhang Ping

In the area of thermodynamics of martensitic transformation, the published papers were concentrated on binary or ternary systems such as Fe-C, Fe-Mn-C, Fe-Ni-C, Fe-Cr-C and etc. The present paper develops the thermodynamics of martensitic transformation in Fe-Mn-Ni-C, and predicts the M_s temperatures of the materials in the system. Several thermodynamic models were utilized in the research, especially Fisher's, KRC, LFG, all of which were combined with Zener's treatment. As compared with the data obtained experimentally, the thermodynamically predicted M_s temperatures were successfully consistent with them.

222. Experiments and Modeling of Partial Hysteresis Loops in Thermoelastic Martensitic Transformations (WITHDRAWN)

Jordi Ortin

223. Local Atomic Arrangements of Fe-Ni Steel

B.D. Butler and Jerome B. Cohen [TO BE PRESENTED BY G.B. OLSON]

There is no significant local order or clustering involving Fe and Ni in the austenite phase of Fe-26 pct. Ni -0.9 C and more conclusive data have been obtained that C atoms are in octahedral sites in a similar steel (in Fe-13 pct. Ni, 1 pct C) than was available. The displacements of Fe atoms around a C atom have been measured for the first time out to several neighbors and from these experiments a new Fe-C potential has been obtained directly. A high density of {011} twins occurs on transforming to martensite, with a twin volume of 17(4) pct.

224. Some Aspects of the Behaviour of Virgin Martensite at Low Temperatures
Y. Liu and Juhani Pietikainen

Many works have been concerned with the behaviour of virgin martensite at low temperatures since 1960's, but few of them have been concentrated on the behavioural differences between different morphological type of martensites. In the present study, the low temperature behaviour of two different morphological type of martensites, thin plate martensite and lenticular martensite, have been studied by means of X-ray diffraction, electrical resistivity, Magnetic susceptibility and internal friction methods. It has been found that the behaviours were quite different between these two kind of martensites. The reason of the differences were due to the differences in martensitic substructures.

225. HREM Study on the Microstructures of the Membrane Stress Assisted Martensite in an Fe-Ni-C alloy at Low Temperature
Z.L. Zie and Juhani Pietikainen

Fe-20Ni-1.2C alloy was first cooled in liquid helium to form completed twin thin-plate martensite and then deformed by membrane stress at liquid helium temperature. The microstructures of the isothermal martensite formed under membrane stress and the crystallography relationship between the thermally formed thin-plate martensite and the isothermal martensite formed under membrane stress have been studied by means of optical microscope and high resolution transmission electron microscope.

226. Effects of Cold Deformation on the Morphology and Lattice Structure of Fe-Ni-C Thin-Plate Martensite
Markku Nieminen and Juhari Pietikainen

Fe-25Ni-0.7C thin plate martensite samples were deformed in virgin state at -60 °C and after ageing at room temperature. Despite the relative high carbon content deformation degrees of 50-60 % were achieved without breaking the samples when virgin martensite was deformed. Optical microscopy studies revealed severely deformed martensite plates. Smooth, regular interfaces between austenite and martensite had become very irregular and the internal twinned structure of the plates was also changed. Beside morphological changes deformation mechanisms were also studied using transmission electron microscopy. Changes of lattice structure were observed with X-ray measurements. Because of deformation the tetragonality of martensite had disappeared and lattice had become cubic. This phenomenon was related to change of position of carbon atoms in the iron lattice and a new model is presented to explain this phenomenon.

227. An Acoustic Emission Study on Martensitic Transformation in Fe-Ni-C Alloy During Cooling and During Tensile Testing
Zhu Zuming, Long Q.Y., Zhang Xiumu and Li D.F.

The dynamic process of martensitic transformation (MT) in a Fe-29%Ni-0.15%C alloy during cooling and during tensile testing at different temperature has been studied by means of acoustic emission (AE). It is found that the process of MT during cooling has two stages; more than 80 pct of austenite has transformed into martensite in the first stage; the relation between the AE events H and the temperature T is $H = 1 / (a + b e^{-\alpha(M_s - T)}) - 1 / (a + b)$ in this stage, while in the second stage the relation between H and T is $H = C - d e^{-\beta(M_s - T)}$, where a , b , c , d , α and β are constant; in addition, the AE energy emitted by unit volume of martensite is lower in the first stage than in the second stage; the frequency spectra will shift to the higher frequency region as the MT proceeding from stage 1 to stage 2. It is also found that the MT during tensile testing is strongly dependent on the temperature; as the testing temperature is close to M_s , very strong AE activities produced by MT are observed even if in the elastic deformation stage; as the temperature increases, the AE activities emitted by the MT decreases; and the morphology of the transformed martensite is also gradually varies with the testing temperature; the analysis of the waveforms of the AE signals shows that different waveforms result from different morphology of the transformed martensite.

228. In-Situ and Continuous Observation of Transition of Martensite Morphology and Substructure in Alloy Fe-Ni-C

Gong Hai, Zhang W.Y., Wang Xiaochin and Zhang Xiumu

Up to now it is conceded traditionally that the martensite morphology or substructure is determined by the "formation temperature", the lath martensite is followed by the plate martensite and the slipping takes place before twining in the sequence of martensite formation. In this paper, the ordinary, in-situ and continuous observations are made for the mixed martensites in alloys Fe-23Ni-0.10C, Fe-24Ni-0.14C, Fe-29Ni-0.31C and Fe-30Ni-0.34C by means of optical and electronic microscopes. The continuous observation is recorded by a video under a differential interferogram with a low-temperature carrier controlled by a electronic computer. The results show that the sequences of martensite formation are butterfly \rightarrow plate \rightarrow lath, thin plate \rightarrow lenticular in the same a parent phase when the mixed martensites are formed mainly by plastic accommodation. A single martensite growth might appeared to be a complex formation during which the substructure might be transited. The sequence of substructure transition shows complete twin \rightarrow partial twin \rightarrow dislocation. It is found from synthetic analysis that the austenite yield strength and the austenite dislocation configuration play an important role on the shear mode and morphology transition of the martensite; a large number of dislocations produced by the plastic accommodation in the austenite block the formation and development of transformation twins. It can be considered that the relationship between the martensite morphology and substructure and the formation temperature is not essential.

229. Structure and Aging Behaviour of Iron-Nitrogen Martensite

V.G. Gavriljuk, Vladimir M. Nadutov, and Kari Martti Ullakko

Nickel-rich Fe-2.39N martensite is characterized by an abnormally high tetragonality at the freshly formed state which we assume to be caused by the coherent bond at the interface between virgin martensite and the ordered regions in retained austenite. Evidence for the imperfect Fe₄N structure in austenite was obtained by Mössbauer spectroscopy. This structure pointed out to undergo magnetic ordering between 100 K and 300 K. Tetragonality is decreased during ageing between 100 K and 200 K, which is accounted for by the break of coherency possibly assisted by some dislocation process. Tetragonality of the virgin Fe-7.3Mn-0.83N martensite is reduced slightly in this temperature range. According to the present measurements nitrogen atoms are redistributed above 200 K. This redistribution can be regarded as a long range atomic ordering before the precipitation of α'' phase without the formation of clusters.

230. Martensitic Transformation in Fe-31Ni-0.25C Steels Bordered Upon the Vacuum Condensate

A.G. Yakhontov, N.P. Kylosov, Z.H. Fuxman and V.I. Chumakov,

Thin martensitic plates with high anomalous tetragonality of the lattice appear in steels on the border of TiN influenced by the magnetic field. When heated up to 373 K the degree of tetragonality is reduced. Magnetic contents decrease 20 % nevertheless cementite is not found. Strips of phase contrast are observed in austenites on the border of martensitic crystals as a result of high stress. α - γ -transformation begins with the interphase borders and transformation duobles. The transformation results in the appearance of dislocations accumulations of high density left by the martensitic plate on the interface border. Martensitic contents halve when heated up to 473 K, the degree of tetragonality approximates to 1.008 and cementite is found. α - γ -transformation completes entirely at 673 K and it does at 773 K in check samples.

231. The Morphology of Martensites and Their Transiting Process

Wang Ruixiang, Gu Nanju, Zhang Jianxin and Yin Fuxing

The morphology of martensites and its changing law have been studied. The research results are as follows

- (1) The dislocation-M form first in low and medium carbon steels, however the twined-M may form first in higher carbon and high alloy steels.
- (2) The changing orders of its habit planes are with the increasing of the strength of parent phase being $\{575\}f \rightarrow \{111\}f \rightarrow \{252\}f \rightarrow \{529\}f \rightarrow \{10,3,15\}f$, generally.
- (3) The plate-M may transform into fine lath-M as well as their habit planes from $\{252\}f$ into $\{111\}f$, when the dislocation density of parent phase is very high.
- (4) The wide lath-M form at the grain boundary first and its sub-structure is dislocation of high density.
- (5) The change of martensitic morphology may depend on the competition between the plastic-accommodation of parent phase and the self-accommodation for different martensitic variants, such as twin and matrix in a martensitic plate, both of which result in the decreasing of strain energy. The dislocation-M form, when the plastic-accommodation of parent phase was dominant, however the twined-M form, when the self-accommodation of martensites variants was dominant. Using this viewpoint, the observed results of above may all be explained.

232. Effects of Heat Treatment Cycle on Martensite Formation in a Dual Phase Steel

H.K. Khaira, A.K. Jena and R.K. Ray

A steel containing 0.197%C, 0.98%Mn, 0.46%Si and 0.47%Cr was investigated. Three cycles, intermediate quenching (IQ), intermediate normalizing (IN) and step quenching (SQ) were such that the steel was martensitic, ferrite-pearlitic and austenitic respectively prior to intercritical annealing. The annealing temperatures were 750, 770, 790 and 810°C. The annealing time was 15'. The volume fraction of martensite at a given annealing temperature was minimum for the cycle, IN and maximum for the cycle SQ. The martensitic phase formed during the IQ cycle was globular, that produced during IN cycle was elongated and the SQ cycle generated large and lumpy regions. The IQ and IN cycles yielded highly dislocated laths of martensite arranged in packets. Two predominant lath orientations were observed. The laths found after SQ cycles were also dislocated, but many lath orientations were found. A few twins were detected after IQ and SQ cycles at annealing temperatures, 790 and 750°C. A partial equilibrium model which assumes no partitioning of substitutional solutes but partitioning of carbon, predicts volume fraction of martensite accurately at low annealing temperatures. The compositions of martensite predicted by this model are consistent with the observed microstructural features. The IQ cycle imparts the most favorable combination of properties to the dual phase steel.

233. Catalytic Formation of Butterfly Martensite

Q.Z. Chen, X.F. Wu, R.Q. Rong and Tsun Ko

Butterfly martensite forms from austenite in a suitable temperature range of Iron-nickel-Carbon alloy of certain composition. The butterflies show an autocatalytic effect with the result that they pile up in a row with almost equidistance between each other. It is proposed that this is the result of an interplay between nucleation in an inhomogeneous matrix and the stress field around the butterfly shaped martensite. This stress field has been estimated from a model of martensite in which two prisms with an obtuse-angled triangle section are coupled together and introduced into a prismatic hollow with dimensions smaller than the prisms by a volume corresponding to the austenite-martensite expansion. The elastic stress field caused by the expansion is then estimated by conformal transformation. Only volume expansion has been considered, as the multi-shear process of the transformation has reduced the stress field induced by shear to a value small enough to be neglected. The result shows that stress fields near the wing tip and in the region ahead of the butterfly are most favourable for the tensile nucleation of a new butterfly martensite plate in front of the previous one.

234. Thermoelastic Martensite in Fe-Ni and Fe-Co Based Alloys

Vladimir V. Kokorin

Ferrous aging alloys with the thermoelastic martensite were proposed in 1979. Particularly Fe-Ni based alloys with the composition being close to some maraging steels were studied. Among Fe-Co based alloys the ausaged alloys with thermoelastic $\gamma \rightleftharpoons \alpha$ transformation were offered also. Main factors which determine reversible character of the martensite transformation in Fe-Co alloys are the same as in Fe-Ni ones. The system of γ' -phase fine coherent particles is forming during ausaging. These inclusions being inherited by the martensite cause anomalously high tetragonality of its crystal lattice. The relationship between martensite crystal lattice tetragonality and $\gamma \rightleftharpoons \alpha$ temperature transformation hysteresis has been established: the higher tetragonality degree (c/a) corresponds to the lower thermal hysteresis. The observed increase of c/a on Ni content increasing can be explained by growing the volume fraction of γ' -phase inclusions.

235. Surface Microstructure and Fatigue Property of Laser Transformation Hardening Steel

Liu Changsheng and Cai Qingkui

The surface microstructure and fatigue property of laser transformation hardening low alloy steel was investigated. The microstructure was studied by light microscopy and transmission electron microscopy, experimental results show that the microstructure of hardened layers is inhomogeneous because of short duration of heat and the surface fine structure is twin martensite. The twins are also observed in plate martensite. These can be reduced by high phase transformation driving force and adjusting of local stress. Contrary to expectation, twin martensite has an advantageous effect on the fatigue property of low alloy steel. Fatigue tests were conducted on untreated and laser transformation hardened specimens, results indicated that case depth, microstructure and hardness of laser hardened surface layer are important parameters which affect fatigue property. Under selected technological regions, laser transformation hardening increased the fatigue life by a factor 4 while raising the fatigue limit by as much as 30 percent.

236. Technological Problems of Regulation of Structure and Properties in Martensitic Steels by Thermomechanical Treatment

Yurij D. Zhelesnov, Ljudmila M. Kaputkina and Sergei V. Dobatkin

237. Structure, Morphology and Transformation of Martensite obtained by Quenching after Laser Heating or by Splat-Quenching

Ljudmila M. Kaputkina and Sergei D. Prokoshkin

238. Structure and Properties of Maraging Steels Undergoing Thermomechanical Treatment

Alexander F. Edneral, D.M. Perkass and Vera G. Prokoshkina

239. Factors Affecting the Morphology and the Size of Martensite Crystals of As-Quenched Low-Alloyed Medium-Carbon Steels

Peng Zhifang, Huang Guanghua and Liang Huanwen

It was found through different heat treatments (including commercial-, single- and double-thermomechanical ones) that given chemical composition changing the dislocation density and controlling the dislocation mobility of austenite prior to quench would obviously change the morphology of martensite crystals of 40Cr and 45Cr steels. The martensite crystals formed in differently treated samples were characterized by exhibiting typical and/or anomalous laths and unformed laths plus plates in appearance, and by being dislocated and/or twinned in substructure, respectively. Besides, twins initiated from prior deformed-austenite could be inherited by martensite in quench. It was also found by double-revealing etching method that under the condition of reaching an equivalent prior austenitic grain size, two kinds of martensite crystals with remarkably different sizes could be obtained by using the single- and the double-thermomechanical quench treatments respectively. On the basis of physical metallurgy and dislocation theory, the above experimental results are explained, and a tentative quantitative analysis on the effects of the dislocation density in prior austenite on the martensite morphology is also discussed in this paper.

240. Evolution of Magnetic Field-Induced Martensitic Transformation

Vissarion D. Sadovsky and LN. Romashev

Recently in some of our investigations of the induced by a magnetic field ($\gamma - \alpha$) transformation in chromium-nickel steels with martensitic points displaced to the liquid helium temperature the important phenomenon has been detected. It turns out that the thin plate martensite formed in austenite by the pulsed magnetic field at low temperatures can considerably broaden (grow) even in the absence of magnetic field at the same or even higher temperature. Separately placed thin martensite plates become lenticular crystals, closely placed parallel plates become "many-midrib" martensite crystals and great martensitic "complexes". As a result, the total amount of martensite in steel is increased by several times. The thin martensite plates growth takes place only in certain temperature range, and this process flows with the changing velocity. The evolution of pulsed magnetic field-induced martensitic transformation can occur at fixed temperature and it is a specific isothermal martensitic transformation whose product is lenticular martensite crystals. To our opinion, the martensite transformation evolution is connected with relaxation of the elastic tensions existing around thin martensite plates. The relaxation depends on the magnetic and elastic properties of austenite.

241. Crystallographic and Structural Changes Resulting from the Reverse Martensitic Transformation in High-Chromium Steels

V.V. Sagaradze, I.G. Kabanova and Vissarion D. Sadovsky

High-chromium ferrite-austenite steel Kh28N9M2 was chosen as a model material for investigating the mechanism of heating-initiated BCC-FCC transformation in order to realize this process in dislocation-free polyhedral ferrite. The crystal-geometric peculiarities of the α - γ transformation at different rates of heating were studied. The possibility of inheritance and forming new dislocations as a result of the BCC-FCC transformation was analysed. It was shown that a plated γ_1 -phase possessing all signs of a martensitic transformation (orientation relationships, 24 crystallographic orientations, shear strain, martensite habit plane $\{4.11.15\}_\alpha$) could form during accelerated heating by the shear mechanism. Decreasing the heating rate gives rise to disperse rod-like γ_2 -phase crystals formed with the participation of diffusion processes in the redistribution of alloying elements. New dislocations form during the BCC-FCC shear transformation and the dislocation density increases up to $3 \cdot 10^{10} \text{ cm}^{-2}$, a fact which indicates that a normal ferrite to austenite hardening occurs during heating. Three cases of interactions between growing γ_1 -plates and dislocations in ferrite were found: inheritance of dislocations, the inheritance and redistribution of dislocations in the growing phase, the absence of the inheritance-displacement of dislocations on the front of growing γ_1 -plates. We review investigations into the structural mechanism of α - γ transformation.

242. Crystallography of Ferrous $\{252\}_f$ Martensitic Transformations

Wang Shidao and Zhang Xiumu

Crystallographic theory, formulated by the semi-twin shear-rotation strain mechanism has been applied to the $\{252\}_f$ martensitic transformation and satisfactorily predicted its crystallographic features. Single lattice-invariant shear and the variant interlock suggested by W-L-R were also adopted to explain the complex crystallographic features, such as transmitted faults in front of the plate tip, wide scatter of the shear strain directions and multiplicity of the martensite substructure. The current theories on the $\{252\}_f$ martensitic transformation were discussed.

243. Martensitic Transformation in Fe-Ni-C Alloys Under Intensive Influence

A.G. Yakhontov and S.S. Mishchenko

The effect of additional twinning in martensitic transformation under pressure (1000-1500 MPa) is discovered in an Fe-31Ni alloy. The transverse and longitudinal additional twins, as well as transformation twins are formed in lenticular martensite at the same time. Under pressure 1500 MPa a cellular dislocation substructure is formed in martensitic crystals instead of transformation twins. A martensite in thin plates is formed in Fe-31Ni-0,25C alloy at 77 K in impulsive magnetic field (26 MA/m). While heating at 293 K the martensite in thin plates transforms into austenite the transformation beginning from the boundaries of martensitic crystals.

244. Martensitic Transformation in a Trip Steel

M.A. Nagaev, A. G. Yakhontov and B.G. Tugelbaeva

The plastic deformation at 293 K is proved to be accompanied by the formation of thin twin-plates of the $\{111\} \langle 112 \rangle$ type and ϵ - martensite in austenite. Deformation speed rise from $10s^{-1}$ to $5 \cdot 10^3 s^{-1}$ leads to the considerable structure coarsening and to the increase of ϵ - martensite amount, especially in the sphere of large deformations. The appearance of fragmented band structures with habitus of the 259A type is being observed. They are developing mainly in the localized deformation zones. Orientated correlations of austenite lattices, of twins and ϵ - martensite are defined by the dark-field method. The regularities of trip-steel property changes are determined according to its processing conditions.

245. Martensitic Transformation in an Fe-32%Ni Alloy Deformed by a Stroke

A.G. Yakhontov and A.F. Bayman

The influence of the impulsive deformation of the austenite on the kinetic and morphologic peculiarity of the martensitic transformation have been studied. The impulsive act by temperatures of 223...373 K increases the beginning of the martensitic transformation. Martensitic point is found out after the impulsive deformation by the temperatures of 573...773 K. The stabilisation by the weak deformation is bound with the raising of the parameters of the nearest order of the atoms. The stabilisation of the austenitic phase in the process of high deformation is defined by the dispersional structure and disorientation of the crystallite structure in microvolumes. The morphology of the martensitic crystals is studied in the dependence of the temperature and the degree of the preliminary pressing. The correlation between structure and properties alloy is established.

246. The Deformation Behavior of Martensitic Lath in a Cold-Drawn Low Carbon Dual-Phase Steel

Zhang Bing, Ge J. and Zhou Z.

The cold-drawn deformation behavior of martensitic islands in a low carbon dual-phase steel was studied by TEM. There are many fine martensitic lath beams in the island distributed in ferrite matrix. When the true strain increases, the deformation behavior of martensitic lath consists of two steps. The first one is the rotation of laths towards to the cold-drawn direction. The other is that the laths are prolonged along the cold-drawn direction. In some field, martensitic laths almost become fibres with the increase of true strain. The analysis shows that it is the distribution character of three dimensional stress in cold-drawing that makes martensitic laths have considerable deformability, thereby low carbon martensitic laths have a good combination of toughness and strength in martensite/ferrite dual-phase steel.

247. The Relation Between M_s Temperatures and Contact Fatigue Resistances of the Metastable Austenitic Alloys in Fe-Mn-Ni-C System

Zhang Ping and Xu Binshi

The contact fatigue resistances of Fe-Mn-Ni-C metastable austenitic alloys were investigated through contact fatigue test. By means of martensitic transformation thermodynamics, obtained was the correlation of environmental temperature T , M_s temperature and contact fatigue resistances of the materials involved. When $|T-M_s|$ was at the minimum value, the contact fatigue resistance reached the maximum, martensitic transformation was induced by plastic strain when the specimens were subjected to Hertzian stress. But when $|T-M_s|$ was great, different mechanisms dominated or the austenite was too stable to transformed martensite, or it was so unstable that a lot of martensite had been transformed. In order that the material achieve the best performance, the critical factor is to control the M_s temperature according to the environmental temperature T . Since mature elastic analysis has given the result that the maximum principal shear stress is in the subsurface when two solids contact each other, the application of strain-induced martensitic transformation provides a unique advantage that the initial micro-plastic-strain establish perfect hardness distribution below the surface, the greater the initial strain is, the greater the increment of the strength.

248. Peculiarities of Transformation in Textured Fe-18% Cr-10% Ni Alloy

Volodimir V. Karpovich, V.N. Dneprenko and L.N. Larikov

Peculiarities of polymorphous transformations in thermomechanically treated Fe-18%Cr-10%Ni alloy have been investigated both through the thickness and in different texture components. Complex of techniques including X-ray texture analysis, TEM and computer simulation was used. It is shown that different own variants of orientational relations are selected in texture components $\{001\}<110>$ and $\{111\}<211>$ of rolled sample. Independent texture components of γ -phase are formed by $\alpha \rightarrow \gamma$ transformation in the region with orientation $\{112\}<110>$ corresponding to the basic partial fibre components overlapping. In this case the number of selected variants is greater then in the basic texture components.

Peculiarities of transformations in texture components are inherent in other steels. But their revealing may be somewhat different. It is found that depending on heat treatment γ - ϵ transformation in surface layer of rolled Fe-20%Mn alloy may be realized in one or another texture component or practically don't be realized. The influence of dislocation structure and thermal stresses on variant selection has been also investigated.

249. Anisotropic Growth of Bainite Plate in Cu-Zn-Al Alloys
Kazuyoshi Takezawa, Shin'ichi Sato and Kenzaburo Marukawa

The bainite plates are usually observed as a pair with a chevron shape on the surface of Cu-Zn-Al alloys. A morphological examination has previously been made to determine the three-dimensional shape of the pair in the author's laboratory and concluded a form of long hinge. (pp.625-630, Proc. ICOMAT-86). Since this particular form is thought to be originated from the growth anisotropy of plate, an attempt is made in the present work to measure the growth rate separately in two directions on the habit plane, parallel and perpendicular to the expected direction of transformation shear. Growth velocities of 2.9×10^{-7} m/s and 9.3×10^{-8} m/s are obtained in the parallel and perpendicular directions, respectively, i.e., the former is about three times faster than the latter. An activation energy of growth, 28 Kcal/mol.K, is also obtained from the temperature dependence of these velocities, which is about the same as that associated with the diffusion of solute atoms in the matrix crystal. The present results suggest that the bainite lattice is formed by the atomic shear mechanism as well as in the martensitic transformation and also that the growth process is controlled by the diffusion of solute atoms. The obtained anisotropy can be understood by considering the stress distribution at the growth front of plate.

250. Monte Carlo Simulation of Lamellar Products at Middle Temperature Range
Feng Hua and Kang Mokuang

In this paper the nucleation kinetics of lamellar products at middle temperature range has been simulated in atomic scale with Monte Carlo method, in which the quantitative effects of dislocation pile-up and grain boundary on nucleation kinetics have been taken into account. Monte Carlo simulation results indicated that (A) A carbon depleted region will appear in super cooled austenite during incubation period, in which lamellar products nucleate more easily than in others; (B) In the lower part of middle temperature range shear mechanism dominates; (C) In upper part diffusional nucleation mechanism dominates. Moreover, random point and line scanning analysis of carbon content in super cooled austenite of steel within incubation period at middle temperature range by Auger microprobe has recently confirmed the existence of carbon depleted region near austenite grain boundary.

251. Time-Temperature-Transformation Diagram Within the Bainite Reaction in Some Alloy Steels
Kang Mokuang, Chen Daming, Hu G.L. and Meng X.K.

Time-temperature-transformation (TTT) diagram within the bainitic reaction of some alloys is found to be composed of one or two or three kind(s) of C-curve(s). Investigation on the bainitic TTT diagram of a β brass shows there is only one kind of C-curve corresponding to bainite. But to a middle-carbon alloy steel, the TTT diagram is composed of two separate kinds of C-curves, and the microstructure in this occasion is upper bainite or lower bainite, depending on the higher or lower location of the C-curve in the TTT diagram. Furthermore, carbide-free(meta)upper bainite or lower bainite will be obtained if the steel contains Si. In a lower carbon alloy steel, the TTT diagram possesses three separate kinds of C-curves, each corresponding to the microstructure of granular structure or upper bainite or lower bainite, also depending on the location of the C-curve in the TTT diagram. A single type of bainite can be obtained only in the primary stage of the bainitic reaction, while a mixture of bainites or bainite and other phase occurs during longer transformation times.

252. Thermodynamics of Bainitic Transformations in Fe-C- ΣX_i Multiple-Element Systems
Wei Quiming, Chen Daming and Kang Mokuang

Through the introduction of Zener's bi-parameter method, the X-K model has been extended to obtain a thermodynamic description of the bainitic reactions in Fe-C- ΣX_i multi-element systems. Calculations for steels 9CrSi, 40CrMnSiMoVA and 15SiMn3Mo show that, if carbon depleted region in austenite is taken into consideration, bainitic reactions can be put into the category of shear type transformations. A critical carbon content, which is 0.01(at.pct.), has been suggested for the carbon content of carbon depleted region in austenite. This critical carbon content is a result of the thermodynamic analyses of this paper. 1 1 1

253. Thermodynamic Analyses of Bainitic Transformation in Fe-C Alloys at the Initial Stage

Zie Zhaoyang and Kang Mokuang

A model of the bainitic transformation in Fe-C alloys during the initial stage of transformation (without carbide precipitation) has been proposed in which carbon partitioning is prior to the formation of bainitic ferrite through martensite-type shear. A thermodynamic analysis of the bainitic transformation using Xie-Kang's regular interstitial solution treatment of Fe-C solid solution is given. The analysis suggests that the carbon content of bainitic ferrite during the initial stage of transformation be calculated by letting the free energy change ΔG^{Fe} take the minimum to carbon content at the Bs temperatures.

254. On the Pre-Bainitic Phenomenon

Yang Y.Q., Wei Qiuming, Yang Q.M. and Kang Mokuang

The pre-bainitic phenomenon in several ferrous alloys and copper alloys was investigated by means of Internal Friction, Scanning Auger Micro-Probe and Analytical Electron Microscopy. The peaks of internal friction of carbon or zinc atoms diffusion in austenite of ferrous alloys or in β brass, respectively, were related to the carbon or zinc depleted region formation within the bainitic incubation period observed by composition measurement. The possibility of bainite nucleation in solute depleted regions by shear for Ms temperature in those regions increases to holding temperature was analysed. It is pointed out that the pre-bainitic phenomenon is a behavior of solute depleted region formation by diffusion and bainite nucleation by shear.

255. The Midrib and its Formation Mechanism in Lower Bainites

Sun Jialin, Chen Daming, Kang Mokuang and Lu Hongxiu

Modern physical methods have been used to examine the midrib existing in lower bainites of steels containing silicon. A small misorientation of 2-4 degrees between the midrib and the bainitic ferrites (BF) has been observed with a μ -diffraction technique. EELS(Electron Energy Loss Spectra) analyses show that the carbon content of the midribs is ca. 40pct lower than the mean carbon content in BF. No significant interface has been found between the midribs and the ferrites. The results of morphological and crystallographic studies and carbon content measurements have indicated that the midrib is actually a very thin penny-shaped area, formed with BF nucleated by shear and with the subsequent rapid growth of the nuclei. The midrib plane is therefore the habit plane of bainite nucleation. The thickening of BF is carbon diffusion controlled.

256. The Source of Carbide Precipitation in Lower Bainite

Sun Jialin and Kang Mokuang

The crystallography of carbides formed during lower bainite transformation in a silicon contained steel was studied by transmission electron microscopy(TEM). Significant differences in crystallographic aspect were detected between carbides precipitating from bainitic ferrite and those from austenite. This implies crystallographic analysis is a possible way for carbide source determination.

257. Substructural and Crystallographic Features of Lower Bainite

Sun Jialin and Kang Mokuang

Transmission electron microscopic investigations to the substructure of lower bainites in two steels containing silicon show the existence of a plastic accommodation defect in austenite prior to bainite transformation. The formation of bainitic ferrites is associated with an inhomogeneous shear. The magnitude of the macroscopic deformation (shear) has been evaluated, together with the measurements of the crystallographic features of the two investigated steels. A crystallographic model has been founded by taking into consideration the plastic accommodation double shear processes. The theoretical crystallographic predictions for the two investigated steels given by the newly founded model show a good agreement with the experimental results.

258. Shape Memory and Trip-Effect in Bainitic Steels after Isothermal, Thermomechanical Treatment

Sergei A. Faldin and Octai V. Samedov

The TRIP-effect in retained austenite of bainitic steels was studied. Low-temperature thermomechanical by regulated regimens leads to increased bainite volume fraction and creates conditions for pronounced TRIP-effect realization. Such a treatment improves plasticity and cracking resistance at high strength. The mechanism of γ - α transformation can be studied by an observation of the shape memory effect realization in such bainitic steels.

259. Growth Kinetics of Widmanstätten and Bainitic Ferrite

Wang Shidao

Two kinds of edgewise growth kinetics approaches has been developed for the plate precipitation of the proeutectoid and bainite ferrite in order to investigate the growth mechanisms of them. A mixed diffusion-interface controlled model of the ferrite growth suggested on the basis of determination of the interface kinetic effect using the diffusibility inside boundary. Following the kinetic thermodynamics of bainite growth proposed by the author, the another competent model of the bainite growth below the B_s temperature has a paraequilibrium shear growth mechanism. The model shows that the carbon partition of a partial equilibrium occurs simultaneously with the shear movement of iron interface. The comparison of the predictions by means of the two kinds of growth models with experiments shows that the growth kinetics of Widmanstätten ferrite above 550°C is consistent with the mixed diffusion-interface controlled, the paraequilibrium shear growth model is of the dominant operation mechanism of the bainite growth kinetics below 500°C, and the kinetics competition occurs in the temperature range between 550°C and 500°C. The above results are obtained in Fe-0.43wt%C alloy, The transition temperature of growth model in kinetic competition is higher than 500°C for the lower carbon alloys whereas lower than 500°C in the higher carbon alloys.

260. Widmanstätten and Upper Bainitic Ferrite Crystallography

Wang Shidao

The present paper will deal with the crystallography of Widmanstätten and upper bainite ferrite by means of different crystallographic approach. Both Widmanstätten and upper bainite ferrite exhibit a number of similarities. Such similarities make the understanding of their reaction mechanism so controversial that some investigators strongly hold the ledge diffusion mechanism but another stand for the shear one applying to both of them. A new crystallographic approach developed on the basis of the fault shear-dominant lattice deformation has been applied to the upper bainite ferrite and satisfactorily predicted the experimentally observed crystallography which has recently reported. It is important to find that the crystallographic variant correspondance of bainite ferrite is just the same as the martensites have. But Widmanstätten ferrite shows a distinct crystallographic variant correspondance from the one of martensites. An approach of elastic plane stress state in the epitaxial interface of the Widmanstätten ferrite has been suggested with the use of the strain Mohr circle. There is no any additional inhomogeneity in order to establish the IPS of Widmanstätten. And the lattice correspondance in it has no significance of the lattice deformation as that of martensites.

261. The *In-Situ* Observation of Bainitic Transformation in Cu-Zn Alloy

Yang Y.Q., Liu D.H., Kang Mokuang and Sun Y.

In situ observation of the growth process of bainite in Cu-Zn alloy by means of high-temperature TEM is conducted. It is found that the stacking fault substructure exists just in the growing tip of fresh bainitic plate and so does the shear stress field in the matrix around the tip shown by the change of bend extinction contours. The growth ledges are observed. The broad and narrow faces of the ledges are parallel to the fault plane and habit plane, respectively. The moving direction of ledges is parallel to the fault plane. It is shown that the thickening at one side of bainitic plate is faster than that at the other side. The mechanism of bainitic transformation in Cu-Zn alloy is discussed.

262. Effects of the Ultrasonic Treatment on the Bainitic Transformation Kinetics of Constructional Steels

O.V. Abramov, Elena V. Konopleva, N.M. Bayazitov, E. V. Kisterev and A.B. Ivanov

The isothermal transformation kinetics in the 30Cr3, 30CrMnSiNi2 and 08Cr2Mn2V steels was studied using the installation consisted of ultrasonic part and balance magnetometer. The UT (resonance frequency 18,5 kHz, amplitude of relative strain $\leq 10^{-3}$; the UT time ≤ 180 s) was carried out at a temperature in a metastable austenite range after previous austenitizing and cooling to 530°C. For comparison the kinetics after austenitizing and direct cooling to the isothermal transformation temperature and after austenitizing, cooling to 530°C and holding for ≤ 180 s at this temperature has been measured too. The effects of step treatment on the bainite transformation kinetics depend on holding time at 530°C and alloy composition. The UT did not change the reaction rate in the lower part of bainite range and retarded it in the upper part (only in the 30Cr3 and 30CrMnSiNi2 steels) compared to step treatment. The structure of the specimens transformed to pearlite or bainite was examined.

263. Stabilization of Martensite and Ordering of the Parent Phase in a Cu-Zn-Al Alloy

Chen Shuchuan, Xu Zuyao (T.Y. Hsu), Yang Fan and Zhang Jihua

The reverse transformation has never occurred in a quenched and aged specimen upon heating from room temperature to 320°C at which the martensite disappears thoroughly. Both $B2 \rightleftharpoons 9R$ and $DO_3 \rightleftharpoons 18R$ coexist in step-quenched and short-time isothermally treated specimen. As prolonging the isothermal holding, the $B2 \rightleftharpoons 9R$ disappears and the $DO_3 \rightleftharpoons 18R$ intensifies. $B2 \rightleftharpoons 9R$ occurs only in specimens quenched and up-quenched immediately to 100 – 150°C. Rapid quenching from high temperature will depress the $B2 \rightarrow DO_3$ ordering but not the $A2 \rightarrow B2$ one. An enough concentration of vacancy will promote the $B2 \rightarrow DO_3$ ordering. The possible mechanism for the stabilization of martensite in a Cu-Zn-Al alloy was also discussed.

264. Influence of the Interactions of Order-Disorder Phenomena with Thermomechanical Cycling on the Hysteresis of the Martensitic Transformation in a Cu-Zn-Al-Ni Alloy

Laurent Buffard, Pierre Charbonnier, J.L. Macqueron, and E. Weynant

The use of shape memory alloy springs in industrial products of high temperature accuracy needs an increasing reproductibility of the hysteresis of the martensitic transformation. It has been established that in copper based alloys, the evolutions of the hysteresis is due to an instable order of the matrix. This order is partial and imperfect and can be modified by the temperature, the stress and heat treatments.

We present results of industrial probes carried out on springs whose transformation characteristics were analysed by acoustic emission. This technique gives an access to dynamic parameters of martensitic transformation and allows the analysis of the evolution of the state of the alloy during transformation cycles.

In addition to acoustic emission, electrical resistivity and calorimetry measurements allow us to better characterize the evolution of the atomic order.

265. Martensite Ordering and Stabilization in Copper Based SME Alloys

Osman Adiguzel

Stabilization behaviour of the martensite in shape memory CuZnAl and CuAlMn alloys has been studied by the x-ray measurements and electron microscopy. In these alloys influenced by both quenching and post-quench heat treatments the degree of stabilization depends on quenching conditions, and stabilization process is mainly due to the structural change and atomic arrangement in martensitic lattice inherited from the parent phase. From x-ray results it was suggested that stabilization and loss of memory are directly related to disordering in martensitic state. In the present study, it was concluded that the spacing differences (Δd) between some selected pairs of diffraction planes of type $(h_1 k_1 l)$ and $(h_2 k_2 l)$ satisfying the relation $(h_1^2 - h_2^2)/3 = (k_2^2 - k_1^2)/n$, with $n=1$ for 9R and $n=4$ for 18R martensites reflect the degree of ordering in martensite, in addition to the lattice distortion parameters defined as $\phi = |\sin^2\theta_{202} - \sin^2\theta_{122}|$ and $\phi' = |\sin^2\theta_{320} - \sin^2\theta_{040}|$.

266. α_1 Precipitates Induced by Constraint Aging in a Cu-Zn-Al SMA

Hu Chen-Ti and Leu Shyue-Shang

The constraint aging treatment to induce two way shape memory (TWSM) effect has been reported at TiNi SMA, i.e. the all-round shape memory (ARSM) effect. In this study, the various tensile-loaded aging treatments have been conducted on a Cu-27.4Zn-3.7Al SMA. The acceleration of precipitation process of needle-like α_1 precipitates due to the constraint stress was discovered. In addition a TWSM character with extensive strain has been observed in constraint aged CuZnAl specimens which is opposite to the contractive character of TWSM in constraint aged TiNi alloy. It is suggested that an internal compressive stress has been developed at the interfaces between precipitates and matrix after the Cu-Zn-Al specimen been constraint aged. Once the testing specimen was cooled below M_s , those martensite variants which contributing to decrease or eliminate the internal compression stress nucleated and grew preferentially, moreover caused the extensive TWSM character.

267. A Study on Aging Stabilizing of Martensite in Cu-Based Shape Memory Alloy

Wang Yonggang, Zhou Hefeng, Li Shulin and Hou Zhengshou

The memory property and the martensite aging stability of Cu-23.12Zn-4.37Al and Cu-26.34Zn-3.24Al-0.67Mn (Wt%) hot rolled sheet under different conditions as hot rolled, marquenching and oil quenching have been studied. It is found that not only the memory property is good enough, but also the resistance to martensite aging stabilizing is high under hot rolled condition with higher hardness. By using X-ray diffraction method, it is discovered that microscopic internal stress exists in hot rolled sheets under all the three conditions. Among them the internal stress under hot rolled condition, is the highest, but it relaxed very slowly during aging process, while the internal stress with marquenching or oil quenching is some-what relaxed. According to the test results, a stress relaxation model is proposed for martensite aging stability of Cu-based shape memory alloy. During the process when Cu-based shape memory alloy is used or laid aside in martensite state, the coherent interface among different martensite variants as well as between martensite and parent phase was destroyed due to relaxation of microscopic internal stress. For this reason, it is difficult for different martensite variants to combine and martensites come into aging stabilizing.

268. Influence of Mn Addition on the Thermal Stability of Cu-Al-Ni SMA

Inahi Hurtado, Jan Van Humbeeck, Muthuswamy Chandrasekaran and Luc Delaey

Potential shape memory applications at higher temperatures in recent years have stimulated the search for alloys with transformation temperatures above 373K. Among these the Cu-Al-Ni alloys have received a special attention because of their good thermal stability and low cost. In order to improve their mechanical properties various elements are added, such as Ti for reducing the grain size, Mn for improving the machinability, etc. In the present work, the role of Mn on the thermal stability of Cu-Al-Ni alloys is investigated by means of Differential Scanning Calorimetry (DSC), Thermoelectric Power (TEP), X-ray Powder Diffraction and Transmission Electron Microscopy (TEM). The variation of the martensitic transformation characteristics, i.e. temperatures, hysteresis, etc., are compared with those of the previously studied Cu-Al-Ni-Ti-Mn alloys.

269. Study on the Precipitation of the Stable Phases on Cu-Al-Ni Shape Memory Alloys

Vicente Recarte, Inahi Hurtado, J. Herreros, Maria Luisa No and Jose San Juan

About the Cu-Al-Ni shape memory alloys, one of the matters that limits the maximum using temperature is the precipitation of the stable phases. On the other side, for the interesting concentrations of this alloys, the phases equilibrium diagrams are not exactly determined, specially on the low temperature range.

In this paper, the stable phases showed at the different temperatures and for some different concentration of Cu, Al and Ni have been characterized by optical and electronic microscopy, dilatometry and X-ray diffraction. On the same way the T.T.T. curves for this alloys have been obtained by quenching dilatometry, studying the precipitation kinetic of the stable phases inside the metastable β phase.

270. Research on Ageing Processing of AF1410 Steel

Xu Changgan and Ma Jing

The quantity of martensite and residual austenite in high-alloy ultra-strength AF-1410 steel quenched by different manner is various. The characterization of microstructures quenched by oil, air, etc. and separately aged in 430°C, 500°C, and 570°C, are different. In aged process the precipitation from quenched martensite, the coarse precipitated cementite and the inversional austenite from martensite simultaneously induce to decrease hardness of steel. By the verified result of electron diffraction the second hardening phenomenon with Mo_2C precipitating in AF1410 steel yet is presented.

Key words AF1410 steel, martensite, aged of steel.

271. Further Information about the Tempering of Martensite

Mstislav A. Shtremel, Ljudmila M. Kaputkina, Sergei D. Prokoshkin and Dmitriy E. Kaputkin

272. Martensitic Interface Crystallography and its Effect on Tempering Precipitation

Wei Fugao (F.G. Wei)

The crystallography of tempered cementites and the interfaces on which cementites precipitate is characterized in terms of the exact coincidence site lattice (CSL) misorientation between the two martensites separated by the interfaces, deviation from the misorientation and the orientation of the interfaces. A high silicon-content medium steel was used for this investigation which contained lath martensites and a few of micro-twin martensites. Theoretical calculation shows that all the martensite interfaces within a packet are classified into seven CSL types with a reasonable deviation. Results of TEM observation reveal that CSL misorientation plays an important role in the nucleation of cementites and their orientation with both matrices beside them and deviation from the exact CSL misorientation is of significant importance in the selection of variants and the growth behavior of the precipitates while the orientation of interfaces appears to have a weak effect on the precipitation probably because of the high density of dislocations in the martensite matrices.

273. Ti-Rich Precipitation and Martensitic Transition in Ti-Rich Ni-Ti Alloy

Zhu J.S and Li J..

Internal friction (IF), modulus ($\propto f^2$), electric resistance and zero position shift were measured in Ti-rich NiTi alloy before and after aging at 500°C for over 1 h. An anomaly of IF and corresponding to a variation of modulus, electric resistance and zero position shift on the low temperature side of M_s were observed in sample after aging at 500°C over 1 h. A further experiment indicated that the anomaly of IF has characteristic of first order phase transition i.e peak height of IF is proportion to the temperature rate and inverse proportion to the measuring frequency. SME and X-ray diffraction technique were used to clarify the observed phenomena. Grain shape precipitates which have rich-Ti composition were found by SME in aged sample. It is also confirmed by X-ray diffraction, large enhancement of diffraction lines for Ni_2Ti_3 phase was observed in sample after aging. As we know, the appearance of Ti-rich precipitate phase reduces Ti content in area near precipitate phase. A decrease of martensitic transition point in this range was found because it has more Ni content. The observed anomalous in IF, modulus, electric resistance and zero position shift are attributed to the decreasing in the area near Ni_2Ti_3 precipitate phase in aged sample.

274. Acicular Martensite Induced by Low Temperature Aging of an Arc-Melted $\text{ZrO}_2\text{-Y}_2\text{O}_3$ Alloy

Motozo Hayakawa, Y. Onda, and M. Oka

Aging of a coarse-grained $\text{ZrO}_2 - 2\text{mol}\% \text{Y}_2\text{O}_3$ specimen at 250°C induces the t (tetragonal) $\rightarrow m$ (monoclinic) transformation. The transformation exhibits two distinct types of morphology, i.e., herringbone type and acicular type. The crystallographic feature of the former has been previously studied[1]. The present paper describes the structure and the mechanism of the formation of the latter. Acicular martensite was typically several hundred μm long and a few μm thickness. It penetrates into the material about 100 μm below the surface, thus it is a thin plate form. A two-surface trace analysis uniquely identified the habit plane to be a $\{100\}_t$ plane. Despite the well defined habit plane, the surface relief did not correspond to a simple invariant plane shear. Electron microscopic observation of a plate revealed that the plate comprised many small variants of lenticular or triangular shape. The arrangement of these plates were not regular. In the neighborhood of a fully grown plate, thin plates were often observed running parallel to the thick plate. These thin plates were single variant with the same $\{100\}_t$ habit. Even though a phenomenological calculation[2] predicts an irrational $\{207\}_t$ habit plane, if the lattice invariant shear is inhibited for some reason, the lattice strain associated with the $t \rightarrow m$ transformation will be roughly a shear on a $\{100\}_t$ plane, but with strain mismatch on the interfaces. The stress resulting from the strain mismatch would explain the preferential formation of the smaller variants alongside.

[1]M. Hayakawa, K. Adachi, and M. Oka, *Acta metall. mater.*, **38**, pp. 1753-59 (1990)

[2]M. Hayakawa and M. Oka, *Acta metall.*, **37**, pp. 2229-35 (1989)

275. Surface Relief in Ceramics During Transformation

Kunio Wakasa, Chou Chen-Chia and C. Marvin Wayman

Surface relief effects were investigated in various ceramics using interference microscopy. Relief phenomena in certain ceramics are very similar to that of martensite in metals (invariant plane strain) and interference microscopy is a promising way to investigate structural transformations in ceramics. Surface tilt angles were determined from interference fringes, and are related to lattice parameters, crystal symmetry and other microstructural characteristics. Combining different techniques, such as optical microscopy, X-ray and transmission electron microscopy we can construct general structural information on transformations in ceramics. For instance, in lead titanate crystals, surface tilting, variant distributions, and self-accommodation were characterized from optical and interference microscopy. The twinning system was explicitly identified as $\{110\} \langle 110 \rangle$ using transmission electron microscopy. Lattice parameters were derived by the X-ray technique. All structural information is interrelated, and well explains the transformation crystallography in PbTiO_3 single crystals. Similar investigations were conducted on other ceramic materials, such as ZrO_2 , PSZ, Gd_2O_3 and BaTiO_3 crystals and the results are compared and discussed.

275A. Shape Memory and Pseudoelastic Behavior for Ceramics with Field-Induced Antiferroelectric-Ferroelectric Phase Transformations

Pin Yang and David A. Payne [TO BE PRESENTED BY W.A. KRIVEN]

Electrically induced deformations associated with antiferroelectric (AFE)-to-ferroelectric (FE) phase transformations in tin modified lead zirconate titanate (PZST) ceramics are reported. The total strain is comprised of a (i) spontaneous strain which occurs at the phase transformation and a (ii) strain associated with domain alignment on poling. Therefore, the total induced strain is greater than the converse piezoelectric effect normally associated with ferroelectric materials, and as such, is attractive for potential device applications. Depending on reversible and irreversible characteristics, associated with the temperature of operation and thermal hysteresis, the deformation process can be classified as superelastic or shape memory behavior. Superelasticity is observed at temperatures above the FE-AFE transformation temperature (T_A) with immediate strain recovery upon release of the electric field. Electrically induced irreversible strains, within the thermal hysteresis region ($T_F < T < T_A$), are recoverable upon heating above T_A ; and give rise to a shape memory effect, the extent of which is dependent on the magnitude of the AFE sublattice coupling. Shape memory and superelastic behavior are explained in terms of competing thermodynamic stabilities for the AFE and FE phases. Implications to other ceramic systems are indicated.

276. Phase Changes at Zirconium Ceramics Thermocycling

O.N. Kanigina, I.P. Gerashenko, E.M. Pak and I.G. Sevastjanova

Zirconium ceramics samples ovened at 1873 C were studied 4 hours before and after thermocycling by SCAN, TEM, RSA methods. The samples contained poreproducing addings e. i. hollow corundum microspheres from 2 to 20 percent in mass. The Thermocycling was achieved by heating and cooling at the rate of 260 degree/min. Thermosolidity was judged by the cycles number the samples stood before the distruction. Thetragonal-monoclean martensite change of zirconium dioxide occures at thermocycling its intensity depends on microsphere containance. The samples thermosolidity is defined by the phase martensite intensity samples with maximum thetragonal phase contence before cvcling are the most thermosoled. They can stand three times more thermocycles. The distruction takes place after the phase change finished.

277. TEM Study on the Concrete Process Details of the Martensitic Transformation in (Y,Mg)-PSZ Ceramics

Dai Zhurong, Li Baocheng, Wu Houzheng, Chen Yuru and Liu Wenxi

The martensitic nature of the transformation from tetragonal structure($t\text{-ZrO}_2$) to monoclinic structure($m\text{-ZrO}_2$) in zirconia ceramics is well known and has been the subject of many studies. When a few contents of Y_2O_3 was added into the material on the basis of the composition of magnesia partially stabilized zirconia(Mg-PSZ), the phase of tetragonal zirconia($t\text{-ZrO}_2$) tended to be stabilized, so that the process and details of $t\text{-ZrO}_2 \rightarrow m\text{-ZrO}_2$ martensitic transformation were clearly displayed. In this paper, the concrete process details of the martensitic transformation, including its nucleating and developing, in (Y,Mg)-PSZ were observed in situ by means of TEM. The results indicated that as the effect of the contact stress between $t\text{-ZrO}_2$ precipitates, a group of martensitic subplates was generated early at the phase boundary of $t\text{-ZrO}_2$ and $C\text{-ZrO}_2$, then they were advanced through the tetragonal precipitate and finally, another group of martensitic subplates was induced within the spacing between the early formed subplates as a result of the elastic strain relaxation. Both groups of martensitic subplates formed into the relationship of (100) m reflection twinning in essence. In addition, the crystallograph on the martensitic transformation was studied. The conversion matrices between martensitic subplates and tetragonal phase are M_M and M_T . They are given by $M_M = S_M \cdot B_M$ and $M_T = S_T \cdot B_T$, where $S_{M,T}$ and $B_{M,T}$ represent the shear matrices and Bain distortion matrices respectively. The martensitic transformation matrix M in whole range of the tetragonal precipitate is equivalent to the composite reaction of M_M and M_T . That is $M = xS_M \cdot B_M + (1-x)S_T \cdot B_T$, where $x = 1/2$ is the volume fraction of a group of twin-related subplates.

278. Effect of Martensitic Transformation on Mechanical Properties of $\text{Al}_2\text{O}_3\text{-ZrO}_2$ Ceramics

O.N. Grigor'ev, Yu.G. Gogotsi, V.K. Sulzhenko, G.E. Khomenko, N.A. Orlovskaya and G.S. Krivoshey

The structure, stressed state and fracture of hot-pressed, transformation toughened alumina (ZTA) ceramics are studied by transmission and scanning electron microscopy and X-ray diffraction. The influence of processing and composition (content of ZrO_2 and Y_2O_3) on strength and fracture toughness is investigated. It is shown that the martensitic $t\text{-m}$ phase transformation, as well as microcracking and crack deflection, is responsible for the mechanical properties of ZTA ceramics. The contribution of stress-induced (that is, occuring in the region ahead of a crack tip) $t\text{-m}$ martensitic transformation to fracture toughness of ceramics is evaluated. The materials with the constant fracture toughness values of $8.5 \text{ MPa}\cdot\text{m}^{1/2}$ in a wide concentration range (10-40 mass % ZrO_2 and 0, 2, 3 mol % Y_2O_3) are developed. The maximum strength was observed for ceramics with 30 mass % ZrO_2 and 3 mol % Y_2O_3 .

279. Transformation Plasticity of Ceramics in Non-Proportional Compression
Sun Qing-ping

In this paper, by using moiré interferometry and strain gauges, the experimental observation of the anomalous plastic behavior of ceria-stabilized tetragonal zirconia polycrystals (Ce-TZP) under non-proportional compression are presented and the microstructural mechanisms of such behavior are discussed. The non-proportional compression is realized by two stages, i.e., first compressing the 10mm × 10mm × 10mm sized specimen along axial direction to cause transformation plastic deformation and unloading, then reloading the specimen along the radial direction to cause further plastic deformation. Two strain gauges, along axial and radial directions respectively, are attached on one surface of the specimen to continuously record the stress-strain curve during loading and unloading by two X-Y recorders. At the same time, a moiré grating is attached to the other surface of the specimen to record the corresponding in-plane strain distribution. The experimental results are analyzed and compared with the theoretical model proposed by the author.

280. Microstructures of Athermal and Stress-Induced Martensites of Ti-V-Al Shape Memory Alloys
J. S. Lee Pak, C.Y. Lei, Ming-Hsiung Wu, H.R.P. Inoue and C. Marvin Wayman

Microstructures of both athermal and stress-induced martensites in Ti-4.0Al shape memory alloys containing vanadium between 14.1 and 16.8 (in weight per cent) have been investigated by means of electron microscopy. These two β_1' martensites have an ordered face-centered orthorhombic structure and transform from the β_1 parent phase with an ordered tetragonal structure. The athermal martensite forms in the shape of plates around 400nm wide containing a high density of internal faults, or $(101)\beta_1'$ (or $(\bar{1}12)_{\beta_1}$) microtwins. On the other hand, the stress-induced martensite forms in the shape of rather intricate zigzag patterns of thin plates (around 200 nm wide) which are slightly smaller than the athermal martensite, but also have a high density of internal faults parallel to the $(101)\beta_1'$ plane. Variants of the stress-induced martensite have a $(111)\beta_1'$ (or $(\bar{1}01)_{\beta_1}$) twin relationship.

281. Influence of the Solution Treatment on the Martensitic Transformation Temperature and on the Microstructure of a Cu-Zn-Al Alloy
Michel Morin, David Rios-Jara and Gerard Guenin

The effect of various step quench has been studied on a Cu-Zn-Al alloy with 8 wt pct Al. The temperature of the martensitic transformation (M_s) as a function of the step quench temperature is found to exhibit a maximum near the T_{B2} temperature (temperature for the transition from the disordered to B2 ordered beta phase).

A systematic study of the microstructure of this alloy step quenched at different temperatures has been carried out. From this work, it is shown that the T_{B2} ordering has a large influence on the microstructure obtained after a step quench.

282. Stress-Induced Martensitic Transformation and Deformation Behaviour of Single Crystal of the NiAl Alloy
Kazuyuki Enami, M. Togawa and Valeri V. Martynov

The stress-strain behaviour, structural and microstructural change during tensile deformation of the single crystal of 63.2at%Ni-Al alloy with $[001]$ and $[011]$ axes were investigated by in situ optical microscope observation and X-ray Laue method. In the specimen with $[001]$ axis, two stage pseudoelastic deformation was found to exist above M_s temperature. The first stage yield corresponds to the formation of the seven layer 52 structure and the second one the beginning of the formation of the "single variant" crystal of the L10 martensite phase at the expense of 52 M phase. From in situ optical microscope observation and X-ray analysis, it was found that the L10 M phase formed at the crossed region of two different variant crystals of the preceding 52 M phase. In the specimen with $[011]$ axis on the other hand, only 52 M phase formed and L10 M phase did not form until the specimen was ruptured. This difference is well explained by the shear mechanism and its orientation dependence of 52 M to L10 transformation. From the temperature dependence of the stress-strain behavior, a phase diagram of the stress-induced transformation of the NiAl alloy in the temperature-stress space was established.

283. Martensitic Transformation and Sub-Structures of Martensites in Ni-Al Alloys with Different Quenching Rates

Cheng Tian*, (T.Y. Cheng)

Rapidly solidified Ni-21wt%Al alloys with different cooling rates were manufactured by melt spinning process. The microstructures of spun ribbons have been investigated by TEM, EDS, XRD and DSC.

It has been found that the martensitic transformation of β -NiAl was suppressed partly and replaced by pre-martensitic transformation. The extent of suppression related directly with cooling rates during rapid solidification or quenching rates of ribbons. Moreover, NiAl martensites with different sub-structures such as twins and stacking faults with different morphologies have also been observed.

The effects of quenching rates on martensitic transformation of β -NiAl and different sub-structures in NiAl martensites and a possible mechanism have been discussed.

*Permanent address: Metal Materials Section, Beijing Institute of Technology, P.O.Box 327, Beijing 100081, P.R.China

284. Isothermal Martensitic Transformation in Cu-Base Alloys

V.A. Lobodyuk

The isothermal kinetics of martensitic transformation in the nonferrous metals was firstly reported for Cu-23.5% Sn-2.0% Ga [1]. It was shown that after formation of first portions of athermal martensite slow transformation takes place at constant temperature. This transformation continues during 20-60 min; transformation rate has a maximum value in the initial moment decreasing with time. It was discovered that in Cu-(23.5-24.0)%Sn-2.0%Ga the isothermal transformation occurs when the magnitude of Vickers hardness is equal to 3-4 GPa. Such values can be reached after ageing at 100-200°C for 1-5 min or after rolling on 5-10%. In aged alloys there are different successions of isothermal and athermal kinetics. It was determined the temperature rate dependence of isothermal martensitic transformation: with lowering temperature the transformation rate is essentially decreased. Transmission electron microscopy observations have shown that quenched Cu-Sn-Ga alloys were always ordered. Partial decomposition which occurs during quenching is followed by the formation of the precipitates of FCC δ -phase ($a=1.795$ nm). An additional decomposition proceeds during ageing at 100°C for 5 min or at 200°C for 1-2 min resulted in considerable hardening effect. It was supposed that transformation kinetics in Cu-Sn-Ga alloys is influenced by the stress relaxation processes which depend on the state of alloys.

1. V. A. Lobodyuk, T. G. Sych, L. G. Khandros. *Metallaphysica*, 1981, 3, 124

285. Damping Capacities in Fe-X%Mn Martensitic Alloys

Chong-Sool Choi, J.D. Kim, T.H. Cho, S.H. Baik and G.H. Ryu

The damping capacity has been investigated at room temperature for the as-quenched Fe-Mn alloys having manganese content from 5 to 28 wt%. In these alloys, the Fe-17%Mn alloy shows the highest damping capacity, $SDC = 28$ at $\gamma_{max} = 8 \times 10^{-4}$. The damping capacity of the Fe-17%Mn alloy increases with increasing the ϵ martensite content, showing a peak value at and around 50 vol.% ϵ , and decreases with further ϵ martensite content. This suggests that the damping capacity of the alloy is closely related to the total γ/ϵ interface. Thus, the reason why the Fe-17%Mn alloy shows the highest damping capacity in the Fe-Mn system may be attributed to the following factors: (a) Since the Fe-17%Mn alloy has a lower value of stacking fault energy than other Fe-Mn alloys, the γ/ϵ interface can move easily even by the slight stress such as the vibration stress. (b) The as-quenched structure of the Fe-17%Mn alloy is composed of about 50 vol.% ϵ corresponding to the maximum value of the γ/ϵ interface in the mixture structure of γ and ϵ .

286. Reversible and Irreversible Transformation Plasticity Deformations in Fe-Ni-C Alloys

J.S. Zhang, Elisabeth Gautier and A. Simon

Transformation plasticity deformation has been measured versus the progress of the transformation for different thermomechanical paths. Anisothermal creep tests and tensile tests have been performed on two Fe-Ni-C alloys whose M_s temperatures are about -35 and -150°C . The reversible part of the transformation deformation has been determined by rapid heating up to temperatures above A_f , and cooling. The variation of that reversible deformation versus the martensite content and the thermomechanical conditions of transformation have been obtained. For anisothermal creep tests, the results show that concerning transformation plasticity deformation versus martensite content, it increases rapidly at the beginning of the transformation and the increase lowers as transformation content increases. Comparing the two alloys, they show a similar behaviour if we consider the effect of the applied stress normalised to the flow stress of the parent phase. For the tensile tests, transformation plasticity has been measured at different tests temperatures, confirming the difference in behaviour in the elastic and plastic deformation range observed previously (1), low deformation associated to the transformation in the elastic range and larger ones in the plastic range. The measurements of the reversible part of the transformation deformation show a larger reversibility in the plastic deformation range. On a microstructural point of view, observations are performed in order to quantify the anisotropy of martensite orientation.

These results are discussed considering the origins of transformation plasticity, anisotropic plastic accommodation of transformation strains, orientation of martensite plates and the factor which can modify these contributions (transformation accommodation mechanisms).

1 - E. Gautier and A. Simon, Proc. Phase Transformation 87, The Institute of Metals, Ed G.W. Lorimer, 285, 1987.

287. Study of the Thermomechanical Fatigue of a Cu-Al-Ni Alloy Subjected to a Bending Test

F. Trivero, Michel Morin and Gerard Guenin

The thermomechanical fatigue of a Cu - 13.5 wt pct Al - 4 wt pct Ni shape memory alloy, which transforms close to 70°C , has been studied. A static bending force has been applied to parallelepipedical samples during a large number of thermal cycles (about 5000). Small chockes have been stucked on the samples to realize the bending. The thermal cycling has been made between two oil bathes at 20°C and 150°C . For each cycle, the Stress Assisted Two Way Memory Effect is induced, due to the martensitic and reverse transformations of the samples.

The influence of the applied stress and thermal cycles number have been measured as well as the memory strain amplitude. By changing the thickness of the chockes, the effect of the strain amplitude has also been observed.

Finally a previous thermal cycling with higher stress than the test stress has been applied. The results obtained after this treatment have been compared with the first measurements. It is shown that this previous thermal cycling improves the toughness to the thermomechanical fatigue of this alloy.

288. Deformation Twins and Martensite in Ductile B2 Alloys of the Zr (Pd, Ru) System

R.M. Waterstrat, Leonid A. Bendersky and Raymond Kuentzler

A martensitic transformation that occurs in the equiatomic compound ZrPd at about 540°C can be reduced to room temperature by the substitution of Ru atoms for about 28% of the Pd atoms. A hardness minimum and a sharp maximum in the electronic specific heat coefficients are observed at the approximate composition $\text{Zr}_{50}\text{Pd}_{35}\text{Ru}_{15}$. Ordered B2 phase crystals having this composition exhibit significant ductility when tested in tension and evidence for crack stabilization is observed prior to fracture. Deformation twinning of the (114)-type and a relatively high density of dislocations has been observed in TEM studies. Martensite formation occurs at lower temperatures in this same composition range. The structure, orientation relationship and morphology of the martensite crystals were analyzed by TEM. Competing mechanisms of dislocation slip, twinning and martensitic transformation for accommodation of the deformation will be discussed.

289. Anharmonic Behaviour of Cu-Zn-Al Alloys

B. Coluzzi, Andrea Biscarini, Fabio M. Mazzolai, C. Costa, S. Ceresara and A. Giarda

Internal friction and Young's modulus have been measured as a function of temperature in a CuZnAl alloy at varying amplitudes of the resonant flexural vibrations. It has been found that anharmonicity is low in the parent β phase and only shows slight premonitory effects of the martensitic transition above M_s . The alloy system becomes very anharmonic in the transition region, where the amplitude dependence of the Young's modulus passes through a pronounced maximum. The source of such anharmonicity is believed to be related to the lattice metastability. Below M_f anharmonicity is high, approximately temperature independent and, likely, is associated with hysteretic motions of martensite-martensite interfaces.

290. Internal Friction and Microdeformation of Ni-Ti-Nb Shape Memory Alloys

Jose San Juan, V. Recarte, Maria Luisa No and Jan Van Humbeeck

A new Ni-Ti-Nb shape memory alloy family has been recently developed. This alloys show the advantage of having a very good ductility, they also exhibit a high transformation hysteresis which is of great interest for some specific sorts of applications. Otherwise the microscopic mechanisms responsible for this important hysteresis has not been well precised yet.

In this work, we have studied, by internal friction and microdeformation the behavior of a 47Ni-44Ti-9Nb alloy, in the whole temperature range including the transformation cycle. The results we have obtained show clearly an important asymetry on the transformation cycle depending on whether the temperature increases or decreases. In addition to this, this alloy shows a high damping ability on the martensitic phase.

291. Morphology and Fracture of an Isolated Martensite Packet

Yuri G. Andreev and Mstislav A. Shtremel

Specimens of various orientations cut of a large martensite packet, which is formed in a quenched austenite singlecrystal of .37C-1.5Cr-3.0Ni steel, have been studied by metallography, TEM, micro- and X-Ray diffraction. The three-dimensional model of a packet, consisting of six types of laths, have been constructed. Crystallography of laths is predetermined by the six systems of K-Z homogeneous shear. Habit plane of laths is approximately $(111)_\gamma$ plane, being their common plane of the "first" shear. The long axes of laths are close to $[011]$, $[110]$, $[101]_\gamma$, which are their "second" shear directions. The tetragonality axes lie at an angle of 45° to the direction of the "first" shear $[112]$, $[121]$, $[211]_\gamma$. Experimentally observed G-T orientation relationship, as well as dispersion of orientations, found to be in agreement with the calculated rotation of lattice from plastic accommodation. The packet grows from the single lath. Self-accommodation of laths of different orientations, determines the mode of their stacking and, therefore, the structure of the packet. All the interlath boundaries within the packet are low-angle or close to special (regular) twist ones, formed by the systems of screw dislocations, generated by plastic accommodation. These boundaries are of low mobility. In the BCC lattice they have a long-range stress field and thus are resistant to moving dislocations. The interfaces between the packets are of the facet type with 77% of high angle irregular boundaries. Torsion and bend tests of microspecimens, cut of the packet, show strong anisotropy. Common $(111)_\gamma$ of the packet is the plane of the easiest slip. Stereophotogrammetry and optic reflectometry of fracture show, that $(001)_\alpha$, normal to tetragonality axis, is the only cleavage plane. The difference in fracture relief on the two halves of the fractured specimen shows, that cleavage occurs in front of the main crack, and the facets join the crack after plastic flow and shear along the edges.

292. The Effect of Oxygen and Carbon on the Fracture Behaviour of Cu-Al-Ni Shape Memory Alloys

Stephan Eucken, G. Otto and G. Viehhaus

A Cu-Al-Ni alloy was remolten and meltspun in different atmospheres. Shape memory, fracture strain and fracture behaviour of the ribbons were determined by tensile testing directly after production or after ageing treatments. While unaged ribbons produced in He-atmosphere performed a favourable shape memory effect and a high fracture strain, the ribbons meltspun in air and aged specimen exhibited a brittle intergranular fracture after small fracture strains. While there was no significant difference in microstructure visible at all ribbons used for this investigation whether in light, electron or transmission electron microscope, an auger spectroscopic analysis on oxygen and carbon indicated layers on grain boundaries of all brittle fractured specimen and just very small amounts of these elements on the fracture surfaces of the favourable ribbons.

293. Effect of Microstructures on the Impact Fatigue Properties of 40CrMnSiMo VA Steel

Chen Da-Ming, Kang Mokuang and Tan Ruo-Bing

Impact fatigue properties of ultra high strength 40CrMnSiMoVA steel have been investigated. Four kinds of notched specimens and five different heat treatments were employed in the test. Experimental results show that the bainitic microstructure has longer fatigue crack initiation life $N_{0.2}$, slower crack propagation rate da/dN and longer fatigue crack critical length a_c than the martensitic microstructure. The reason has been indicated in the present paper. As a result, it is queried whether the static K_{Ic} value could be used to determine the a_c value of a practical part under conditions of fatigue loading.

294. Effect of Microstructures on Strain-Controlled Fatigue Properties in an Ultra High Strength 40CrMnSiMo V Steel

Chen Da-Ming, Kang Mokuang and Tan Ruo-Bing

The strain-controlled fatigue properties of different microstructures in an ultra high strength 40CrMnSiMoV steel have been investigated. The results show that the martensite structure obtained by isothermally quenching at 190°C is cyclic softening, while the meta-bainite which consists of ferrite laths and retained austenite films distributed between or in the laths, obtained by isothermally quenching at 300°C, either tempered or not, is sharp cyclic hardening at first, and then slowly cyclic softening during fatigue. As a result, the cyclic stress-strain curve of meta-bainite with a lower original $\sigma_{0.2}$ value is higher than that of martensite. The fatigue life of meta-bainite is longer than that of martensite in the range of $2N_f > 10^3$, which is contrary to the traditional viewpoint. It is believed that for a constant total strain amplitude the cyclic hardening decreases the component of plastic strain and makes the microplastic deformation homogeneous, while the cyclic softening increases the component of plastic strain and concentrates the micro-plastic deformation. Therefore, the lower $\sigma_{0.2}$ value and $\sigma_{0.2} / \sigma_b$ ratio of the meta-bainite is its advantage, other than weakness.

295. Effect of Plastic Deformation on Structure and Reversible Martensitic Transformation in CuZnAl Alloys

Jerzy Morgiel and Jan Marek Dutkiewicz

The stripe of CuZnAl alloys with M_s equal -17 and -74°C were rolled up to 10 and 30% deformation. The structure changes were monitored through optical and transmission electron microscopy, while the electrical resistivity measurements were used to assess the characteristic martensitic transition temperatures. The height reduction of hysteresis loop of reversible martensite transformation with increasing deformation was found to correspond to increasing amount of martensite introduced during rolling. The hysteresis height reduction is accompanied by down shifting the start of martensite transformation. The electron diffraction showed that, small part of martensite introduced during rolling has 2H structure while the rest was 18R e.l. the same as formed during cooling. The *in-situ* cooling and heating experiments showed that in thin foils, where some strains from rolling are relaxed, the previously stable deformation martensite may either resume its growth during cooling or start to shrink during heating, confirming its full similarity with athermal martensite.

296. Texture Transformations During Strain-Induced Martensite Formation

Ljudmila M. Kaputkina, Sergei D. Prokoshkin and Tatiyna V. Morozova

This work was aimed at studying structure, texture and mechanical properties of steels after rolling and tensile in range of M_d - M_s (Fe-0,06C-14,1Cr-6,0Ni-1,5Mo-1,9Cu) and M_s - M_f (Fe-0,06C-14,3Cr-7,6Ni-1,6Mo). In this range the existence of deformation temperature area in which the final martensite texture transforms from $\{112\}\langle 110 \rangle$ to $\{111\}\langle uvw \rangle$ has been detected. After rolling yield strength increased up to 1600 MPa while anisotropy of steel strip was absent. The study of reverse martensite transformation has showed the existence of linear shape memory effect.

297. Strain Induced Martensite Transformation in a Low Carbon-Low Alloy Triphase Steel

Shen Lian and Li Hua

A low carbon-low alloy triphase (F-M-A) steel containing 7~16% retained austenite is obtained by composition design and intercritical annealing. The strain induced martensite transformation in the retained austenite during tensile deformation and its effect on tensile properties have been studied by X-ray diffractometer, tensile test machine and transmission electron microscope (TEM). The experimental results show that the retained austenite is an isolated type and it is unstable mechanically. The strain induced martensite transformation occurs in it during tensile testing. The amount of retained austenite decreases from 16% to 2.64% at uniform elongation of 7.85%. The strain induced martensite transformation process is observed *in situ* deformation by TEM. The sequence of transformation is retained austenite (f.c.c.) \rightarrow stacking fault (h.c.p.) \rightarrow martensite (b.c.c.). The effect of retained austenite on tensile properties of steel is remarkable. σ_b , n_1 , n and δ_u are enhanced, σ_1 , σ_1/σ_b , δ_1 and Ψ are decreased and the resistance to formation of necking is increased.

298. The Influence of Volume Change on Stress Induced Martensitic Transformation in Tension and Compression

Sun Qing-ping

Constitutive relations and the accompanying microstructural changes in the stress induced martensitic transformations of two kinds of alloys, one with volume expansion and the other with volume contraction, are studied respectively in present paper. Based on the micromechanics and thermodynamics constitutive model developed by the author, the theoretical results for uniaxial tension and compression are derived respectively and compared with the experimental data of two polycrystalline iron alloys. One was an Fe-29% Ni-0.2% C which formed α' -martensite with a volume expansion of about 4%, and the other was an Fe-32% Mn-0.2% C which formed ϵ' -martensite with a volume contraction of about 2%. A good agreement between theory and experiment is obtained.

299. The Orientation Dependence of Ti-Ni Single Crystals Mechanical Properties

Yu.I. Chumlyakov, N.S. Surikova and A.D. Korotaev

The orientation and temperature dependence of the resolved shear stresses τ_r , plastic deformation and fracture have been investigated systematically by tensile testing in Ni-rich TiNi single crystals ($M_s = 208$ K and $M_s = 243$ K). A strong orientation dependence of the resolved shear stresses, plasticity and the mechanism of fracture have been found. At first, it has been shown that τ_r in B2-phase in a "hard" orientations $\langle 001 \rangle$, $\langle 011 \rangle$ are about three times larger than τ_r for "soft" orientations $\langle 111 \rangle$ and $\langle 112 \rangle$. Secondly plasticity of the $\langle 111 \rangle$ crystals in B2-phase is 30 + 50 times larger than in $\langle 001 \rangle$. Thirdly, the "hard" crystals have been brittly destructed without the plasticity of transformation in the temperature range M_s - M_d , and M_d in $\langle 001 \rangle$, $\langle 011 \rangle$ crystals is about 100 + 150 K larger than in $\langle 111 \rangle$ orientation. Experimentally obtained results have been discussed in details. The main prominence is given to the role of slip localization during the deformation in the high temperature B2-phase and a high level of the stresses achieved in $\langle 001 \rangle$ crystals and a change of acting slip systems in "hard" and "soft" orientations.

300. Variation in Dislocation Substructure During Tensile Deformation of Tempered 300M Steel

Zhao Jingshi and Zhang Lin

The variation in dislocation density and dislocation cell size during tensile deformation of quenched and tempered 300M steel was investigated. The dislocation density increases with increasing strain. The dislocation cell size decreases with increasing strain, and reaches to a critical size. After that the cell size remains constant, even while the strain continues increasing. The local stress-local strain curve shows that stages II and III work hardening exist even in quenched and tempered ultra-high strength steel.

301. A Study of Impact Toughness of Fe-Cr-X Damping Alloys

Lu Junsheng, Liu Xiaodong, Zheng Wenjie, Wu Baorong, Bi Hui and Wang Guijin

Fe-Cr-X damping alloys are prevented from being widely applied due to their poor impact toughness caused by coarse ferrite grains and carbides as high solution temperature and low cooling rate are adopted in order to obtain satisfactory damping property. The emphasis of this paper is placed on investigating how to improve impact toughness of Fe-Cr-X damping alloys. It is concluded that two measurements may be utilized. One is suitable for alloys of single phase of ferrite, when damping capacity as high as possible is mostly desired. The other is becoming important when the combined properties of damping capacity, strength and toughness are needed. Of the two the latter one is more convenient and economical and therefore is discussed in a little detail. It is found that the small martensite islands in the ferrite matrix can enhance impact toughness significantly, but lower damping property drastically at the same time. So a balance should be made between mechanical properties and damping capacity by properly controlling the volume fraction of tempered martensite in dual-phase damping alloys.

302. Step-Wise Transformations in Shape Memory Alloys

Graziella Airoidi, S. Besseghini and Guido Riva

The Stimulated Step-wise Martensite-Austenite Reversible Transformation (SMART) is here examined in NiTi, NiTiFe and AgCd alloys. SMART looks consequent to local microstructural "memories" imprinted following a sequence of incomplete thermal cycles on heating from full martensite phase, freely selected with a decreasing rank within the reversion temperature range $[A_s, A_f]$. SMART is here reconsidered at the light of recent X-ray diffraction data, which clearly evidence the reversibility of the underlying process. Results related to SMART on NiTiFe and AgCd alloys are here given and the general key features of the SMART are pointed out. At the light of recent papers on the hysteretic behaviour of Shape Memory Alloys (SMA), SMART experimental phenomenology is discussed.

303. Two-Way Shape Memory Effect Generated By Deformation of Parent Phase in Ni-Ti

Shoichi Edo

The two-way shape memory (TWSM) effect generated by deformation of the parent phase in Ni-Ti alloy has been investigated. The start samples are cold-drawn polycrystalline Ni-Ti wires with the diameter of 1 mm and a nearly equiatomic alloy composition. Aged samples with linear shape are deformed in bending or tensile mode and then heated under constraint so as to generate the TWSM. The spontaneous shape changes on cooling and heating are measured as a function of ageing temperature, constraint temperature, and constraint time. As ageing temperature increases, the amount of shape change designated ϵ_{TWSM} increases. The increase of the transformation heats with ageing treatment are observed by differential scanning calorimetry (DSC). This phenomenon is thought to be related to the relaxation of strains introduced at wire drawing which inhibits the transformations. Such strain relaxation promotes the plastic deformation under constraint heating and the residual internal stress fields generating the TWSM. As constraint temperature increases, the critical shear stress for reverse transformation of stress induced martensites (SIM) increases, while that for usual slip deformation decreases. This results in an increase in ϵ_{TWSM} , because the residual internal stress fields are formed more easily by the plastic deformation. ϵ_{TWSM} increases and decreases depending on constraint time. The phenomenon suggests the presence of accumulation and relaxation processes of the internal stress fields under constraint heating.

304. X-Ray Diffraction of Rapidly Solidified Ti-Ni-Cu Shape Memory Alloy

Minoru Matsumoto, T. Suzuki and Yasubumi Furuya

Ti-Ni-Cu shape memory alloy has excellent mechanical properties. $Ti_{50}Ni_{50-x}Cu_x$ ($x=0-20$) shows one step martensitic transformation ($x=0-10$) and two step one ($x=10-20$). The object of this paper is to clarify the crystal state of rapidly solidified $Ti_{50}Ni_{50-x}Cu_x$ ($x=0-20$). The specimen was made by a melt-spinning machine which was used in rapid quenching. The specimens were 2mm in width and 35 μm in thickness. X-ray diffraction to $Ti_{50}Ni_{50-x}Cu_x$ ribbon was performed using diffractometer of Cu $K\alpha$. The temperature was changed from 230 to 370 K. From the diffraction pattern, (1) specimens were a perfect crystal, (2) a part of $Ti_{50}Ni_{50-x}Cu_x$ specimen seemed to be in an amorphous state, (3) the measurement diffraction intensity of (200) in the parent phase was larger than the calculated one as a powder specimen, then the preferred orientation was observed and (4) thermal hysteresis was observed in diffraction intensity on the thermal cycle by heating and cooling.

304A. Martensitic Transformation in Rapidly Solidified Ti-47 at.% Al Alloy Powder

Minoru Nishida, T. Tateyama, R. Tomoshige, K. Morita and A. Chiba

The microstructural characterizations of PREP'd Ti-47 at.% Al powders have been made in the present study. There were two kinds of powders, i.e. M and D powders, with respect to surface and cross-sectional morphologies. M powder had a surface relief of a martensitic phase and D powder had a dendritic structure. The former consisted of α_2 lath plates with twin relationship and the primary phase during solidification was deduced to be the β -phase. The latter consisted of α_2/γ lamellae and γ phases decomposed in the α_2 matrix. These features suggested that the cooling rate of M powder was larger than that of D powder.

304B. Junction Plane of TiNi Martensite Variants

Minoru Nishida, Kiyoshi Yamauchi, A. Chiba and Y. Higashi

Internal structures of martensite in Ti-50.1 at.%Ni shape memory alloy have been studied by transmission electron microscopy (TEM). Internal defect of martensite variant was confirmed to be $\langle 011 \rangle$ Type II twinning by electron diffraction. Spear-like $(11\bar{1})$ Type I twinning planes were observed at many of junction planes between martensite variants. It suggested that $(11\bar{1})$ Type I twinning was variant accommodation twinning which is introduced as a means of mutual accommodation of shear strains between variants.

305. Formation of Ti-Ni Shape Memory Films by Sputtering Method

Akira Ishida, A. Takei and Shuichi Miyazaki

A thin film of Ti-Ni is a promising actuator for micro robots. In this study Ti-Ni films in the range of 48.9 to 51.4 at.%Ni were formed by magnetron sputtering under various conditions. The compositions were determined by the electron probe micro analysis. As-sputtered films were amorphous materials or crystals depending on the sputtering condition. The films were heated for solution treatment or age treatment. Their shape memory behavior were estimated by thermal cycle tests under a variety of constant loads. The results revealed that they exhibited a stable shape recovery characteristics.

306. Effects of Grain Refinement on Phase Transformation Characteristics and Mechanical Properties of a Ti-Ni Shape Memory Alloy

Yoshinobu Motohashi, Taketo Sakuma, M. Suzuki, Tajii Hoshiya and K. Ohsawa

The grain sizes of Ti-50.7 at.%Ni alloy and Ti-50.2 at.%Ni alloy having no effect on precipitates were reduced by means of a thermo-mechanical treatment. Then, specimens having different initial grain sizes ranging from 4.0 to 50 μm were made, and the grain size dependence of martensitic transformation temperature M_s was studied. Moreover, a tension test in a temperature range from 77 to 423K and a thermal cycling test under a constraint stress were conducted, and the effects of the grain refinement on mechanical properties and shape memory characteristics were discussed. Based on these results, it is concluded that the grain refinement is a fairly effective method for improving the shape memory characteristics of the Ti-Ni alloys without lowering other properties.

307. Intrinsic Transformation Influenced Mechanical Behaviour in a NiTi Alloy

Paul G. McCormick, Shuichi Miyazaki and Yinong Liu

Shape memory alloys are well known to exhibit thermal effects associated with the stress induced martensitic transformation. Local temperature rises of up to 25K may be generated by the transformation. In conjunction with the relatively large temperature dependence of the transformation stress, such temperature rises can significantly influence mechanical behaviour. In this paper we report measurements of the effect of specimen-ambient heat exchange on the stress-strain characteristics of a Ni-49%Ti alloy. It is shown that the temperature rise associated with the formation of stress induced martensite acts to stabilise against transformation localisation, causing the transformation to occur in a spatially uniform manner.

308. Effect of Hydrogen on Mechanical and Shape Memory Properties of Ti-Ni Alloy

T. Asaoka, H. Saito and Y. Ishida

Effect of hydrogen on mechanical and cyclic shape memory properties of Ti-Ni alloy was studied. For the study, the original shape memory cycle test machine was constructed. The shape memory cycle was realized by electric current charge heating and cold air spray cooling, in the manner of tensile stress loading. Results show that even a small amount of hydrogen, which is not sufficient to form hydride, lowers cyclic shape memory properties of this alloy. From the results of mechanical test, it is supposed that hydrogen does not affect on the displacement process of martensite variants. Observed decrease in cyclic shape memory properties due to hydrogen was attributed to the interaction of mobile hydrogen with dislocations which were introduced during cyclic deformation.

309. Martensitic Transformations and Shape Memory Effect in Multicomponent Compounds on the Basis of TiNi

V.P. Voronin, Vladimir N. Khachin and V.G. Pushin

Ternary and multicomponent compounds of TiNi with the simultaneous alloying by Cu and one of the following metals (Al, Fe, Co) were investigated by electron microscopy, electron and X-ray diffraction and mechanical test. It was established, that the following sequences of martensitic transformations (MT) realize in the alloys. $B2 \rightarrow R \rightarrow B19'$, $B2 \rightarrow B19'$ and $B2 \rightarrow B19 \rightarrow B19'$. The connection between the MT, the structure of premartensitic and SME parameters under alloy composition variation were determined. The laws of alloying with the purpose of creating of materials with assigned properties were also determined.

310. Martensitic Transformation and Shape Memory Effect in ZrCu Intermetallic Compound

Yu.N. Koval, G.S. Firstov, and A.V. Kotko

Structural investigation of martensitic transformation (MT) in ZrCu equiatomic compound was carried out by an optical metallography, transmission electron microscopy (TEM) and X-ray diffractometry. Formation of the two monoclinic martensites with internal structure of different kinds has been observed in as-cast condition. Examination of shape memory effect (SME) behavior show that ZrCu alloy demonstrate considerable shape recovery and recovery stresses. Influence of thermal cycling on MT and SME characteristics has been studied. The shape memory aspects of ZrCu alloy are discussed.

311. Shape Memory Effect, Structure and Properties of Ti-Ni Alloys After Thermomechanical Treatment

Sergei D. Prokoshkin, Ljudmila M. Kaputkina, Irene Yu. Khmelevskaya, A.A. Kadnikov, S.A. Bonareva, Ljudmila P. Fatkullina and S. V. Oleynikova

312. Effect of Aging on Martensitic Transformations in Ti-50.7 at.% Ni Alloy

S.V. Oleynikova, Irene Yu. Khmelevskaya, Sergei D. Prokoshkin and L.M. Kaputkina

This paper presents the studies of the effect of heat treatment (solid solution and aging) on martensite transformation (MT) temperatures, recovery strain and yield stress in various semi-manufactured objects made of Ti - 50.7 at.%Ni alloy. It shows the possibility of smooth regulation of MT temperature intervals with the help of aging and the possibility of obtaining Af near 37 °C for application in medicine. The stage-by-stage character of direct MT in the aged specimens-in case MT develops under a low stress is a consequence of an external stress influence on the MT development in grains with various orientation.

313. Electronic Pulse Beam Induced Martensite Transformation and Shape Memory Effect

V.E. Domrachev, L. A. Monassevich, V.V. Myasnikov and Yu.I. Pascal

The lamellate specimens of Ti/Ni based alloys, containing 49.3 (alloy 1), 50.3 (2), 50.6 (3) at.% Ni, 1 mm thick were irradiated with an electronic pulse beam. The pulse duration was 10^{-8} s, the current density varied from 0.1 to 1.6 kA/cm². The diffractogram was read before and after the treatment from both specimen surfaces. To exclude the influence of radiation damage and warming up on the phase state of the material a buffer plate of the same materials was placed before the specimen, the acoustic contact of the latter with the specimen was ensured. Some experiments were also carried out without a buffer plate. The current density being 1.4-1.6 kA, residual changes of the phase state were found. The irradiation in martensite state in alloys 1 and 2 results in a reverse martensite transformation. On both specimen surface from 40 to 100% of high-temperature phase was found. 5-10% of martensite phase is formed in alloy 3 as result of irradiation in high-temperature state. The observed phase state changes are established to be induced by pressure pulse, formed by a thermoelastic mechanism. The martensite hysteresis loops before and after the irradiation were compared. As a result of irradiation the hysteresis loop stretches and shifts towards lower temperatures. The hysteresis loop change is similar to that induced by a mechanical cold hardening and is accompanied by broadening of x-ray profiles of a high-temperature phase. This enables to conclude that the observed changes are due to a plastic component of a pressure pulse and a material cold hardening induced by it. Under certain conditions shape restitution of a material preliminary deformed in a martensite state as result of the electronic pulse irradiation was observed. This enables to expect some interesting practical application.

314. The Variety of Method of Phase Transformation Caused by Thermo-Strain Cycles on NiTi Shape Memory Alloy

Long Shen, J.F. Guo and M. Zhu

The variety of the method of phase transformation caused by thermo-strain cycles on 55.2wt%Ni-Ti SMA was studied in this paper. Special method of thermo-strain cycles test has been designed and done. The curves of internal friction in phase transform (Q-T) and the curves of resistance in phase transform (P-T) have been measured on the sample before and after its cycles test. Following conclusions are made by analysing results: 1) temperature range of phase transformation was enlarged by thermo-strain cycles, and hysteresis was increased. 2) the method of phase transformation (MPT) are changed by thermo-strain cycles from taking B2 \leftrightarrow R \leftrightarrow M as main MPT into taking B2 \leftrightarrow M as main MPT. 3) to large strain ($\epsilon=8\%$) cycles, B2 \leftrightarrow M MPT is good for decreasing the fatigue degradation rate of shape memory effect.

315. The Effects of Aging on the Transformation Behaviours in Ni-Ti-Nb Shape Memory Alloys

R.H. Yu, Y.S. Li and Y.B. Jin

It is known that Ni-Ti-Nb alloys exhibit a wide transformation hysteresis after overdeforming in the martensitic phase because the microstructure of them consists a hard ordering matrix(NiTi phase) and a fine dispersed soft second phase(Nb-rich phase) which is cubic. The formation of the soft second Nb-rich phase can be influenced by heat treatment and alloy content.

The effect of heat treatment temperature on the martensitic transformation temperature and the latent heat of transformations in Ni₄₇Ti₄₄Nb₉ and Ni_{47.5}Ti_{44.5}Nb₈ Alloys were investigated and calculated. Heat treatment after solution at 1173K were carried out in the range of 623-1123K and then cooled in water. Martensitic transformation temperature and latent heat of transformation were measured using a differential scanning calorimeter (DSC).

Both of two composition alloys showed wide transformation hysteresis(about 150K) after deforming in the martensitic phase. The transformation temperature and latent heat of transformation strongly depend on the ageing temperature. That is, Ms of Ni₄₇Ti₄₄Nb₉ alloy increased with increase ageing temperature while the latent heat initiatively increased, reached maximum at 823K then decreased. Only martensitic transformation take place in this alloy that heat treated at all ageing temperature. Ms of Ni_{47.5}Ti_{44.5}Nb₈ alloy changed irregularly with change ageing temperature while latent heat of transformation reached maximum at 773K. The R-transformation takes place while specimens were heat treated at some temperature. The latent heat of transformation in both alloys was related to the transformed amount of phases.

316. Stress-Induced Martensitic Transformation in a Ni-Ti-Nb Shape Memory Alloy

Cai W., Zhang C.S. and Zhao Liancheng (L.C. Zhao)

Stress-induced martensitic transformation has been investigated in a Ni-Ti-Nb wide hysteresis shape memory alloy by means of tensile tests at various temperatures and TEM analysis. During the deformation at the temperatures between Ms and M_s^{*}, the stress-induced martensitic transformation occurs and the relationship between the critical stress for martensitic transformation and deformation temperature satisfies the Clausius-Clapeyron equation, while the slope of the linear relationship is lower than that of stoichiometric NiTi alloys. The TEM observations show that a majority of the stress-induced martensite variants exhibit self-accommodation, but some of the variants around the β -Nb particles exhibit lower self-accommodation. The substructure of the stress-induced martensite is mainly type I (111)_Mtwins and (001)_Mtwins and antiphase domain boundaries are occasionally observed. The orientation relationship between the parent phase and the stress-induced martensite with type I (111)_Mtwins was determined to be $[1\bar{1}\bar{1}]_{A_1} // [1\bar{1}0]_M$, with (101)_{A₂} 5° away from (001)_M.

317. The Two-Way Memory Effect and the Martensitic Transformation of Two-Way Driving Element in Ni-Ti

Zhou Shou-Li and Zhang Yun-Guo

The two-way memory effect and the martensitic transformation of two way driving element in Ni-Ti have been studied by using electrical resistance measurement, x-ray diffraction and TEM. The complete and incomplete cycle φ -T curve and θ -T curve have also been studied. The new procedures were adopted to keep the two-way memory effect remain stable. The electrical resistance peak effects and R phase transformation in the driving element were found to exist during the procedure of two-way memory. There is a resistance peak at A_s followed by a range of leaving off during the reversible procedure. It is suggested that the procedure of transitions of two-way memory is: $B_2 \rightleftharpoons I \rightleftharpoons R \rightleftharpoons R + B_{19}$. The observation on φ -T and θ -T curve leads to the conclusion: the rotation in the temperature range of driving element has good response and less thermal hysteresis. This element exhibit great value for extensive application. Furthermore, it is also proposed that the widening of the electrical resistance peak at A_s relates to residual martensites.

318. The Uneven Deformation with Drawing Wire The Shape Memory Effect Behaviour in Ti Ni

S.V. Shchukin, S. Yu. Kondratjev and N.G. Kolbasnikov

The uneven deformation with drawing TiNi alloy wires on the shape memory effect properties is investigated. It is determined in experimental results that the transformation plasticity, shape memory effect, residual deformation is decrease in 1.5-1.7 times with the fractional deformation of TiNi wires. It is shown that the hysteresis loops is more closed with uneven deformation.

319. TiNi-Base Alloy Mechanical Properties and Shape Memory Effect Parameters

Ljudmila P. Fatkullina, S. V. Oleynikova, A.B. Kainov and E.B. Markova

The effect of technological deformation, thermomechanical and thermal treatment on mechanical properties and shape memory effect (SME) parameters has been thoroughly studied for alloys of various compositions. It has been shown that the temperature of martensitic transformation is effected by alloying on one hand and by ageing of alloys containing more than 50 at.% Ni on the other hand. The temperatures of martensitic transformation attained depend both on temperature and time of ageing, and on chemical composition, deformation treatment of semiproducts and homogenization condition prior to ageing. Among other SME characteristics, reactive stress which correlates with materials strength is of practical importance. Main factors promoting the strengthening of material have been defined. They are dispersed and uniformly distributed TiNi phase and polygonized substructure. Wide range of TiNi alloys semiproducts commercially produced by VILS and knowledge of the peculiarities of the effect of main technological procedures on the SME parameters alloys us to meet various requirements of customers.

320. Study of Superficial Oxide Coats and Composition Changes in Cu-Zn-Al-Ni Alloys after Heat Treatments

Pierre Charbonnier, Michel Morin and Laurent Buffard

Prolonged heat treatments have been carried out on Cu-Zn-Al-Ni alloys. Different changes in martensitic transformation temperature with thermal treatment conditions (temperature, duration) and sample geometry have been observed. The growth, at the sample surface, of an oxide layer essentially constituted of alumina was shown in a previous paper. Surface analysis confirm this tendency and chemical analysis show losses of zinc and aluminum during heat treatment. We explain the increases of transformation temperatures by the loss of these two elements.

321. Effects of Compressive Pseudoelastic Cycling in Cu-Zn-Al Single Crystals: Characteristics of the Induced TWSME

Eduard Cesari, Catalina Picornell and Marcos Sade

Single crystals of Cu-Zn-Al have been trained under compressive pseudoelastic cycling. As a result, the two way shape memory effect (TWSME) was found to appear for a smaller number of cycles than in the samples submitted to tensile experiments. Temperature induced transformations were studied by calorimetry in samples mechanically trained. Many of the characteristics of the thermally induced martensitic transformation produced by tensile cycling also appear in this case, but some of them (i.e. hysteresis width increase) become important after a higher number of cycles than in tensile training.

Samples which show the TWSME after compressive mechanical cycling, are able to overcome an applied opposing stress during the $\beta \rightarrow M$ transformation. A "threshold value" can be defined as the higher stress that can be overcome by the sample before the degradation (measured as length change) of the TWSME starts. This value increases with the number of compressive mechanical cycles and its dependance on the orientation of the sample, critical stress applied, etc., has been also studied.

322. The Effect of γ Precipitates on the Two Way Memory Effect in Cu-Zn-Al

Jaume Pons, Marcos Sade, Francisco C. Lovey and Eduard Cesari

Small γ -phase precipitates ($O(100\text{\AA})$ in size) can be produced in the β -matrix of Cu-Zn-Al alloys by specific thermal treatments. When samples containing this type of precipitates are subjected to tensile pseudoelastic cycling through the martensitic transformation, the two-way memory effect (TWME) is induced after a relatively lower number of cycles (about 200 cycles) comparing to precipitate-free samples. Once the TWME is present the sample can deliver a small amount of work against an external force on cooling. It is shown that this capacity to produce work increases with the number of cycles in the case of initially coherent precipitate distributions.

Transmission electron microscopy studies were carried out in order to find a relationship between the microscopic changes in the specimen and the appearance of the TWME. The results show that the precipitates are deformed after pseudoelastic cycling, thus braking the cubic symmetry in favour of the induced martensite variant. The internal stresses produced by the precipitates deformation could account for the induction of TWSME.

323. Effect of Ni Content on the Phase Stability of Martensites in β Phase Cu-Al-Ni Shape Memory Alloys

Hidekazu Sakamoto, M. Yoshikawa, and Ken'ichi Shimizu

The effect of Ni content on the phase stability of three kind of martensites, γ_1' (2H), β_1' (18R₁) (or β_1'' (18R₂)) and α_1' (6R), thermally formed or stress-induced in Cu-Al-Ni shape memory alloys has been studied. The phase stability was evaluated by using our previous data on the pseudoelastic behavior examined as a function of temperature in single crystals with $\langle 100 \rangle$ orientation of Cu-14.1Al-xNi (x=2.1, 3.2 and 4.3 mass%) alloys. Using the thermodynamics of the stress-induced martensitic transformations and the thermodynamic parameters such as equilibrium stress, which was the midpoint between the forward and reverse transformation stresses, and the transformation elongation, it has been calculated that, with decrease of 1%Ni, the chemical free energy G^* of the β_1' increases by about 9 and 8 J/mole relative to those of the γ_1' and α_1' phases, respectively. The stress-temperature phase diagram in binary Cu-14.1Al alloy was constructed by using equilibrium temperature T_0 and temperature dependence of equilibrium stress which were extrapolated from those of the Cu-14.1Al-xNi alloys to x=0. It was found that Ni atoms more stabilizes the β_1' phase than for the γ_1' and α_1' phases.

324. Mechanical Behavior of Memory Brass

Scott Berry and Wally Peters

This paper describes the testing and analysis of the mechanical behavior of memory brass. Specimens were cut out of a large piece of metal obtained from Memry Corporation to be tested in uniaxial tension. The tension tests were done at different temperatures to ascertain the change in behavior with changes in amount of martensite. Tests were also performed to measure the constrained and restrained recovery properties of the material.

325. Differences in the Kinetic Grain Growth Between Cu-Zn-Al, Cu-Zn-Al-Mn, Cu-Al-Mn and Cu-Al-Mn (Si) Shape Memory Alloys

F.J. Gil and Josep M. Guilemany

In the shape memory alloys a great influence of grain size on singular transformation temperatures is observed, and also on thermodynamic values, elastic and frictional energy and mechanical properties among others. The main aim of this work is to show how the grain size can be predicted for different copperbased shape memory alloys at different temperatures and heat treatment times. The kinetic grain growth was studied in β -phase alloys at room temperature. For each of these alloys, 30 slices were cut from the same bar, measuring 5 mm in diameter and 4 mm in height. Two of them were used as reference samples, whilst the rest were subjected to different heat treatments at 750, 800, 850 and 900°C and for 3, 5, 10, 15, 20, 30 and 60 min at each temperature. The metallographic observations have been carried out by means of light microscopy and the image analysis. After the optimization process, grain size parameters were identified and quantified. In the copper based shape memory alloys studied very fast grain growth is observed at a given temperature for up to 10 to 15 min heat treatment but it becomes slower after this time, giving a constant grain size at times above 60 min at the test temperature. The growth order ranges from 0.69 for Cu-Zn-Al to 0.35 for Cu-Zn-Al-Mn. The activation energy has also been calculated assuming a simple diffusion law. This energy ranges from 50 to 100 KJ/mol for the different alloys.

326. The Effect of Melt Spinning on Shape Memory Behaviour of a Melt Spun Copper-Based Shape Memory Alloy

J.H. Zhu, Druce P. Dunne, G.W. Delamore and Noel F. Kennon

CANTIM 125 is a Cu-Al-Ni-Ti-Mn alloy which is commercially produced as a high strength, high temperature SM alloy. Although grain refinement is achieved through the presence of relatively coarse X-phase $[(\text{CuNi})_{0.5}\text{Ti}_{0.25}\text{Al}_{0.25}]$ particles, the grains in hot rolled strip are still relatively coarse ($\sim 200 \mu\text{m}$) and the ductility is still limited.

In the current investigation, the rapid solidification technique, i.e. melt spinning, was employed to form thin strip directly from the melt, and to produce marked refinement of the parent β grain size. An average grain size of $2.4 \mu\text{m}$ was obtained and both coarse and fine X-phase precipitates were suppressed. Using DSC thermal cycling and repeated bend tests, the transformation behaviour and shape memory effect of melt spun ribbons was examined. A reproducible shape memory effect was clearly shown in ribbon samples. The transformation temperatures for both forward and reverse transformations were much lower than those of bulk material formed conventionally. However, melt spun material which was reheated to 900 °C then quenched in KOH solution did not show reproducible transformation characteristics or shape memory effect on thermal cycling, as the martensite started to decompose by tempering rather than reverting to parent phase. By means of TEM and SEM observations, it has been established that the X-phase precipitates formed at 900 °C in the melt spun alloys adversely affect the reversibility of the martensitic transformation.

It is concluded that the martensitic transformation and SME in this alloy are highly sensitive to the state of X-phase precipitation.

327. Pseudoelasticity and Shape Memory Effect in Mn-18.6at.%Cu Alloy Single Crystal

Hiroyuki Kato, H. Morishita and Sei Miura

Pseudoelasticity and shape memory effect in Mn-18.6at.%Cu alloy was examined using a single crystal grown by Bridgman method. The analysis of the results of dilatometric measurements leads to the assumption that through the martensitic transformation a fcc single crystal becomes a twinned face centered tetragonal (fct) structure, in which only one twinning system operates and the twin-related two fct layers have an equal thickness. This configuration of fct crystals can explain the appearance and the characteristics of three different types of stress-strain behavior observed in tensile testings of a single crystalline specimen.

328. An Investigation of the Grain Size Effects on the Corrosion Behavior of Copper-Based Shape Memory Alloys

D.N. Adnyana and S. Katili

Two Cu-Zn-Al alloys containing a small quantity of zirconium were chosen for the study of grain size effects on corrosion behavior in copper-based shape memory alloys. To vary the grain size, the two alloys were solution treated at various temperatures ranging from 750°C to 900°C. At room temperature, one alloy exhibits beta phase while the other shows martensite. Corrosion tests were carried out at room temperature using accelerated tests and electrochemical measurements. The results showed that the dezincification rate on either beta phase or martensite tends to increase with increasing grain size. However, the beta phase showed higher dezincification rate compared to that of martensite. The difference in the corrosion behavior of the two alloys will be discussed.

329. The Effect of Constraint Aging of Two-Way Shape Memory Effect of Cu-Zn-Al Alloy

Ren-Der Jean, H.J. Lai and S.C. Cheuh

The two-way shape memory (TWSM) effect has been a hot topic in the development and applications of shape memory (SMA). The amount of this effect showing on materials, as well as its stability in thermostatic applications, has everything to do with the training procedure. Among some others, constraint-aging training has been confirmed to be an effective training method. The experiment of this paper employed this very method on a Cu-Zn-Al alloy of a designated composition and worked systematically to vary the temperature and aging time under which the TWSM effect was developed. Experimental results are given here which shows the influence these two factors have over the TWSM effect obtained. A look into the thermal stability of this effect has also been made and the result is summed up. To account for all the phenomena observed in this experiment, and explanatory model is presented as well.

330. The Decomposition of β_1 Phase after Hot Extrusion of Cu-Zn-Al Shape Memory Alloy

Svatoboj Longauer, V. Spetuch, M. Longauerova, S. Sladik and K. Czach

The effect of cooling mode after hot extrusion of Cu₁₄,6Zn₈,7Al (wt%) alloy on morphology of β phase decomposition products arising during tempering was studied by light and electron microscopy. It was shown that decomposition occurs via eutectoid reaction when extruded rods were quenched into 20°C water immediately after extrusion. Morphology of $\alpha + \gamma_2$ lamellar eutectoid indicates that it could arise by discontinual precipitation. Thickness of lamellas is about 50 nm. Quite different morphology is after slow cooling of rods in 20°C air after extrusion. During subsequent tempering at same conditions as in former case β_1 phase decompose to γ_2 needle shaped and/or nodular particles in α matrix. The particles follow orientation of martensite plates. Most significant feature which differs from eutectoid morphology is thickness of particles which is about 10 times higher than in case of lamella in eutectoid. Differences have been also observed in substructure. In water quenched case martensite plates has some signs of shape deformation with higher dislocation density and smaller antiphase domain dimensions. In air cooled case martensite was not deformed, and antiphase domains have been substantially larger.

• 331. **Martensitic Transformation of a Cu-Zn-Al SMA Under Thermal-Mechanical Cycling**

Shidong Wang, Jinping Zhang and Guangjun Shen

The change in morphology, crystal structure and defects of martensite under thermal-machanical cycling was investigated in detail by optical and transmission electron microscopy. The stress-induced martensite α' and irreversible dislocation debris were observed and expected to be the reason that results the degradation of the shape memory effect under thermal-machanical cycling.

332. **Shape Memory Behavior of Ti-V-Al Alloys**

C.Y. Lei, J.S. Lee Pak H.R.P. Inoue and C.Marvin Wayman

The shape memory effect of Ti-V-4Al alloys was studied using optical microscopy, DSC, and tensile tests. All alloys showed a Clausius-Clapeyron relationship between the triggering stress for martensite formation and temperature. Metallographic observations revealed that shape recovery is associated with the reversible movement of the martensite-parent interfaces.

333. **On the Stability of ϵ Fe-Mn-Si Martensite by Neutron Diffraction at Low Temperatures**

K. Tamarat, T. Bouraoui, Alain Lodini, G. Andre, M. Perrin and Bernard Dubois

According to the bibliography, the detection of pure ϵ martensite seems controversial and may depend on the experimental process. It could be due to the antiferromagnetic order of ϵ phase. The resistivity measurements published are not clear about Neel temperature.

If Fe-30 wt % Mn-6 wt % Si, is quenched, the magnetic susceptibility yields $T_N = 276$ K and $M_s = 278$ K after one cycle between 200 K and 500 K.

Neutron diffraction experiments were carried out on the Orphee reactor. Up to now, only Neel temperature was detected up to 240 K and a super lattice of γ phase.

New lines also, were obtained related to antiferromagnetic oxides. The failure was attributed either to the thermomechanical treatment of the cubic samples or to the inhomogeneity of the quenched bars.

New experiments are still in progress to determine if the austenite lines are always detected at 1.7 K.

334. **Shape Memory Effect in Fe-Mn-Cr and Fe-Mn-Si Alloys**

K. Tamarat, T. Rouraoui, Laurent Buffard, E. Weynant and Bernard Dubois

Some Fe-Mn-Cr and Fe-Mn-Si shape memory alloys were studied either after hot rolling or as quenched after 1 hour at 1050°C under argon atmosphere.

At room temperature, X ray diffraction, electron and optical microscopy showed the presence of γ austenite and ϵ martensite. More over the α' phase is detected in Fe - 14 wt % Mn - 12 wt % Cr : the S.M.E. appears in this ferromagnetic sample. The electropolishing is very important.

By electrical resistivity measurements obtained from the Laboratory apparatus, clear results concerns Fe-Mn-Si and not Fe-Cr-Mn. In Fe-Mn-Si, it seems difficult to reach the M_f point. For the two alloys, transition temperatures between -50°C and + 150°C were detected by internal function measurements.

The shape memory effect was observed in each alloy after bending : the best recovery was obtained in Fe - 30 wt % Mn - 6 wt % Si but Fe - 20 wt % Mn - 12 wt % Cr was used to make a clip. This alloy present always a shape memory effect four years after training.

335. Oxidized Surfaces and Manganese Distribution in Fe-30 wt % Mn - 6 wt % Si
C. Keller, K. Tamarat, Laurent Buffard, E. Weynant and Bernard Dubois

As received Fe-30 wt % Mn - 6 wt % Si bars were spark machined at a thickness of 2 mm and maintained at room temperature for 18 months. Initially the bar (18 x 18 mm²) was water quenched after maintaining 1 hour at 1100°C. X ray diffraction detected the (111), (200) γ lines, the (110), (200) α' martensite lines and other compounds not well crystallised. The sample was attracted by a magnet. The thickness was reduced to about 200 μ m, and only the (111) (200) γ lines and (1010), (1011) ϵ martensite lines appeared with the same intensity. Reducing the thickness 500 μ m more, the ϵ lines intensities decrease to about 50 %. Local analysis with S.E.M. indicated two layers in the oxidized sample : above, oxygen, iron and silicon were in large quantities and the under layer was enriched in manganese. The above layer contained amorphous compounds partially with OH bands as detected by I.R. spectroscopy. The underlayer manganese enriched would explain the appearance of the ϵ lines. The decrease of the lines with reducing thickness by electropolishing would be due to either a manganese gradient or an incomplete quenching. Electron microscopy showed a small quantity of ϵ needles near the stacking faults. This alloy presented too many difficulties for industrial applications.

336. The SME and HCP Martensitic Transformation in an Fe-Mn-Si-Ni-Cr Alloy
Gu Nanju, Zhang Jianxin, Wang Ruixian, Yin Fuxing, Chen Wei and Liu Qingsue

Using TEM, the HCP martensitic transformations in FeMnSiNiCr SMA has been studied. It was found that the main mechanism of nucleation for HCP-M may be the orderly overlapping of the stacking faults, the resolution of the perfect dislocations and the creation of the stacking faults may occur easily at the boundary of annealing twin, the low-angle grain boundary and the place of which the dislocation array pile up at a grain boundary.

Furthermore, it is advantageous to the nucleation for HCP-M that the dislocations, in a dislocation wall, dissociate into partial dislocations and resulting in the orderly expansion of the stacking faults, and the stacking faults could project from a twined boundary into the annealing twin so that the single orientation HCP-M formed and resulting best SME.

337. Ni₂MnGa as a New Ferromagnetic Ordered Shape Memory Alloy
V.A. Chernenko and V.V. Kokorin

It was found in present work the Heusler's ferromagnetic alloy Ni₂MnGa undergo the thermoelastic martensitic transformation (MT). M_s temperature can be varied from 130 K to 293 K with respect to the composition. The pre-martensitic state in the parent phase was discovered and interpreted as an intermediate phase having crystal lattice modulated along $\langle 110 \rangle$ by the transversal displacement waves with length $\lambda = 6d_{220}$. In the martensitic phase λ was obtained to be $5d_{220}$. MT is accompanied by anomalies of electric resistivity, magnetic susceptibility and elastic constants c_{11} , c' . The volume change associated with MT was about 0,05%. This value was obtained using experimentally determined hydrostatic pressure shift of M_s and latent heat being equal 6 K/GPa and 3,8 Jg⁻¹, respectively. The peculiarities of electromagnetic - to - acoustic transformation efficiency near M_s was investigated. It was proved that Ni₂MnGa possesses the shape memory effect, superelasticity and ability to generate reversion stresses. The maximal reversible strain along axis $\langle 100 \rangle$ was about 4%. The compression along $\langle 110 \rangle$ at 77 K induced the strain accumulation up to 5%. The step-like recovery of the latter strain upon heating was observed. It was confirmed that the reversal intermartensitic transformations take place at the temperatures corresponding to the mentioned step-like recovery of the strain which in turn was accompanied by change of magnetic properties.

338. Effect of Thermo-Mechanical Treatment on Deformation- Induced γ - ϵ Martensitic Transformation and Shape Memory Effect in an Fe-Mn-Si-Ni-Co Alloy

Wang X.X., Wang W.X. and Zhao Liancheng

It has been shown that shape memory effect in an Fe-25.6Mn-5.1Si-4.1Ni-1.8Co(wt%) alloy can be remarkably improved through thermo-mechanical training cycles, which consists of the pre-straining to 3% at R.T and then annealing at 873K for 3 minutes. With increasing cycles, the yield stresses rapidly drop firstly and reach the minimus at 5th cycle; with further increase in cycles the yield stresses gradually increase. The reverse transformation temperature A_f monotonously increases with cycles, while A_s keeps constant. The optical microstructure observation shows that the amount of ϵ martensite increases with cycles. The TEM observation for a series of pre-strained and annealed specimens reveals that with increasing cycles more perfect dislocations are present in the γ matrix. These dislocations usually do not dissociate to partial dislocations during subsequent pre-straining. This is in sharp contrast to the first pre-strained specimen in which a large number of stacking faults is present besides ϵ martensite plates. The shape memory effect may be affected by thermo-mechanical training cycles in two ways: one is the increase of martensite nucleation sites by first several cycles, so that enhances the deformation induced γ - ϵ transformation kinetics; the other is the strengthening of the γ matrix due to the introduction of more dislocations when the cycles are increased.

339. Production Line of Springs of Copper-Based Shape Memory Alloys

Michel Raymond and E. Weynant

The paper describes the production line of a very special mechanism, named "Thermomarker", using the martensitic transformation of a shape memory alloy spring and applied to temperature control. After a brief presentation of each point of the process, the authors will insist especially on the effect of a synergy between the manufacturing tool of production and the laboratory enclosed in the factory.

The paper will explain the kind of synergy used to develop an industrial tool adapted to the high level of performance expected from the alloy. It will exhibit the automatic furnace which can treat a thousand springs at once, using a very repetitive cycle. The thermal treatment is the result of an experimentation based on the industrial working tests of Thermomarkers. Graphes will show the effect of treatment parameters on the working temperature of Thermomarkers.

340. An Application of Ti-Ni Shape Memory Alloy to Partial Denture

Shuichi Miyazaki, S. Fukutsuji and M. Taira

Shape memory attachments for partial dentures have been developed. These attachments enable the partial dentures to be easily attached to and detached from remaining teeth at room temperature, because they become soft at a low temperature. On the other hand, they become harder and recovers the original shape at a higher temperature so that they fix suitably to the remaining teeth and do not detach easily in oral cavity. These attachments have other important functions such as a safety valve and a loose fitting functions. If biting force exceeds a limitation, the attachments will show a large deformation due to the martensitic transformation, playing as a safety valve. The loose fitting nature originates from a low modulus of the alloy, the stress induced R-phase or martensitic transformation, and the design of the attachment. With the loose fitting system, the attachments will not damage the remaining teeth even though external shocks are applied or bone absorption occurs during a long time use. In order to achieve such characteristics of the above attachments, suitable Ti-Ni alloy has been developed by investigating the effects of composition, heat treatment and design of the attachment on the characteristics. An example of clinical case using the shape memory attachment will also be presented.

341. Load Deformation Characteristics of TiNi Orthodontic Archwires
Rohit C.L. Sachdeva, Y. Oshida, Farrokh Farznia and Shuichi Miyazaki

Traditionally the load deformation characteristics of orthodontic archwires have been tested using simple cantilever loading circumstances without multiple constraints as is the case in the mouth. The aim of this study was to compare the load deformation characteristics of TiNi orthodontic archwire when subject to simple cantilever loading, three point bending, five point bending with and without multiple constraints at 0, 22°C, 37°C and 60°C. The results of this study suggest significant variations ($p.001$) occur in the stresses generated by these wires when the loading circumstances are altered. For instance, for a simple beam supported at both ends and not constrained the maximum stress generated was 200 PSI. For a beam of similar length and from the same batch, which was restricted at both ends, a maximum stress of 90 PSI was generated. Also significant differences in the stress strain hysteresis for the wires under different loading circumstances were seen. In conclusion, effective use of these wires in the mouth require understanding of material behavior under conditions that prevail in the oral environment.

342. Characterization of Ni-Ti Orthodontic Archwires
Ren-Der Jean and H.J. Lai and J.J. Lin

In orthodontic applications, the choice of archwire materials is the base for all. Superelastic Ni-Ti shape memory alloy systems are favored over traditional materials due to their relatively small yet stable forces and their great effectiveness. (It is generally believed that forces which are small in magnitude and continuous in nature evoke the optimal biological reaction.) Therefore, Ni-Ti alloys demonstrating low moduli of elasticity have been targeted for application to the field of orthodontics.

The aim of this article is to compare the various commercial Ni-Ti archwires. Our studies indicate that the DSC properties of these wires can be classified into three major categories: work-hardened, superelastic and a mixed type. Currently, the DSC properties of the archwires found on the market differ to a great extent from one brand to another. This has caused a significant amount of confusion on the dentists' part over which archwire to use. Therefore, this paper also tries to address this problem by presenting the results of our study on the thermo-mechanical properties of some of the most commonly used archwires. A discussion of their importance and implications for clinical applications is also included.

343. Medical and Dental Applications of Shape Memory
James Stice

344. Physical and Mechanical Properties of Cold Drawn and Heat Treated Ni-Ti Alloy Wires

Frank Sczerzenie, D.K. Zoeckler, B.K. Eckler and S.O. Mancuso

Special Metals Corporation is developing a database on the physical and mechanical properties of Ni-Ti alloys which are used for superelastic and shape memory applications. Properties are affected by the alloy formulation, the amount of cold work and the heat treatment. Transition temperatures as reported by Differential Scanning Calorimetry are correlated to Transition Temperature Range determined in a thermal bath heated at a controlled rate. Springback, stiffness and kinking resistance are correlated to superelastic strain limit, upper stress plateau and lower stress plateau. Tensile strength, elongation and modulus are reported for different alloy formulations, cold work levels and heat treatments.

345. Characteristics of Shape Memory X-Y Microstage and Necessity of Material Improvement in SMA Actuator Application

Yasubumi Furuya, T. Teshima, K. Abe, Minoru Matsumoto and C. Marvin Wayman

Exploratory investigation of in-plane X-Y positioner was constructed using joule heated coils fabricated from a Ni-Ti shape memory alloy (SMA). These coils work in bias with steel coil spring, and stage movement in two directions (x, y) was achieved by varying the current applied to the SMA coils. The coils were either fan-cooled or naturally cooled in still air. The oscillation could be reduced to as small as ± 0.1 microns and its movement was very smooth by using a more sensitive positioning sensor and by improving the stage control system (i.e., magnitude of the heating current, pulse wave form, etc.), however, improving the response speed remains a more difficult problem. Lastly, some discussions will be done about the SMA material problems with the shape memory actuator application and its control.

346. Methods to Produce a Two-Way Effect

Peter Tautzenberger, Hans-Peter Kehrer, H. Nusskern and H.H. Kocher

347. Diffusion Bonding of Copper Based Shape Memory Alloys to Steel

F.A. Calvo, Jose M. Gomez de Salazar, A. Urena, F.J. Mendez, M. Aparicio and Josep M. Guillemany

In order to achieve a massive technological application of Shape Memory Alloys, it is necessary to find the suitable joining methods to resolve the derived problems of welding Shape Memory Alloys themselves and with other technological materials. Taking in account a previous researches on diffusion bonding of Shape Memory Alloys, the authors have carried out a study of the Shape Memory Alloys-Steel diffusion bonding interface. Light microscopy and SEM images show the important role of the local martensitic transformations occurred in the bonding interface on joining processes.

348. Applications of Shape Memory

W. Van Moorlegghem

349. Development of New Shape Memory Applications

A. David Johnson and John D. Busch

350. New Fabricated Shapes of NiTi Alloys

Darel Hodgson

Over the last several years, increasingly complex and sophisticated shapes have been produced from the NiTi Shape Memory Alloys. Fabrication has generated smaller articles, processing has controlled and enhanced many of the mechanical properties, and secondary operations such as polishing and electroplating have added to the final usefulness of these alloys. A number of such NiTi products being manufactured for various commercial applications will be displayed and described.

351. High Cycle Actuators Using Small NiTi Wires

Wayne H. Brown and Darel E. Hodgson

Small diameter wires of NiTi which have been properly processed to exhibit long cyclic stability and significant memory strain can be used as actuators in a wide variety of applications. Such wires from 0.025mm ϕ to 0.25mm ϕ have been manufactured by Dynalloy, Inc., and trademarked as FlexinolTM. These wires have been incorporated in a wide range of devices to display the potential commercial uses for such shape memory actuation.

352. Performance of the Memoalloy Splitter Using TiNi Alloy in Practical Fields
Kiyoshi Yamauchi, T. Inaba, Minoru Nishida, K. Takashima and K. Kaneko

A newly invented static rock breaker using TiNi shape memory alloy has been proposed by the present authors at ICOMAT-89. The breaker has been produced on a commercial scale and called the MEMOALLOY SPLITTER. It consists of compressively prestrained TiNi rods of 15 mm in diameter and 29 mm in length and a pair of two-layered wedge type platens of steel, and requires no accessory equipments other than heating apparatus. The SPLITTER is inserted into a borehole which is drilled the rock and rock-like objects of breaking. A distance between the SPLITTER and the borehole wall is adjusted by sliding the inner platens. After this operation, TiNi elements recover their original length and generate the recovery force upon heating, associated with the reverse martensitic transformation. The total breaking force of the SPLITTER is about 300 to 900 kN, depending on the number of TiNi elements used. To confirm the performance of the SPLITTER, it has been applied to mortar and high strength concrete walls of buildings and natural boulders in various practical fields. In all cases the objects of breaking were demolished within 5 minutes. It is concluded that the SPLITTER is not lack in terms of performance and is possible to control the direction of crack initiation and growth. That is, TiNi shape memory alloy has a bright prospect and establishes its market as a solid pressure source. A large number of practical applications is presented by table exhibitions at the conference. The performance of the SPLITTER is also discussed as compared with such conventional procedure as expansive agent.

353. The Shape Memory Effect in the Wickered Construction for Vascular Surgery
S.V. Shchukin, S.A. Pulnev, A.V. Karev and N.G. Kolbasnikov

A vascular framework is worked up a cold-drawing wire of TiNi. It is shown that the framework can be used with treatment of the aneurism, stenosis successfully. The description of the framework constructions and the results of clinical test for the mono- and bifurcationary framework is described.

354. TiNi Base Shape Memory Alloys and Their Applications
Ljudmila P. Fatkullina and S.V. Oleynikova

Development of materials displaying a shape memory effect (SME) which can recover the original shape during heating is one of the most important technical problems. Alloys based on TiNi intermetallic compound are of the greatest interest as they have high strength and plastic properties and up to 8% of completely reversed deformation. Research and Production Amalgamation VILS has developed the technology of manufacturing semiproducts in TiNi-base alloys with various alloying additions, known under the common name TN-alloys. At present, we can produce 8 to 230 mm dia rods, down to 0.5 mm dia wire, down to 0.3 mm thick sheets, tubes of different diameters and extruded shapes in TN1, TN1K and TNM3 alloys. The applications of parts made in these alloys are extremely diverse. They help to solve the traditional for air- and spacecraft technology problem of saving the space. Folded and compactly packed antenna, stabilizing mechanisms, solar batteries, etc. are unfolded and moved out under the solar heat after the spacecraft being launched into the orbit. TN1K alloy tubes and rods are used as joints and fastenings. The material is successfully used in medicine.

355. Shape Memory Materials Stress-to-Hydraulic Pressure Transducer
Charles Whitehead

356. Shape Memory Alloy Products
Frank Sczerzenie

Special Metals Corporation has over thirty (30) years of experience in processing Ni-Ti alloys. Our production capabilities include processing from primary melting through to final bar and wire finishing. Our Process Laboratory can supply small heats of custom alloys in bar, wire and plate form. Superelastic and shape memory alloy products will be exhibited including bar wire and strip.